



UNIVERSITY of the  
WESTERN CAPE

**Synthesis and evaluation of 7-substituted 3-propargylamine coumarin derivatives as multifunctional monoamine oxidase and cholinesterase inhibitors for Alzheimer's Disease treatment**

**By Sheunopa C. Mzezewa**

A thesis submitted in partial fulfilment of the requirement  
for  
the degree of Magister Scientae in Pharmaceutical Chemistry  
at the School of Pharmacy,  
University of the Western Cape

Supervisor: Prof Jacques Joubert

Co-Supervisor: Prof Sarel Malan

---

Dedicated to my parents Cornelius and Mukai Mzezewa  
And the rest of my loving family Nyasha, Rumbidzai,  
Tatenda, Chipu, Milani and Tanatswa.



UNIVERSITY *of the*  
WESTERN CAPE

---

## Abstract

Alzheimer's Disease (AD) is a neurodegenerative disease which results from the irreversible loss of neurons in the brain. The disease is characterized by progressive cognitive impairment with recurrent short-term memory loss. AD is the leading cause of dementia and 4th leading cause of death in the elderly. Success in the treatment of AD has been limited, with drugs only treating it at a symptomatic level due to its pathology being complex and poorly understood. However, it is known that the cholinesterase and MAO-B enzymes play an important role in the disease through their association with production of amyloid plaques and oxidative stress respectively, two mechanisms associated with cell death and the symptoms seen in AD. Multi-target directed ligands (MTDLs) have the potential to overcome the failings of the current single-target treatment options by achieving a synergistic therapeutic effect through their ability to interact with multiple disease targets. Coumarin derivatives serve as a good starting point for designing MTDLs due to their wide variety of pharmacological properties, particularly their inherent inhibition of both the MAO-B and cholinesterase enzymes. The aim of this study was to explore the potential of this coumarin scaffold by attaching moieties which would enhance the scaffolds enzyme binding capacity and thus produce multifunctional compounds that may find application in the treatment of AD.

Two series of compounds were synthesized by first attaching either a benzyloxy (series A) or diethyl carbamate (series B) moiety to position 7 of the scaffold via an SN2 substitution. Following this, position 3 of the coumarin was  $\alpha$ -brominated which then allowed subsequent substitution of a propargylamine moiety. A total of 7 novel molecules were synthesised and purified. The structures of the compounds were elucidated using NMR, Mass spectrometry and FT-IR techniques.

*In vitro* biological assays were performed with cell-based assays to screen the compounds for their neuroprotective capability and enzymatic assays were carried out against the MAO and cholinesterase enzymes. The results showed that the compounds had weak activity against the cholinesterase enzymes, showing slightly higher percentage inhibition towards BuChE. Molecular modelling showed that this was because the compounds did not form significant interactions in AChE's active site gorge. Cytotoxicity and neuroprotective studies showed that the compounds were neuroprotective towards neuroblastoma cells, with 75% to 92% of cells compromised with MPP+ surviving following incubation with the compounds. The compounds demonstrated potent inhibition of both MAO enzymes, with exceptional selectivity to the MAO-B isoform. Five of the compounds were more potent than rasagiline, exhibiting IC<sub>50</sub> values between 0.497  $\mu$ M and 0.029  $\mu$ M. Molecular modelling attributed the compounds' activity to their ability to sterically block the entrance cavity and additionally form important interactions in the substrate cavity.


The overall results demonstrated that substitution of the benzyloxy moiety from series A imparted better activity to the derivatives, with the propargylamine derivatives in particular displaying the best MAOB selectivity and neuroprotection. Compounds SM3B and SM4A displayed the best activity profiles and serve as proof that coumarin derivatives show great promise as multi-target directed ligands which can be used in future Alzheimer's Disease treatment.

---

## Declaration

I declare *Synthesis and evaluation of 7-substituted 3-propargylamine coumarin derivatives as multifunctional monoamine oxidase and cholinesterase inhibitors for Alzheimer's Disease treatment* is my own work, that it has not been submitted before for any degree or examination in any other university, and that all the sources I have used or quoted have been indicated and acknowledged as complete references.

Sheunopa Cornelius Mzezewa

Signed.....

Date: 18 March 2020



---

## Acknowledgments

The completion of this thesis has been made possible due to the time, efforts, encouragement and financial support of many people and organisations. I'd like to take this opportunity to express my gratitude and thanks to some of them.

- ▶ The Lord God for protecting me and guiding me up to this point through all of life's joys and tribulations.
- ▶ My supervisor Prof Jacques Joubert and co-supervisor Prof Sarel F Malan for their guidance. I am grateful that you were always willing to lend me your expertise and always had your doors open to me no matter how big or small the issue.
- ▶ My family, particularly my parents Cornelius and Mukai Mzezewa for allowing me to pursue my dreams. Thank you for believing in me as well as supporting me morally and financially throughout.
- ▶ Ms A Ramplin and Mr Y Kippie for their technical assistance and support.
- ▶ Prof. Edith Antunes for assisting with NMR.
- ▶ Dr Sylvester Omoruyi from the Department of Medical Biosciences for his assistance with the cytotoxicity and neuroprotection studies.
- ▶ The National Research Fund (NRF) and University of the Western Cape for providing funding.
- ▶ My colleagues in the Drug Discovery group for all their advice and keeping me encouraged and motivated throughout the course of this research. I am grateful for all the fun we had in and out of the lab.
- ▶ All my friends for constantly encouraging and motivating me to push forward.

---

## Keywords

Alzheimer's Disease

Neurodegeneration

Acetylcholinesterase

Butyrylcholinesterase

Monoamine Oxidase

Multi-targeted Directed Ligands

Propargylamine

Coumarin

Carbamate



UNIVERSITY *of the*  
WESTERN CAPE

---

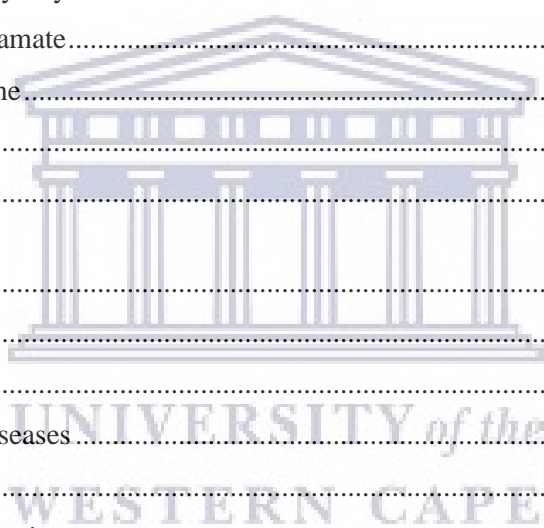
## List of abbreviations

$^{13}\text{C}$	Carbon 13
$^1\text{H}$	Proton
ACh	Acetylcholine
AChE	Acetylcholinesterase
AChEI	Acetylcholinesterase inhibitor
AD	Alzheimer's disease
APP	Amyloid precursor protein
A $\beta$	Amyloid beta
BBB	Blood brain barrier
BuChE	Butyrylcholinesterase
CAS	Catalytic active site
CNS	Central nervous system
DMSO	Dimethyl sulphoxide
FAD	Flavin adenine dinucleotide
GIT	Gastrointestinal tract
IC <sub>50</sub>	Half maximal inhibitory concentration
M	Molar
MAO	Monoamine oxidase
mM	Millimolar
MPP	1-methyl-4-phenyl pyridinium
MTDL	Multi-target directed ligands
MW	Microwave
ND	Neurodegenerative disease
nM	Nanomolar
NMDA	N-methyl-D-aspartate
NMR	Nuclear magnetic resonance
PAS	Peripheral anionic site
PD	Parkinson's disease

---

## Table of Contents

Abstract .....	i
Declaration .....	ii
Acknowledgments .....	iii
Keywords.....	iv
List of abbreviations .....	v
Chapter 1 .....	1
1. Introduction .....	1
1.1 Background.....	1
1.2 Rationale.....	2
1.2.1 Coumarin .....	3
1.2.2 Series A Benzyloxy .....	5
1.2.3 Series B Carbamate.....	5
1.2.4 Propargylamine.....	6
1.3 Aim .....	6
1.4 Conclusion .....	7
Chapter 2 .....	9
2. Literature Review .....	9
2.1 Introduction.....	9
2.2 Neurodegenerative Diseases.....	9
2.3 Alzheimer's Disease .....	9
2.3.1.1 Amyloid hypothesis .....	11
2.3.1.2 Amyloid Cascade .....	12
2.3.1.3 Cholinergic Hypothesis.....	13
2.3.1.3.1 Cholinesterases .....	14
2.3.1.4 Monoamine oxidases .....	17
2.4 Treatment of AD .....	19
2.4.1 Cholinesterase Inhibitors .....	20
2.4.2 NMDAR Antagonists .....	21
2.4.3 Other treatment options .....	22
2.4.3.1 Anti-tau protein strategies.....	22
2.4.3.2 5-HT-6 receptor antagonists .....	23
2.4.3.3 Antioxidants.....	24
2.5 Multi-Target Directed Ligands .....	24





2.6 Coumarins .....	26
2.7 Conclusion .....	27
Chapter 3 .....	29
3. Synthetic procedures .....	29
3.1 Reagents and chemicals .....	29
3.2 Instrumentation .....	29
3.3 Chromatographic techniques .....	30
3.4 General Synthetic Procedure .....	30
3.4.1 7-Hydroxy-3-methyl-2H-1-benzopyran-2-one (SM1).....	31
3.4.2 3-Methyl-7-(2-phenylethoxy)-2H-1-benzopyran-2-one (SM2A).....	31
3.4.3 3-Methyl-2-oxo-2H-1-benzopyran-7-yl-diethylcarbamate (SM2B).....	32
3.4.4 3-(Bromomethyl)-7-(2-phenylethoxy)-2H-1-benzopyran-2-one (SM3A).....	32
3.4.5 3-(Bromomethyl)-2-oxo-2H-1-benzopyran-7-yl diethylcarbamate (SM3B).....	33
3.4.6 7-(2-Phenylethoxy)-3-[[prop-2-yn-1-yl]amino]methyl}-2H-1-benzopyran-2-one (SM4A).....	33
3.4.7 2-Oxo-3-[[prop-2-yn-1-yl]amino]methyl}-2H-1-benzopyran-7-yl diethylcarbamate (SM5A).....	34
3.5 Challenges and optimisation of synthesis.....	34
3.6 Conclusion .....	35
Chapter 4.....	36
4. Biological Evaluation.....	36
4.1 Introduction.....	36
4.2 Cholinesterases activity.....	36
4.2.1 Consumables and instrumentation.....	36
4.2.2 Experimental procedures .....	36
4.2.3 AChE assay results and discussion.....	37
4.2.3.1 Molecular Modelling of AChE.....	39
4.2.3.1.1 Molecular Modelling Methods .....	39
4.2.4 BuChE assay results and discussion .....	41
4.3 MAO Assay .....	43
4.3.1 Consumables and instrumentation.....	43
4.3.2 Experimental procedures .....	43
4.3.3 Results and discussion .....	44
4.3.3.1 MAO-A.....	44
4.3.3.2 MAO-B.....	46

4.3.4 Molecular Modelling of MAO.....	49
4.3.4.1 Molecular modelling methods .....	49
4.3.4.2 Results .....	50
4.3.4.2.1 Series A .....	51
4.3.4.2.2 Series B.....	52
4.4 Cytotoxicity and neuroprotection studies.....	54
4.4.1 Cytotoxicity studies .....	54
4.4.1.1 Experimental procedures.....	55
4.4.1.2 Results and discussion .....	55
4.4.2 Neuroprotection .....	56
4.4.2.1 Experimental procedures.....	56
4.4.2.2 Results and discussion .....	57
4.5 Conclusion .....	58
Chapter 5 .....	59
5.1 Introduction.....	59
5.2 Synthesis .....	59
5.3 Biological Evaluation .....	60
5.4 Conclusion .....	62
References.....	63
<b>Annexure: Spectral Data .....</b>	<b>77</b>



# Chapter 1

## 1. Introduction

### 1.1 Background

Alzheimer's Disease (AD) is a neurodegenerative disease associated with dementia, gradual loss of memory and cognitive skills; ending up in impaired judgment, visuospatial dysfunction, and other Parkinsonian-like symptoms. The disease progresses over an average period of 8 to 10 years leading up to the eventual death of the patient (Bird, 2015).

AD is the leading cause of dementia and fourth leading cause of death in the elderly, with approximately 7 million people worldwide diagnosed with as of 2018 (Alzheimer's Association, 2019). Worldwide the incidence of related dementias has increased by 118 % since 1990 and their prevalence in Africa, particularly Sub-Saharan Africa, can be expected to follow a similar trend to the improved life expectancy of the region (Nichols, *et al.*, 2019). Due to its slow onset and the nature of the disease, AD is associated with great direct and indirect cost which is felt across patients, caregivers and the healthcare systems. AD therefore affects a much larger population than those simply diagnosed with the disease (Allegri, 2006).

AD is characterized by cell death and subsequent loss of neurons localised in the forebrain (Niikura, *et al.*, 2006). The pathophysiology of AD is complex and multifactorial, and researchers have proposed a variety of mechanisms which contribute to the disease state (Swerdlow, 2007) (Figure 1.1).

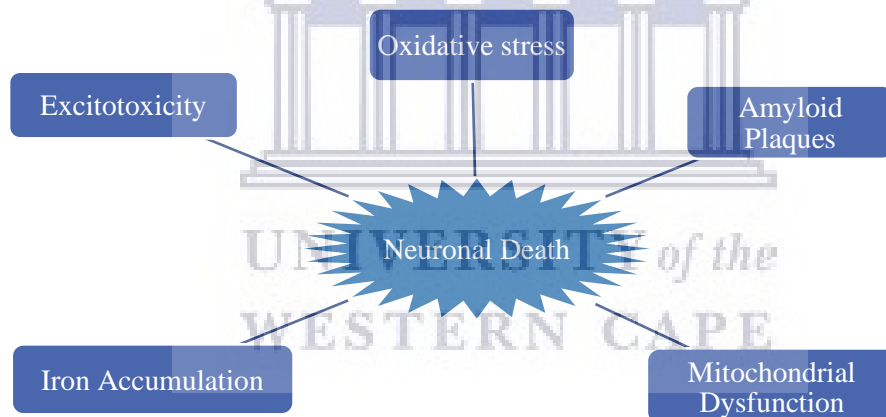


**Figure 1.1:** Mechanisms which contribute to neuron death in AD (Ferrante, 2016).

In spite of these known mechanisms, the underlying cause of this degeneration is not well understood, though genetic and environmental factors play a role as risk factors towards the development of AD. There is no cure for AD and the drugs used in healthcare worldwide offer only symptomatic relief and are not universally efficacious across all patients (Lanctôt, *et al.*, 2009). The main problem with these agents is that they act only at one target. These drugs include the cholinesterase inhibitors (rivastigmine, galantamine and donepezil) as well as an *N*-methyl-D-aspartate receptor antagonist (memantine) (Yiannopoulou & Papageorgiou, 2012). Due to the multifactorial nature of AD, recent research has proposed that the best approach is the use of multitarget directed ligands (MTDLs). MTDLs are single molecules which have the ability to act on multiple targets at pharmacologically effective levels (Figure 1.2) (Cavalli, *et al.*, 2008). Utilizing MTDLs avoids the polypharmacy approach used in other multifactorial diseases such as HIV therapy, wherein a combination of drugs acting on different targets are administered concurrently (Talevi, 2015). Administration of a ‘cocktail’ of drugs in this manner

often has a number of drawbacks due to potential issues with drug-drug interactions, multiplied toxicities and worsened side effect profiles. This disadvantageous nature of polypharmacy is especially undesirable for AD treatment, due to the fact that the majority of patients are elderly and may not be able to tolerate these adverse effects well (Van der Schyf, 2011). In the case of AD, due to its multifactorial nature, there are a number of hypothesis which provide us with potential disease pathways to target.

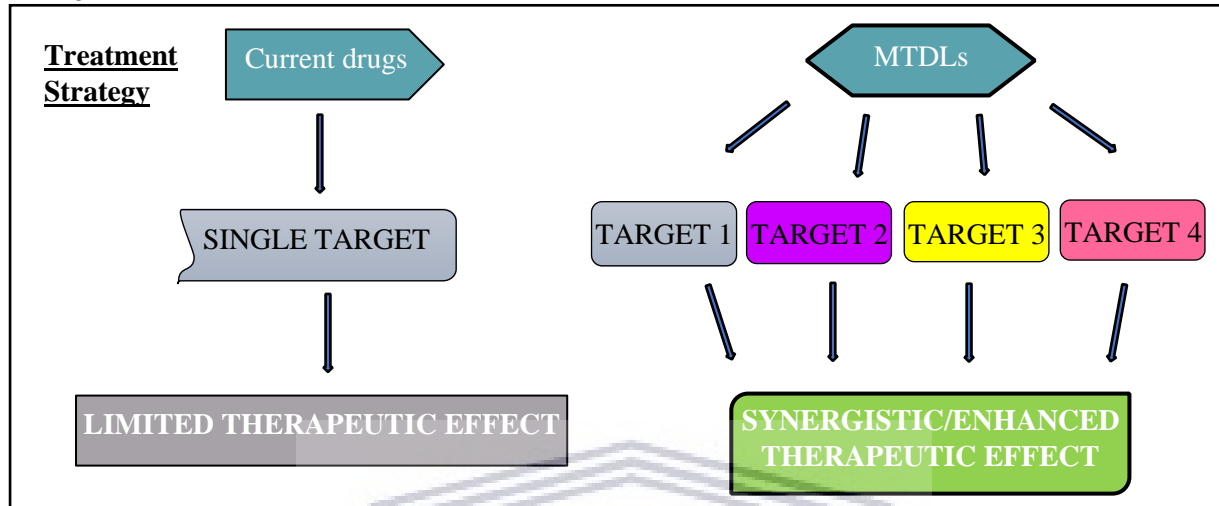


**Figure 1. 2:** Current single target therapy vs the MTDL paradigm.

## 1.2 Rationale

With over a hundred years having passed since Alzheimer's Disease was clinically defined, the disease continues to be a focus of research. With the growing elderly population of the world, addressing the shortfalls in its treatment needs to be prioritised. Though there is limited knowledge on its pathology, the presence of biomarkers such as fibrillary tangles, amyloid plaques and other hallmark signs of the disease pathology have guided treatment research (Blennow, *et al.*, 2015).

The current treatment strategy has been constructed around the role of the cholinergic neurotransmitter system and is termed as the "cholinergic hypothesis" (Terry & Buccafusco, 2003). This hypothesis centres on the fact that the cholinergic neurotransmitter system plays an important role in cognitive processes, with cholinergic neurons playing a key role in memory and learning. Due to its important role in cognition, researchers have found the cholinergic system implicit in many forms of dementia including AD. The main neurotransmitter facilitating impulse transmission is acetylcholine (ACh), whose action is terminated when it is hydrolysed by the cholinesterase enzymes (Greig, *et al.*, 2013). These enzymes are acetylcholinesterase (AChE) (responsible for  $\approx 80\%$  of hydrolytic activity) and butyrylcholinesterase (BuChE) which plays a backup role in hydrolysis.

In AD, significant alterations occur to these various components of the neurotransmitter system. Namely, there is a decrease in ACh synthesis and reuptake as well as a simultaneous increase in the catalytic activity of AChE, cumulatively resulting in lower levels of ACh in synapses and the brain (Schliebs & Arendt, 2006). These changes occur concurrently with the appearance of cognitive impairment and other early symptoms of AD. In addition to playing a role in the observed clinical symptoms of AD, research has found that the AChE enzyme itself has a role in disease progression. This disease progression has been linked to the peripheral anionic site (PAS) of the enzyme, a region of amino acids situated near the entrance cavity to the enzymes' active site (Bourne, 2003). The primary role of the PAS is identifying and trapping various substrates at the enzymes' entrance, however in AD it has been demonstrated to interact and form complexes with amyloid residues (Carvajal & Inestrosa,

2011). These complexes promote the formation of toxic amyloid fibrils and neurotoxic plaques resulting in amyloidosis, tau pathologies and consequently neurodegeneration (Bartus, *et al.*, 1982; Rinne, 2003). The primary therapeutic approach has been to counter cholinergic depletion using acetylcholinesterase inhibitors (AChEIs) and this has thus far been done by using the 2<sup>nd</sup> generation AChEIs such as donepezil, galantamine and rivastigmine. The clinical application of these agents has demonstrated that cholinesterase inhibition leads to modest improvement in cognitive functions, decreased  $\beta$ -amyloid deposition and slowing down the progression of the disease (Linton, 2005). Despite limited therapeutic efficacy, cholinergic inhibition remains an important target due to the cholinergic system's link with AD. To take full advantage of cholinergic inhibition, the goal is to develop agents capable of inhibiting both AChE and BuChE (to ensure there is no back-up hydrolysis of ACh), which also target other contributing factors of the disease outside of this hypothesis.

Monoamine oxidase (MAO) is a biochemically important mitochondrially bound enzyme, existing as two isoforms; MAO-A and MAO-B. The enzymes are distributed throughout the body and modulate the concentration of many biogenic and exogenic amines in peripheral and central nervous system (CNS) tissues. The enzymes are known to metabolize a wide range of substrates including the neurotransmitters serotonin, dopamine and phenylethylamine (Tong, *et al.*, 2013).

During this catalytic breakdown MAO-B produces free radicals, reactive oxygen species and  $H_2O_2$  in the brain. This produces a cascade of effects leading to oxidative stress, neuroinflammation and  $A\beta$  plaque formation; consequently triggering neurodegeneration (Riederer, 2004). MAO-B activity typically increases with age and consequently has been found implicit in other age-related neurodegenerative diseases such as Parkinson's Disease (PD). Similarly, studies have demonstrated a correlation between the increased activity of this enzyme in the AD state and the progression of the disease (Schedin-Weiss, *et al.*, 2017). Inhibition of MAO-B logically has arisen as a viable strategy to combat AD, as it prevents the formation of toxic by-products and triggering of apoptosis. When used in PD and other neurodegenerative diseases MAO-B inhibitors such as selegiline and rasagiline (Figure 1.3) have displayed additional neuroprotective capabilities independent to their enzyme inhibition (Riederer, 2004; Cai, 2014). Patients in long term treatment with these MAO-B inhibitors show improvements in their memory retention and impedes disease progression (Weinreb, *et al.*, 2010).

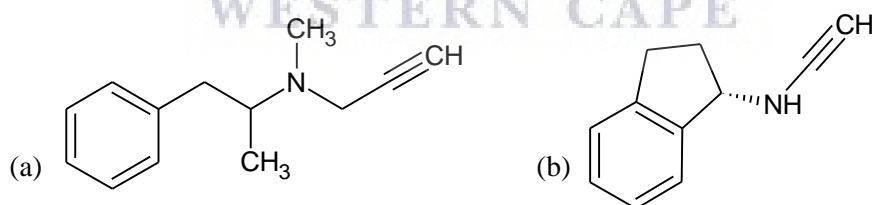


**Figure 1. 3:** MAO inhibitors (a) selegiline and (b) rasagiline.

It is important when dealing with MAO inhibition in AD for potential drug molecules to possess selectivity towards MAO-B, because it is the predominant isoform found in the brain. Furthermore, irreversible inhibition of both MAO isoforms is undesirable as it may lead to an induced hypertensive crisis occurring when patients consume tyramine-rich foodstuffs such as cheese (Finberg & Gillman, 2011).

### 1.2.1 Coumarin

Coumarins are a group of polyphenolic compounds composed out of a benzene ring fused to a pyrone ring. Coumarins have been shown to display a wide array of biological activities and is the key moiety in a range of current and potential drug molecules with uses ranging from anticoagulant, anticancer to

antiviral amongst others (Wu, *et al.*, 2009; Jain & Joshi, 2012). Coumarin derivatives (Figure 1.4) have interested researchers for application in neurodegenerative diseases as they display antioxidant activity, MAO and cholinesterase inhibition and decrease neuroinflammation (Orhan & Gulcan, 2015). Thus, they serve as a good starting point for an MTDL with MAO-B and cholinesterase inhibitory activities, especially because of ease of functionalisation at different positions on the coumarin moiety (Stefanachi, *et al.*, 2018).

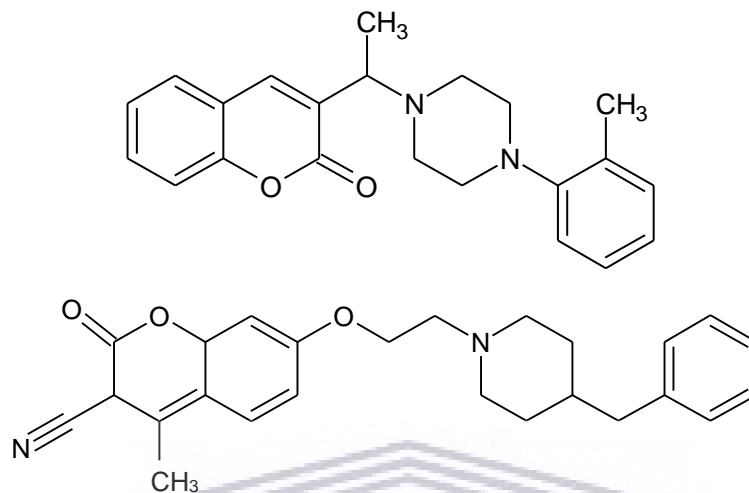


**Figure 1.4:** Examples of promising coumarin based MTDLs for use in Alzheimer's Disease (Joubert, *et al.*, 2017; Abdshahzadeh, *et al.*, 2019).

Several coumarin derivatives have been developed as cholinesterase inhibitors. The scaffold's planar shape and aromatic region impart an affinity towards forming favourable  $\pi$ - $\pi$  interactions with amino acids at the PAS of the enzyme. The molecules thus sterically block the entrance of the enzyme, preventing substrates from reaching the enzyme's catalytic anionic site (CAS) where hydrolysis takes place (Radić & Taylor, 2001). Researchers have found that the best modifications to improve inhibitory activity of the scaffold are the elongation of the molecule (via the addition of a spacer) and substitution of a small moiety capable of forming interactions with the CAS of the enzyme (Yusufzai, *et al.*, 2018). Such modifications would produce a "dual site" binding molecule, capable of simultaneously interacting with the CAS and PAS. The advantage of such compounds, in addition to enhanced inhibitory activity, is that they may prevent the formation of amyloid complexes which occurs at the PAS (Pietsch, *et al.*, 2009). This prevents amyloid aggregation, which is crucial towards slowing down of the disease progression. To achieve these favourable interactions and increased enzyme inhibition, substitutions at position 3 and 7 of the coumarin scaffold have been found as most beneficial (Soto-Ortega, *et al.*, 2011; Farina, *et al.*, 2015).

The design strategy was thus to design two different series of compounds differentiated by the respective substitutions at positions 3 and 7 of the scaffold (Figure 1.5).

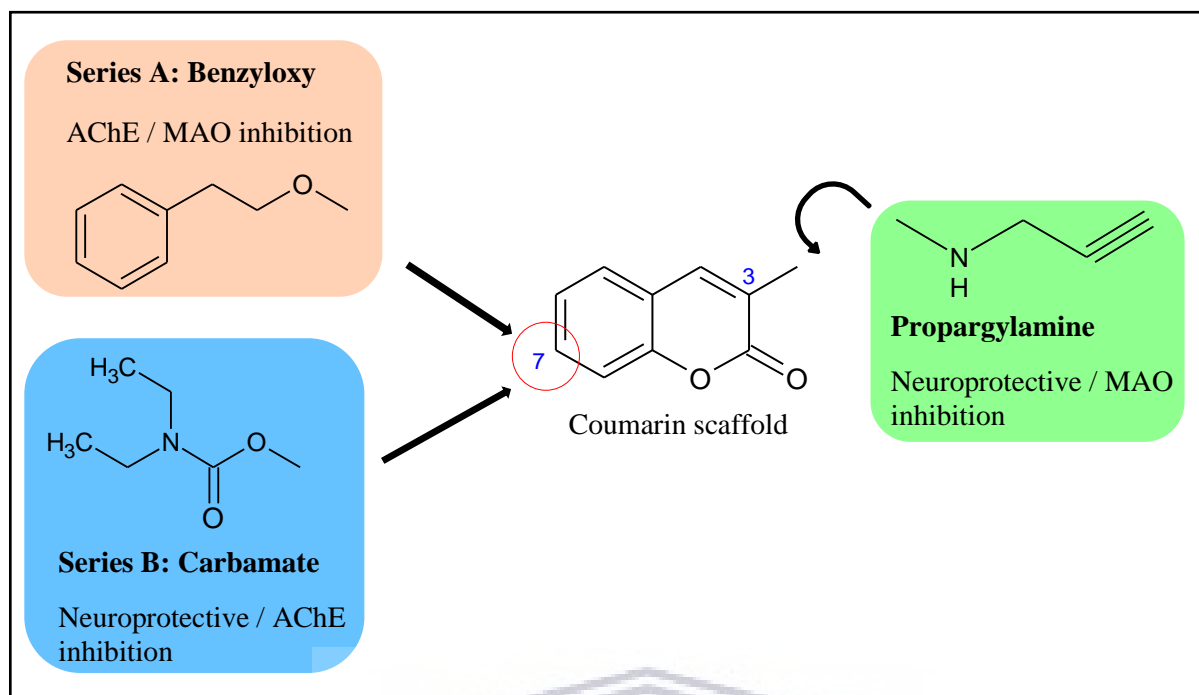


**Figure 1.5:** Design strategy of coumarin derivatives in this study.

### 1.2.2 Series A Benzyloxy

According to studies done by Bruhlmann *et al* (2001) and Foka *et al* (2018) the benzyloxy moiety has been found to form favourable  $\pi$ - $\pi$  interactions in the catalytic site of the cholinesterases. Furthermore, when the moiety was incorporated into substituted coumarin derivatives (Figure 1.6) it was found to confer increased selectivity and inhibitory capacity towards MAO-B. This is the result of the moiety orienting towards the flavin adenine dinucleotide (FAD) co-factor in the active site, which is essential for enzyme function (Pérez V., *et al.*, 1999). In this study, to optimise the final compound's activity towards the enzyme targets, the moiety was attached to the coumarin scaffold via a two carbon linker. This was done to ensure that the designed compounds are sufficiently long to interact with both the CAS and PAS of the AChE enzyme whilst maintaining MAO-B binding interactions by fitting in its active site (Catto, *et al.*, 2006).

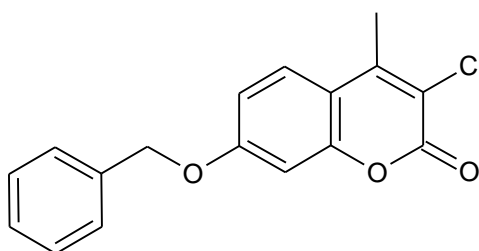


**Figure 1.6:** Structure of the benzyloxy containing compound 3 developed by Foka *et al* (2018).

### 1.2.3 Series B Carbamate

The carbamate moiety is derived from one of the AChE inhibitors on the market, rivastigmine. Numerous studies have found that it confers significant cholinesterase inhibitory effect into various molecules which incorporate it (Denya, *et al.*, 2018; Bak, *et al.*, 2019). The moiety forms moderately stable covalent bonds with the serine residue in the cholinesterase active site. The result of this is that its mechanism of inhibition is reversible, as the bond formed is susceptible to spontaneous hydrolysis,

thus restoring the enzymes catalytic ability (Darvesh *et al.*, 2008; Bak, *et al.*, 2019). Reversible inhibition is desirable as it decreases the chances of acute toxicities occurring (such as cholinergic poisoning) as seen with irreversible cholinergic inhibitors (Colovic, *et al.*, 2013). Consequently, several MTDLs are in development for AD which incorporate the carbamate moiety in their structures, the most prominent of these being ladostigil (Figure 1.7). Having undergone phase II clinical trials, this promising drug displays potent AChE/MAO inhibition as well as neurorestorative properties (Schneider, *et al.*, 2019).

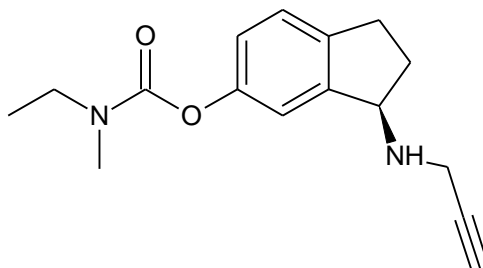


**Figure 1.7:** The structure of ladostigil, a promising MTDL containing a carbamate and propargylamine moiety.

### 1.2.4 Propargylamine

The propargylamine functional moiety has accumulated interest in recent years which came to the forefront in its use in the MAO inhibitors, selegiline and rasagiline. The moiety has been found to form interactions with the FAD cofactor of the enzyme which is vital for the functioning of the enzyme and thus leads to potent inhibition (Zindo, *et al.*, 2015). Independently of this MAO inhibition, the moiety has been able to confer a number of properties pertinent for neuroprotective agents. These include antiapoptosis, inhibiting A $\beta$  aggregation and mitochondrial protection, leading to protection and rescuing of damaged neurons (Naoui, *et al.*, 2003). The incorporation of this moiety should therefore enhance the pharmacological profile of the 7-substituted coumarins. Additionally, to observe the effect of the propargylamine with respect to enzyme inhibition and neuroprotection we will test and compare the intermediate compounds which contain the -CH<sub>3</sub> and -CH<sub>2</sub>Br substituents at position 3.

### 1.3 Aim

The aims of this research are to design, synthesize and evaluate a series of novel compounds for use as potential multitarget directed drug ligands for Alzheimer's Disease treatment. In addition to this, the study aims to expand on the knowledge of how the incorporation of known moieties affects the coumarin scaffolds' ability to act as an AChE and MAO inhibitor. In order to assess the effect of the various substitutions on this capacity, a total of seven compounds will be synthesised and evaluated

- Compound SM1 will serve as the starting coumarin from which modifications will be made;
- Compounds SM2A, SM2B, SM3A and SM3B which are intermediate compounds containing either the benzyloxy or carbamate moiety at position 7;
- Compounds SM4A and SM5A, which contain the propargylamine moiety attached to position 3 in addition to the substitutions at position 7.

To achieve these aims the following objectives have been set for this study:

- To design and synthesise a series of multifunctional compounds based on the (a) benzyloxy and (b) carbamate moieties conjugated at position 7 to various 3-substituted coumarin scaffolds;
- Structural elucidation of the synthesised compounds using analytical techniques such as nuclear magnetic resonance spectroscopy (NMR), infrared and mass spectrometry;



- In vitro evaluation of the synthesized compounds for cholinesterase and MAO inhibitory activity;
- Evaluation of the compounds for neuronal cell viability and anti-apoptotic activity;
- Molecular modelling experiment using docking software to analyze and elaborate on binding interactions and elucidate structure activity relationships.

#### 1.4 Conclusion

Alzheimer's disease is currently a leading cause of death in the elderly population, which has a great effect on society due to the debilitating nature of its symptoms and prolonged disease onset. With the increasing age expectancy, it is absolutely pertinent to address the current lack of effective and disease modifying treatment options. MTDLs offer a promising alternative treatment option and the coumarin scaffold serves as a good starting point to develop such agents (Figure 1.8).

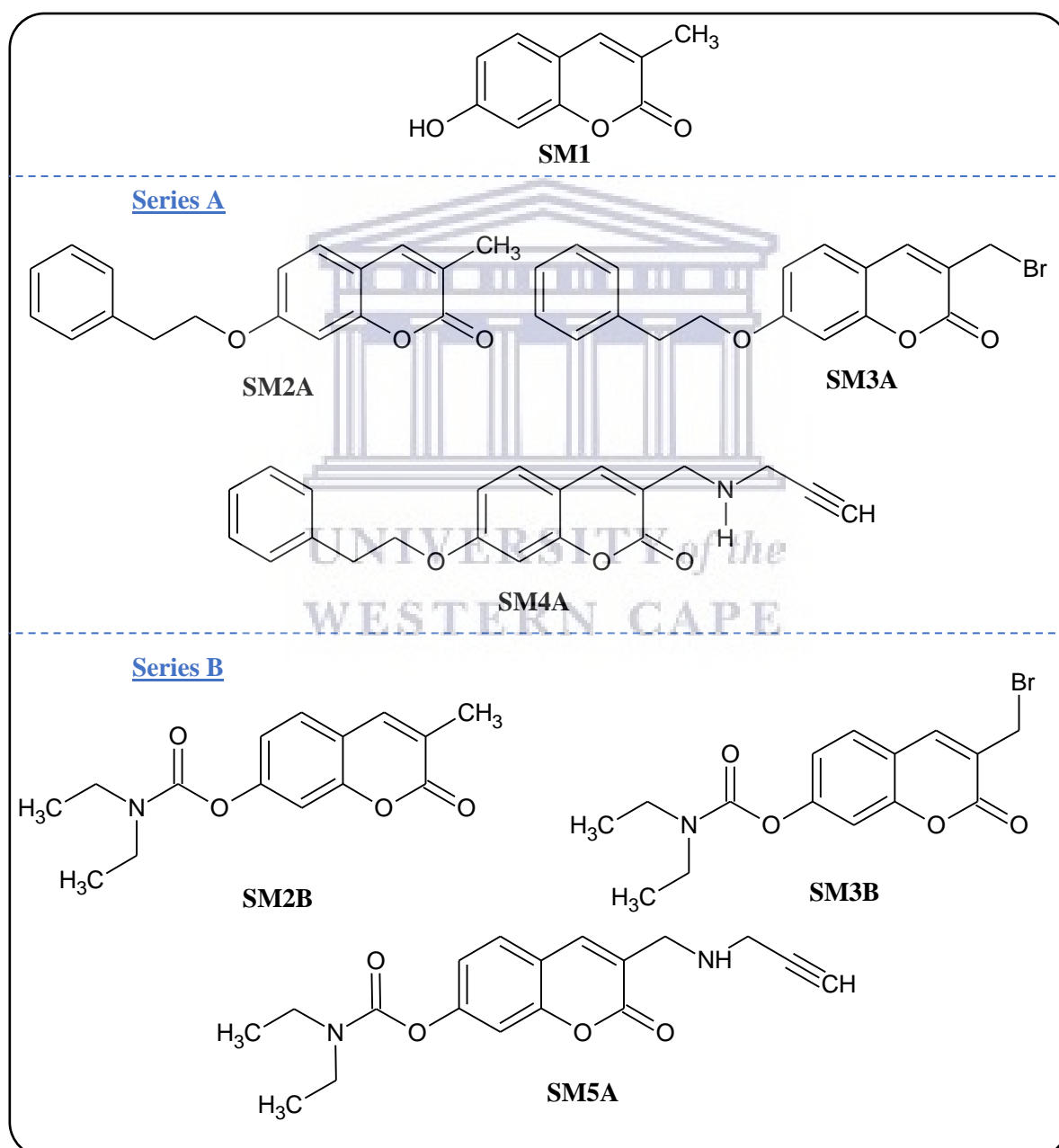


**Figure 1.8:** Proposed series of compounds for synthesis and biological evaluation.

This study aims to explore the synthesise novel coumarin derivatives which can act to inhibit the cholinesterase and MAO enzymes and thus stop or slow down the neurodegenerative process. These molecules will have the potential to relieve the symptoms of AD and slow down disease progression and thus overall reduce the burden of the disease.



UNIVERSITY *of the*  
WESTERN CAPE

## Chapter 2

### 2. Literature Review

#### 2.1 Introduction

This chapter will provide an overview on the background regarding the nature, origin and impact of Alzheimer's disease. The strategies that are being implemented with regards to treatment of the disease and prospective treatment strategies will be explored as well.

#### 2.2 Neurodegenerative Diseases

Neurodegenerative diseases (ND) is an umbrella term used to group diseases which originate from the deterioration of neurons in the brain, leading to various cognitive and movement related disabilities and disorders (Vajda, 2004). There are over 600 conditions classified as NDs and the most prominent of these include Parkinson's disease, multiple sclerosis, Alzheimer's disease and Huntington's disease. Each type of disease has been shown to have unique degenerative patterns affecting specific networks and regions of the CNS (Seeley, 2009). Currently there are no treatments to cure NDs and only symptomatic treatments are available. Even though researchers have discovered and explored multiple mechanisms leading to cell death it has been difficult finding solutions to combat these mechanisms, slow down and reverse degeneration (Van der Schyf, 2011).

The main mechanisms by which neurodegeneration takes place are oxidative stress, mitochondrial dysfunction, inflammation and proteopathy. Proteopathy in NDs centres on the aggregation and deposition of misfolded proteins, with the different diseases arising based on the aggregations pattern, whether it is intra- or extracellular and the composition of causative proteins. In the majority of NDs these proteins are either amyloid beta (A $\beta$ ), Tau or  $\alpha$ -synuclein (Skovronsky, 2006). NDs are typically late onset diseases with increasing prevalence and risk above the age of 60. Ageing is NDs greatest risk factor because with the accumulative effect of DNA mutations, oxidative stress and altered metabolism coupled with the impaired ability for self-repair, it is more likely for the biochemical cascade of events leading to cell death (Daniele, *et al.*, 2018). Exposure to environmental pollutants, particularly heavy metals (such as arsenic, lead, mercury), and some pesticides are also thought to be involved in NDs as they are associated with increased deposition of A $\beta$  peptides and phosphorylation of tau proteins (Chin-Chan, *et al.*, 2015).

The most prevalent ND is Alzheimer's Disease (making up to 60-80% of all NDs) followed by Parkinson's disease, although problems in diagnosis (particularly of dementias) may mean these figures are higher. The burden of these diseases is set to increase with the increase in life expectancy of the world's population and growing population of those aged 65 and above (Erkkinen & Mee-Ohk, 2017). NDs that affect motor functions are set to overtake cancer as the second most prevalent cause of death in adults. Thus, the need for research in treatment is urgent now more than ever (Durães & Pinto, 2018).

#### 2.3 Alzheimer's Disease

Alzheimer's disease (AD) was first classified by Dr Alois Alzheimer in Germany in 1906. As mentioned earlier, AD is the most prevalent ND and the most commonly occurring form of dementia, accounting for about 70% of cases. It is a chronic illness with gradual onset which is irreversible and incurable (Takeda, 2019). The typical progression of the disease occurs over 8 to 10 years and the disease progresses in four stages, namely; mild impairment, mild AD, moderate AD and severe AD (Figure 2.1).

The symptoms for AD, especially in its nascent stages, are often mistaken for old age as the patient initially presents as having difficulties in higher cognitive functions such as planning, but the hallmark symptom for early stage Alzheimer's is short term memory loss. From there the patients' cognitive functions start worsening, experiencing difficulty remembering recent events, speech difficulties which progresses to confusion and loss in reading and writing skills. Once the disease progresses to moderate AD the patient experiences behavioural and personality changes, mood swings and neglects hygiene and eating. When the disease is at its advanced stage the individual is now completely dependent on caretakers for support with worsening of cognitive functions and movement leading to them being bed bound (Lyketsos, *et al.*, 2011). Often this neurodegeneration can spread to other key areas in the brain, that may lead to a change in breathing and swallowing behaviour, leading to difficulty in eating and a higher risk of lung infections (Brunnström & Englund, 2009). While it is difficult to attribute death directly being caused by AD, death occurs due to complications arising from external factors such as malnutrition, deep vein thrombosis, infections and decreased cognitive functions of the patient (Bird, 2015; Apostolova, 2016).

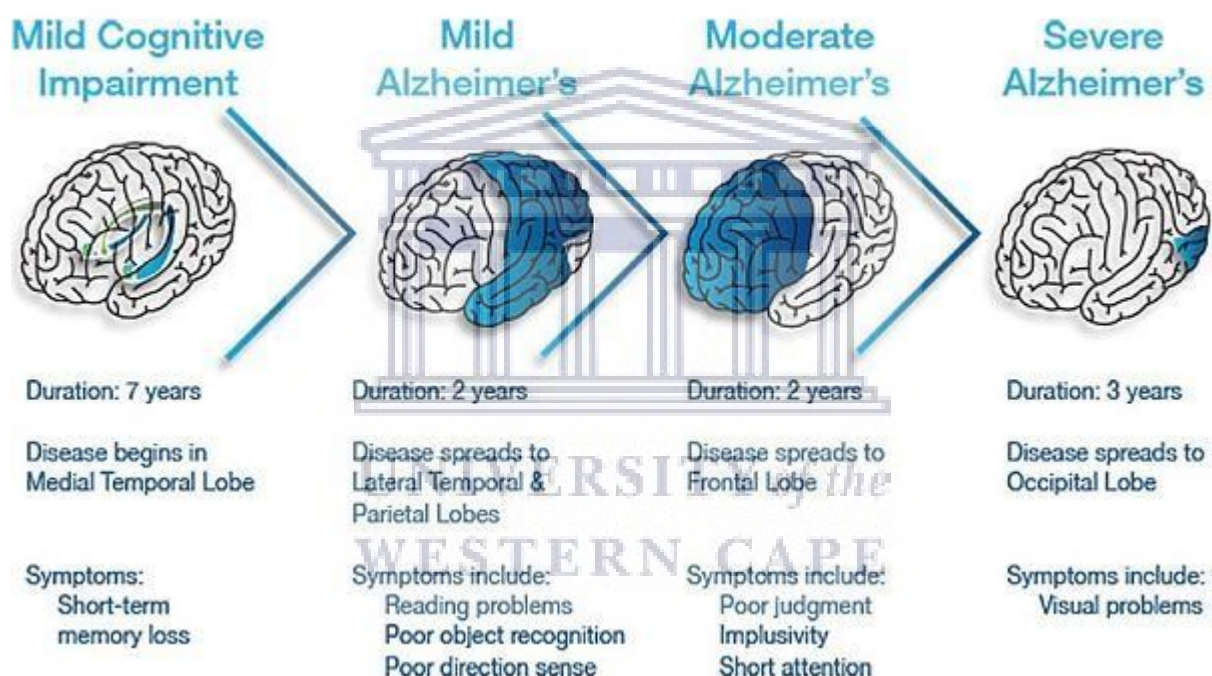


**Figure 2.1:** Progression of Alzheimer's Disease in a typical patient. (East, 2017).

### 2.3.1 Burden of the disease

Around 30-45 million people worldwide are thought to have AD and as mentioned before, this figure may be higher as less than half of the patients with AD are diagnosed. In South Africa, as of 2011, 2.2 million patients were diagnosed with related dementias and as with other NDs this number is set to increase greatly with a global total of 101 million patients predicted to have AD by 2050 (de Jager *et al.*, 2017; Alzheimer's Association, 2019).

The impact of AD also extends to the families and caregivers of the patients due to its prolonged onset. In majority of cases it is reported that the families of the patients often have to become the primary caregivers and as most are not trained to do so, are unable to give the patient the specialised care they require (Kasper *et al.*, 2015). Additionally, as they are not professionals this has led to the majority of these family members experiencing adverse effects ranging from physical, psychological and

economical. This impact is felt especially in low to middle income households where professional care cannot be afforded on top of the high medical costs incurred by the patient (Adams, 2007).

### 2.3.1 Aetiology and pathophysiology

AD is typically diagnosed through a combination of observations of the clinical symptoms with neuroimaging, neuropathological findings and cerebrospinal fluid analysis. The presence of A $\beta$  plaques and neurofibrillary tangles serve as the biomarkers observed for confirmation of AD (Snider, *et al.*, 2009). AD has no known underlying cause, although studies have hypothesised that the disease is primarily familial for both early onset and late onset AD with genetic factors playing an important role in the underlying aetiology. Regardless, the initial causes of the neurodegeneration are not well understood (Gatz, *et al.*, 2006).

There are two main forms of AD:

1) Sporadic AD ( $\approx$  90% of cases):

This has no known trigger although it is associated with certain risk factors such as a history of head trauma, type II diabetes, ischaemia and environmental factors e.g. drinking water with aluminium.

2) Familial AD ( $\approx$  10% of cases):

Stems from genetic mutations and proceeds faster than sporadic AD (Dorszewska, *et al.*, 2016).

Alzheimer's disease has long posed a challenge to researchers due to its complex nature and multiple interlinked aetiologies. Though not well understood, several hypotheses have been proposed based on the characteristic hallmarks; extensive loss of neurons, the presence of amyloid- $\beta$  deposits (plaques) and neurofibrillary tangles.

#### 2.3.1.1 Amyloid hypothesis

Amyloid  $\beta$  peptides are amino acid peptide residues comprised of 37 – 49 amino acids formed when the amyloid precursor protein (APP) is cleaved by  $\beta$  or  $\gamma$  secretase. APP is thought to have an important role within neural tissue; aiding in synaptic formation, intracellular transport and other homeostatic activities. A $\beta$  peptides are seen to play a role in protection and repair in the CNS, being involved in recovery from traumatic brain injury and plugging leaks in the blood brain barrier (Brothers, *et al.*, 2018). Under normal conditions, a steady state exists where production and clearance of A $\beta$  is such that it is maintained at a constant level. However, as you age there is a dysregulation in this state as the two major enzymes, neprilysin (NEP) and insulin degrading enzyme (also known as insulin-degrading enzyme; IDE), which are believed to be responsible for most A $\beta$  degradation have decreased activity. In rarer cases mutations lead to increased production of the APP (observed in the case for development of familial AD) (Paul Murphy & Levine, 2010).

As individual A $\beta$  monomers amass they form oligomers/fibrils ( $\beta$  sheet configuration) which are insoluble and as these aggregate they form plaques. The longer residues of A $\beta$  particularly A $\beta$ <sub>42</sub> are hydrophobic and prone to forming these deposits (Paul Murphy & Levine, 2010). Normally as build-up occurs microglia ingest and destroy these plaques. However, in the disease state the deposition and formation of these plaques overwhelm the ability of the microglia to act allowing the formation of large insoluble plaques (Edwards, 2019). The build-up and increased amount of these so called senile plaques are one of the classic biomarkers for AD. The amyloid cascade is the leading hypothesis for the development of AD (Chen, 2017).

### 2.3.1.2 Amyloid Cascade

As A $\beta$  builds up outside neurons, the oligomers proceed to bind to a number of receptors in the CNS (Figure 2.2) such as the  $\alpha 7$  nicotinic acetylcholine receptor and metabotropic glutamate receptors (mGluR5) among others. This leads to numerous neurotoxic effects downstream.

Of interest is the direct activation of N-methyl-D-aspartic acid receptor (NMDAR), a calcium ion channel receptor. A $\beta$  oligomers bind to the extracellular subunits of the receptor to directly activate it, causing a disruption in the regulation of Ca<sup>2+</sup> ions (Texidó, *et al.*, 2011). The resulting influx of ions causes oxidative damage as mitochondria produce reactive oxygen species, including NO and other oxidated species such as oxidated proteins and peroxidated lipids. Oxidated species cause harm directly to the cell membrane and the cumulative oxidative stress which results causes synaptic dysfunction and cell death (Alberdi *et al.*, 2010).

Intracellularly, A $\beta$  triggers the hyperphosphorylation of tau (an important protein involved microtubule assembly) and these tau proteins aggregate and form neurofibrillary tangles (NFTs). As this occurs the structure and function of microtubules is compromised and may lead to cell death (Spires-Jones, *et al.*, 2009). While the build-up of NFTs is associated with increased neuron loss, it is debated whether they are directly involved in cell death or have another function in damaged neurons. Regardless, the presence of phosphorylated tau and NFTs in the CSF has long been regarded as classic biomarkers used to identify and diagnose AD, though their appearance is delayed after prolonged period of A $\beta$  deposition (Blennow & Zetterberg, 2018).

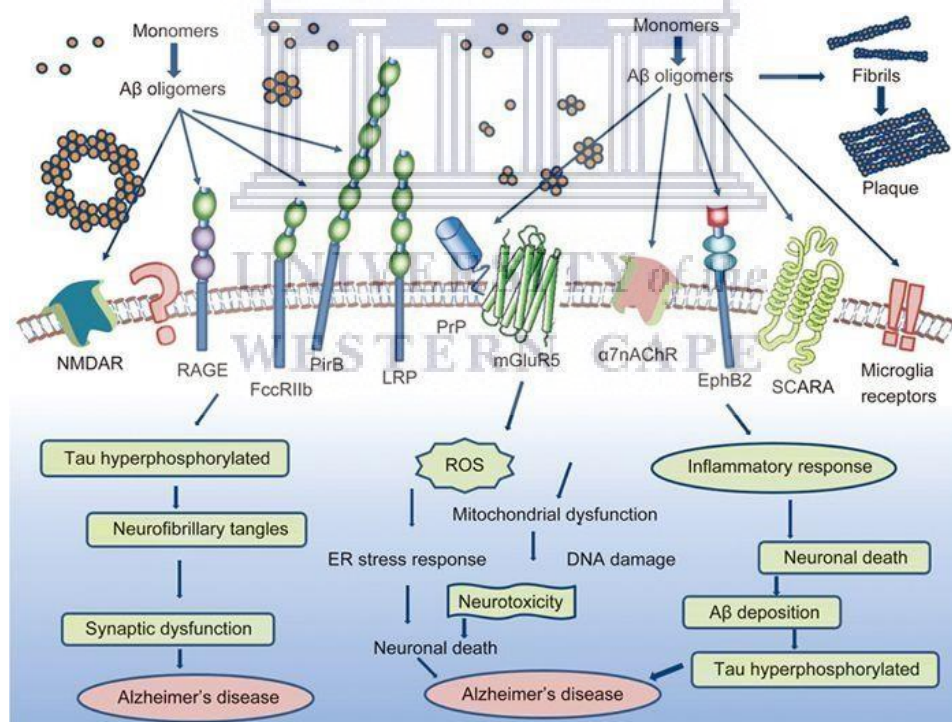


**Figure 2.2:** Amyloid  $\beta$  can interact with several receptors and stimulate pathways which hyperphosphorylate tau proteins, produce reactive oxygen species and cause inflammatory reactions downstream. These can lead to neurotoxicity and neurodegeneration (Chen, 2017).

In addition to the aforementioned effects of A $\beta$ , an inflammatory response also occurs as plaques and oligomers form. Certain amino acid residues such as A $\beta_{42}$  activate surrounding microglia by binding onto membrane receptors. This has the two-fold effect of:

- Causing neural cell death by direct phagocytosis of affected cells.
- The release of immunomodulators and cytokines which activate the cells apoptotic pathway leading to cell death.

This inflammatory response further causes release and production of A $\beta$  peptides and thus the process proliferates further as inflammation becomes chronic (Yuan & Grutzendler, 2016; Spangenberg, *et al.*, 2016). There can be multiple points of damage along an axon. As deposition of A $\beta$  occurs and the affected neuron proceeds to degenerate, the neurotoxic conditions spread to other associated neurons as A $\beta$  oligomers and hyperphosphorylated tau are transported via exocytosis. Over time the neural network is disrupted further and further (Michel, *et al.*, 2013). As loss of neurons is localised mainly in the basal ganglia, temporal lobe and neocortex, memory and cognitive functions are affected.

Familial AD has been the type of AD which is most easily attributed to the amyloid cascade. This is because patients of familial AD have genetic mutations on genes either coding for APP or presenilin 1 (PSEN-1) and 2 (PSEN-2), which lead to amyloidosis (Tanzi & Bertram, 2005). PSEN-1 and PSEN2 are proteins which form the catalytic subunit of  $\gamma$ -secretase, and when these proteins are misfolded they drive the enzyme towards producing neurotoxic A $\beta_{42}$  rather than shorter residues following APP cleavage. In patients with APP mutations however, the most prevalent mutations are those which alter the C terminal of the protein which affect the enzymes cleavage efficiency and selectively in a way which leads to increased production of A $\beta_{42}$  (Xu, *et al.*, 2016). This overall observed increase in the A $\beta_{42}$  ratio is responsible for the early onset deposition of senile plaques (Cacquevel, *et al.*, 2012).

### 2.3.1.3 Cholinergic Hypothesis

Acetylcholine (ACh) (Figure 2.3) is the main neurotransmitter involved in the autonomic and somatic nervous system as well as cholinergic synapses in the CNS. Its main role in the body is stimulation of the parasympathetic nervous system in the heart, blood vessels in the eyes and other organs involved in the “rest and digest” response. In the CNS cholinergic neurons are present in many parts of the brain where their primary function is regulation of memory and learning, stress, wakefulness and cognitive functions (Hangya, *et al.*, 2015).

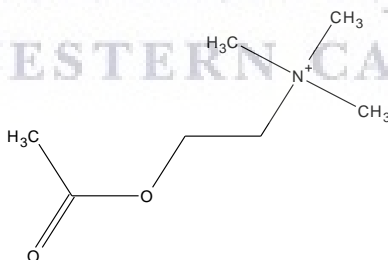


**Figure 2.3:** Structure of the neurotransmitter acetylcholine. The positive charge of the ammonium group plays a role in the recognition of the molecule by nicotinic receptors (Czajkowski, *et al.*, 1993)

ACh is synthesised by choline acetyltransferase (ChAT) from choline and acetyl-Co-A in the presynaptic neuron and stored in vesicles. To transmit a signal, ACh is released into the synapse via exocytosis where it binds to either a muscarinic receptor or nicotinic (ionic receptor). Once bound to a receptor, signal transmission is stopped when a cholinesterase enzyme inactivates the ACh by hydrolysing it, following which it is recycled back to ACh in the presynaptic neuron (Figure 2.4) (Prado, *et al.*, 2017).

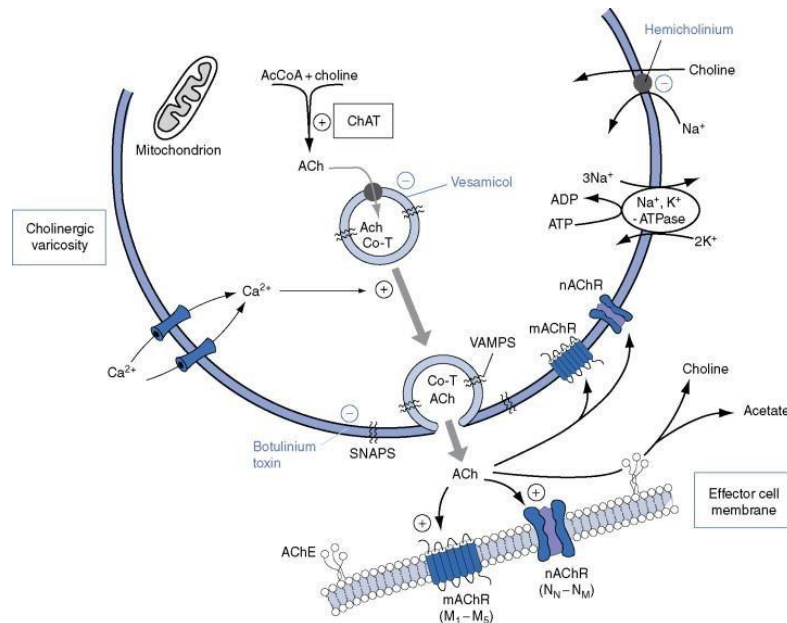


**Figure 2.4:** ChAT synthesises ACh from choline and acetyl CoA, which is then stored in vesicles with other co-transmitters. Ca<sup>2+</sup> voltage gated channels allow Ca<sup>2+</sup> to enter the cell, causing the vesicular membrane to fuse with the cellular membrane and release ACh into the synapse. Once released, ACh will act on muscarinic or nicotinic receptors until its action is terminated by AChE by metabolism back to choline and acetate (Westfall, 2009).

Davies & Maloney (1976) were the first to observe that in AD there is a loss of ChAT activity correlating to cognitive impairment. Bartus, *et al* (1982) further reported that loss of cholinergic activity is observed in the brains of AD patient. These observations gave birth to the cholinesterase hypothesis, which postulates that the symptoms present in AD (particularly decrease in cognition and memory) can be linked to decreased cholinergic function. This decrease in function is attributed to 4 main factors:

- Decreased ACh production due to suppression of ChAT activity in the AD brain (Bowen, *et al.*, 1976, Francis, 2005);
- Loss of a large number of nicotinic receptors (such as  $\alpha 7$  and  $\alpha 4\beta 2$ ) in postsynaptic membranes in the cerebral cortex (Burghaus, *et al.*, 2000);
- Increased activity of cholinesterases (García-Ayllón, *et al.*, 2010);
- Interaction with A $\beta$ ; as A $\beta$  has been shown to affect synthesis and release of ACh, inhibit nicotinic receptors, disrupt vesicular transport and directly damage cholinergic neurons in the basal forebrain (Auld, *et al.*, 1998; Ikeda, *et al.*, 2000).

The memory loss and decline in cognitive function can therefore be attributed to the decreased cholinergic function and concentrated loss of cholinergic neurons in the nucleus basalis of Meynert which is observed AD (Mufson, *et al.*, 2008). The cholinergic theory has long formed the backbone of currently approved AD treatment, with 4 out of the 5 drugs being cholinesterase inhibitors. The theory is further backed by the improvement in memory and cognition that occurs when cholinergic function is restored (Ferreira-Vieira, *et al.*, 2016).

### 2.3.1.3.1 Cholinesterases

The cholinesterases are a pair of enzymes that catalyses the hydrolysis of cholinergic neurotransmitters (mainly acetylcholine) into choline and acetate. They act primarily at the post synaptic neuron (post stimulation) to stop impulse transfer and return it back to its resting state (Giacobini, 2003). There are two kinds of cholinesterases which are differentiated according their structures and their preferred



substrates and kinetics; acetylcholinesterase (known as the “true cholinesterase”) and butyrylcholinesterase (known as pseudocholinesterase). AChE is found mainly in synapses and on red blood cell membranes whilst BuChE is found mainly in blood plasma glial cells and the liver. Both are 3-layer  $\alpha/\beta$  hydrolases with a hydrophobic active gorge sharing 65% of their amino acid sequence (Massoulié, 1980).

The cholinesterases exist in multiple forms:

- Asymmetric - with catalytic subunit attached to a collagen-like tail onto the extracellular matrix. This form occurs more in AChE than BuChE and is specifically expressed in muscles.
- Globular forms – comprised of either 1, 2 or 4 catalytic subunits (also known as the G1, G2 or G4 forms) which are membrane bound. In the brain, the G1 and G4 forms are the most common and are present in varying proportions to each other (Massoulié, 1980; Anglister, Haesaert, & McMahan, 1994).

BuChE is a tetrameric glycoprotein comprising of four subunits each consisting of 574 amino acids and weighing 85 kDa and is produced mainly in the liver. Its substrate selectivity is less specific than AChE's, being able to hydrolyse a wider array of neuroactive peptides (Johnson & Moore, 2012). As such it has other functions in addition to ACh hydrolysis:

- Detoxification – BuChE detoxifies inhaled/ingested poisons e.g. physostigmine and other organophosphates as well as some common drugs such as aspirin (to salicylic acid) and heroin (to morphine).
- Fat metabolism – BuChE's ability to metabolise fat was observed because BuChE deficiency is associated with decreased fat catabolism.
- Scavenging of polyproline rich peptides from cells - BuChE buries polyproline rich peptides into its structure to make them inaccessible for potential interactions with other proteins thereby protecting the cell from unregulated reactions (Lockridge, 2015).

Its primary substrate is butyrylcholine (BuCh) and plays a supportive/backup role to ACh hydrolysis. Kinetically BuChE differs from AChE by displaying substrate activation rather than substrate inhibition although it hydrolyses ACh with reduced efficiency compared to AChE (Chen, *et al.*, 2011).

The BuChE active subunit is a 20 Å deep gorge shaped polyproline rich peptide in the centre of a four helix bundle (Figure 2.5). This active site is larger ( $\approx 500$  Å vs 300 Å for AChE) and bowl shaped due to the presence of residues such as Leu 286 and Val 88 and other aliphatic amino acid residues. This allows for catalysis of bigger substrates such as organophosphates and cocaine (Saxena, *et al.*, 1999).

The active site of BuChE is made up of four regions:

- Peripheral anionic site (PAS)
- Acylation site
- Choline binding site (CAS)
- Acyl binding site

At the mouth of the gorge lies the PAS. Here, Asp 70 and Tyr 332 (which are H bonded) are involved in the initial binding of positive charged substances via  $\pi$  complex with Tyr 332 and the negative charged Asp 70. This triggers conformational change in the monomer as the  $\Omega$  loops come close and the substrate slides down to the Trp 82 binding site, which forms a cation- $\pi$  complex with the substrate (Çokuğraş, 2003).

The oxyanion hole (Gly 116, Gly 117, Ala 199) in the acylation site helps rotate the substrate to the correct orientation where it is hydrolysed by the catalytic triad of Ser 198, Glu 325 and His 438 which is situated at the bottom of the gorge. The catalytic triad catalyses the stabilised substrate site via a charge relay system (Zhang, Kua, & McCammon, 2002 ; Çokuğraş, 2003).

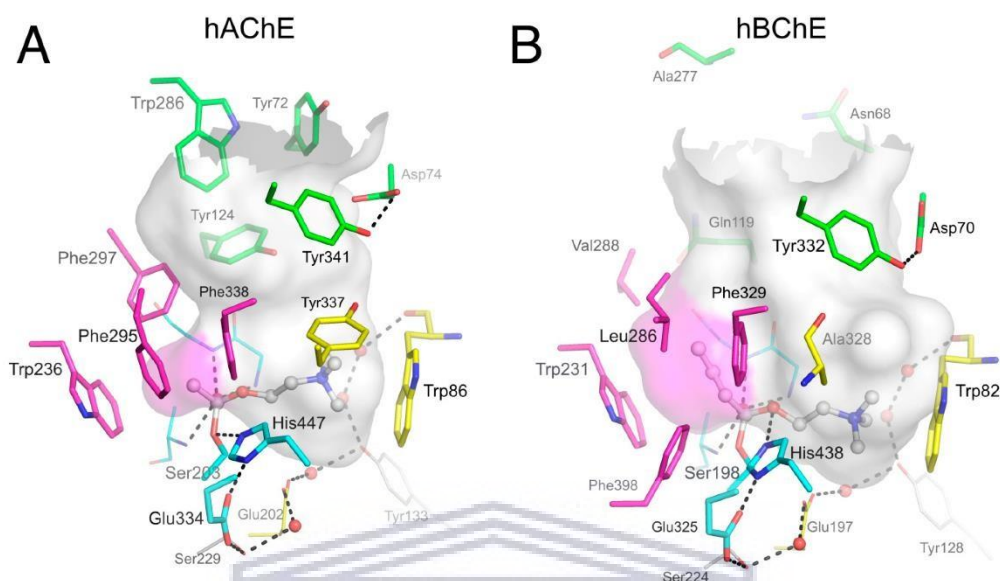


**Figure 2.5:** 3D representation of the cholinesterases' differing active sites (Chiou, *et al.*, 2009).

AChE is an  $\alpha/\beta$  hydrolase folded with an  $\alpha$  helix bound with a  $\beta$  sheet, containing an active site similar to other serine hydrolases (Figure 2.6a). In comparison to BuChE it is found to be nearly two times more effective in its catalysis of ACh breakdown. Similarly to BuChE, the active site of AChE is comprised of the PAS, CAS and catalytic triad (Figure 2.6b). The differences in their amino acid residues account for their difference in activities (Silman & Sussman, 2008; Dvir, *et al.*, 2010).

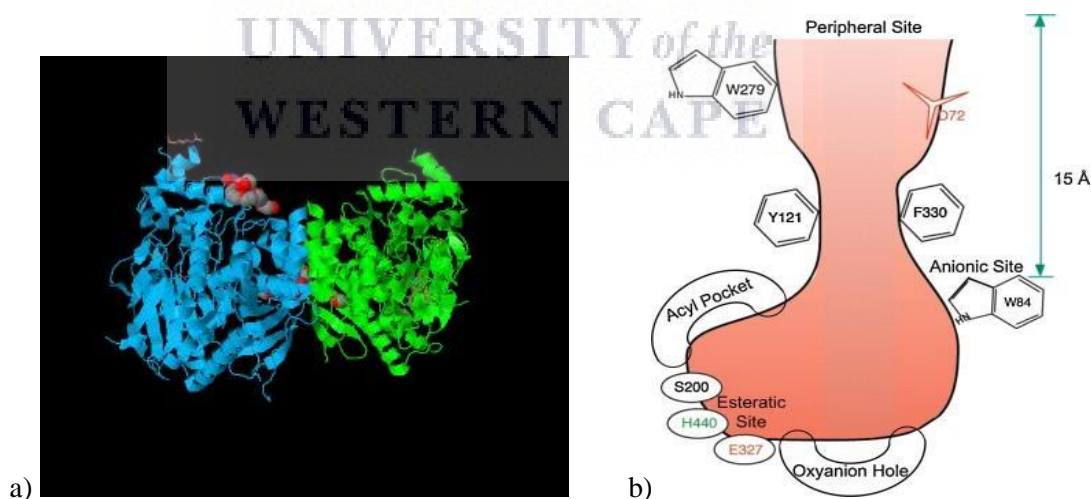


**Figure 2.6a:** Ribbon structure of AChE dimer (Proteopedia.org, 2009); **b:** Structure of AChE active site highlighting some key amino acids important for its activity (Dvir, *et al.*, 2010).

The PAS consists of five residues: Tyr 70, Asp 72, Tyr 334, Trp 279 and Tyr 121 and acts to trap the substrate by  $\pi$  interactions with the substrate. This trapping mechanism enhances the catalytic efficiency, but the shape of this region further mediates the substrate inhibition displayed in AChEs enzymatic kinetics. Additionally, the binding at the PAS induces changes within the gorge allowing the substrate to be further exposed to the esteratic site (Johnson & Moore, 2006). In AD it has been shown

that the PAS plays a role in the formation of A $\beta$  fibrils by forming complexes with the aggregating peptide fragments resulting in particularly stable oligomers which are more neurotoxic than those which form naturally (Alvarez, *et al.*, 1998). The esteratic/catalytic triad made of Ser 200, Glu 327 and His 440 is where hydrolysis of ACh takes place. The Ser 200 residue forms a covalent bond with ACh and reduces its carbon oxygen double bond (Dvir, *et al.*, 2010). Due to its catalytic triad and shape, AChE is not able to hydrolyse large molecular weight esters. The CAS consists of 14 aromatic residues which include Glu 199, Phe 330 and Trp 84. They bind the amino acid region of ACh with Trp 84 being the most essential for interaction with the quaternary portion of choline (Xu, *et al.*, 2008).

### 2.3.1.4 Monoamine oxidases

Monoamine oxidase is an important membrane bound flavoenzyme. It exists in two forms: MAO-A and MAO-B. The two isoforms share 70% of their amino acid makeup and are covalently bound to an FAD cofactor which enables their main biological functions such as the oxidation of primary, secondary and tertiary amines – including neurotransmitters. Each enzyme thus has a separate but overall overlapping function as they have differing substrates. MAO-A metabolizes serotonin, norepinephrine and dopamine while MAO-B metabolizes dopamine, phenethylamine as well other exogenous substances such as benzylamine (Gaweska & Fitzpatrick, 2011). Both enzymes are coded on the same X chromosome and found mainly in the brain in neurons and astroglia. Outside the CNS MAO-A is found in the liver, GIT and placenta while MAO-B is found in blood platelets (Fowler, *et al.*, 2015). MAO-A exists as a 527 amino acid monomer while MAO-B crystallises as a dimer with each unit consisting of 520 amino acids (Figure 2.7). For both enzymes each monomeric active site is made up of 3 domains:

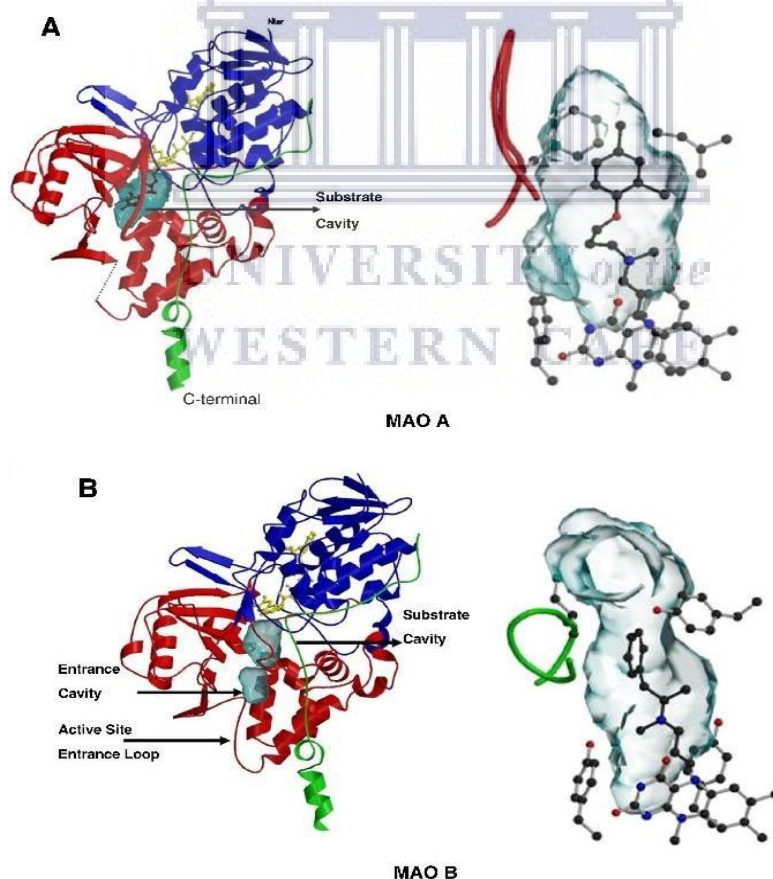


**Figure 2.7:** The active sites of MAO-A (A) and MAO-B (B) complexed with inhibitors, visualised as ribbon diagrams (left) and 3D models (right) (Finberg, 2014).

- **FAD binding domain** – which is nearly identical and conserved in both subtypes (Figure 2.8). A lysine residue (Lys 308 for MAO-A and Lys 296 for MAO-B) binds to the flavin co-factor via the 8  $\alpha$ -methylene of the isoalloxazine ring. The redox active isoalloxazine ring is buried deep within the enzyme oriented towards the substrate binding site (Son, *et al.*, 2008).
- **Membrane binding domain** – Both enzymes bind to outer mitochondria membrane through a C-terminal  $\alpha$  helix of  $\pm 27$  amino acids. In this region lies the entrance cavity by which substrates can enter the enzyme. The entrance cavity is surrounded by a 13 amino acid long flexible loop that must move for substrates to enter. The negative charge of the residues attracts the positively charged amine substrates and thus plays a role in identification of appropriate substrates (Edmondson, *et al.*, 2004). MAO-B has a distinctly narrower entrance cavity with MAO-A's entrance cavity being shorter and wider.
- **Substrate binding domain** - lined by hydrophobic aromatic and aliphatic regions. An “aromatic sandwich” is formed by Tyr 407 and Tyr 44 in MAO-A and Tyr 398 and Tyr 455 in MAO-B. These react with the substrate for oxidation or to activate the amine via a nucleophilic mechanism. The total volume in this active site for MAO-A is 400  $\text{\AA}^3$ . Initially MAO-Bs' active site is smaller, as the Ile 199 and Tyr 326 residues form a gate-like barrier between the entrance and catalytic site. Depending on the nature of substrate or inhibitor present the Ile 199 residue can rotate and functionally, fuse the two cavities to form a larger 700  $\text{\AA}^3$  cavity. Ile 335 (MAO-A) and Tyr 326 (MAO-B) are the key residues that determines substrate specificity (Binda, *et al.*, 2003).

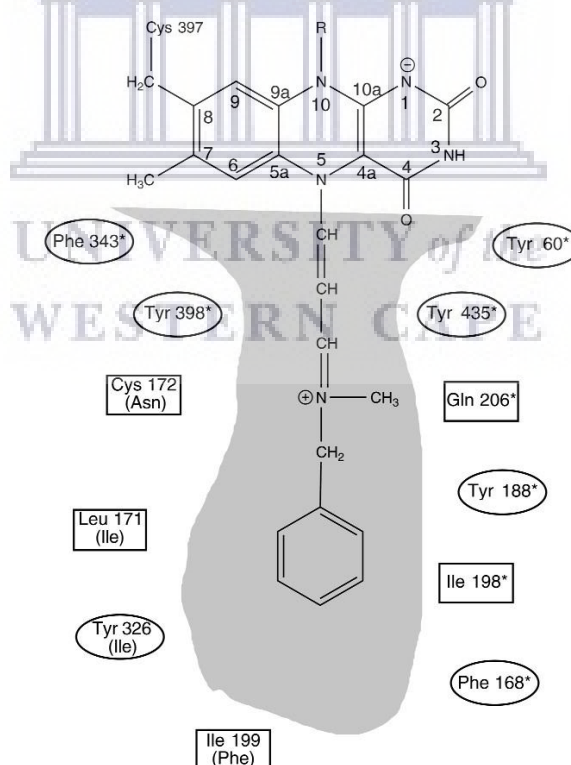


**Figure 2.8:** Diagrammatic representation of the MAO active site complexed with pargyline. The residues conserved across both isoforms are indicated with asterisk and those that differ in MAO-A are in parentheses (Binda, *et al.*, 2003).

Both enzymes follow the same catalytic mechanisms via two half reactions involving a reductive and oxidative step.

### 1) Reduction

The flavin co-factor is reduced by accepting a hydride equivalent, with the most widely accepted means being a polar nucleophilic mechanism. In this mechanism it is suggested that Tyr 435 (MAO-B) and Tyr 444 (MAO-A) have dipole moments which result in the redistribution of the lone pair electrons on the N-atom of the amine. This increases nucleophilicity of the group allowing for reduction to take place. The rate limiting reaction of this step is the cleavage of the  $\alpha$  hydrogen from the substrate. Substrates with neutral amino groups are preferentially bound as there is an increased likelihood for oxidation in the next step (Figure 2.9) (Edmondson, *et al.*, 2004).

### 2) Oxidative phase

Following  $O_2$  entering via the entrance cavity the reduced flavin is reoxidised by oxygen. When this occurs the  $O_2$  is converted to  $H_2O_2$  by the flavonoid hydroquinone (Figure 2.10). The aldehyde product is metabolized and the free radicals produced from  $H_2O_2$  are normally scavenged by antioxidants (such as glutathione), catalase and superoxide dismutase (Finberg, 2014).

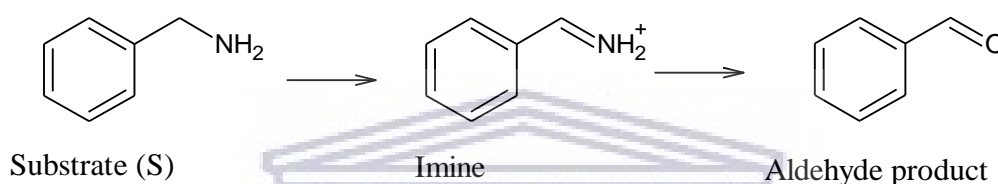


**Figure 2.9:** Oxidation of a typical amine to its aldehyde product.

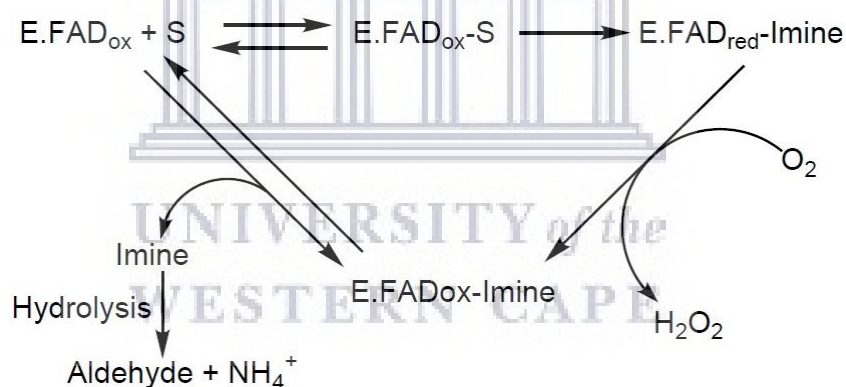


**Figure 2.10:** Redox mechanism of MAO.

If this scavenging of radicals fails and/or there is an increased production of  $H_2O_2$  it can lead to increased oxidative stress within neurons and production of reactive oxygen species (ROS). These are neurotoxic and lead to neuronal death. MAOs are implicated in several diseases which involve neurotransmitters such as PD, depression and AD and in particular MAO-B is overexpressed in AD and so inhibition of its activity could be beneficial in the disease state (Schedin-Weiss, *et al.*, 2017).

## 2.4 Treatment of AD

AD treatment has proven to be difficult due to its complex and interlinked pathology. Of the currently approved drugs none are directly targeted at the underlying cause of the disease and none offer significant neuroprotection or cure the disease. Instead they act as disease modifying agents only slowing down the diseases' progression and improving the patients' cognitive symptoms and memory loss. Regardless, even taking into account their symptomatic alleviation they remain less than desirable treatment options as they do not always work when given to patients. Current treatments fall into two

categories: cholinesterase inhibitors and N-methyl-D-aspartate receptor (NMDAR) antagonists (Touchon, *et al.*, 2013; Frozza, Lourenco, & De Felice, 2018).

### 2.4.1 Cholinesterase Inhibitors

Cholinergic inhibition is regarded as the most important of the multiple proposed targets involved in the AD network (Singh, *et al.*, 2013), being included in current treatment as well as most multi-targeted strategies. Cholinergic inhibition stems from the aforementioned cholinergic hypothesis with AChE inhibitors stopping hydrolysis of ACh therefore increasing the overall levels of ACh and duration of cholinergic action. This increases cholinergic transmission in the brain and compensates for the loss of functioning cholinergic neurons. BuChE is targeted as well due to its takeover role of ACh hydrolysis in AD (Anand & Singh, 2013).

Tacrine (Figure 2.12) was the first drug agent of this class available on the market in 1993, but was discontinued due to its hepatotoxicity. Its impact cannot be understated and its scaffold is still being used in drug discovery endeavours with agents such as bis (7)-tacrine proving to be more potent and potentially safer than the parent compound (Eslami, *et al.*, 2015).

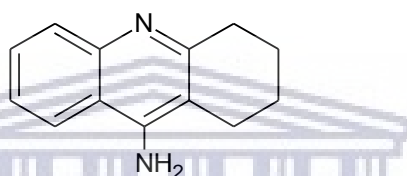


**Figure 2.12:** Structure of tacrine, the first AChEI indicated for AD. It was discontinued due to safety concerns.

The agents currently approved and prescribed for use in mild to moderate AD are donepezil, rivastigmine and galantamine (Figure 2.11). They are all reversible acetylcholinesterase inhibitors (AChEIs) shown to increase cholinergic function and interfere with the synthesis and deposition of A $\beta$  fibrils (García-Ayllón, *et al.*, 2010).

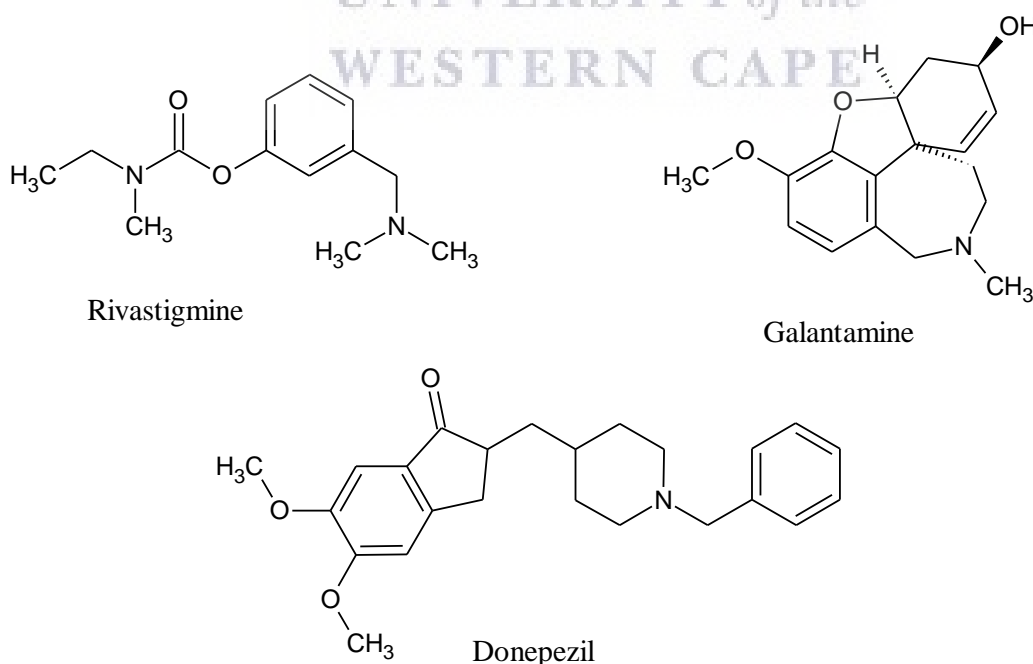


**Figure 2.11:** AChEIs approved for use in AD.

Clinically, patients treated with AChEIs show a decrease in memory loss, increase in cognitive functions and overall delay in the deterioration in mental functions within their treatment duration of 12 to 24 months (Colovic, *et al.*, 2013). All AChEI agents have similar efficacies and show cholinergic side effects such as loss of appetite, dizziness, vomiting and headaches (Johnell & Fastbom, 2008).

Donepezil (developed by Eisai and Pfizer) has been available since 1997 and is also indicated for Lewy body dementia, quickly became the main-stay treatment in mild to moderate AD. It has the benefit in that it is selectively inhibitory to CNS tissue versus peripheral tissue (Jacobson & Sabbagh, 2008). It is also used as a positive control in many lab tests, both *in vivo* and *in vitro*, and acts by binding to the PAS and anionic subsite via its N-benzylpiperidine moiety, which has been incorporated into multiple potent AChEIs being researched for AD treatment (Anand & Singh, 2013; Joubert, *et al.*, 2017).

Rivastigmine is a carbamate based inhibitor which inhibits both AChE and BuChE and together with donepezil form what is known as second generation AChEIs. It has nearly a ten-time higher affinity for brain AChE than peripheral AChE. Transdermal patch formulations were developed to bypass the oral route of administration as this reduces the associated GIT side effects (Mehta, *et al.*, 2012).

Galantamine is an alkaloid (isolated from the plant snowdrop *Galanthus woronowii*) which interacts with the CAS, PAS and aromatic gorge. In addition to enzyme inhibition, galantamine also sensitizes nicotinic ACh receptors and thus increases cholinergic function in the brain (Farlow, 2003).

#### 2.4.2 NMDAR Antagonists

The glutamergic neurotransmission system via NMDA receptors plays an important role in synaptic plasticity and in the consolidation between long and short-term memory. It is noted that in AD (as well as other NDs) there is excessive activity of the NMDARs due to decreased glutamate reuptake in the microglia. The presence of this excess glutamate activity leads to increased  $\text{Ca}^{2+}$  influx, leading to excitotoxicity and cell death (Danysz, *et al.*, 2000; Wang & Reddy, 2017). Therefore, inhibition of NMDAR would improve the condition of AD patients and this is the reasoning behind the development of the NMDAR antagonists. The first of these to pass the drug development pipeline was memantine (Figure 2.13) (introduced by Merz Pharma), approved in 2002 by the FDA and subsequently adopted by many countries including South Africa. It acts as a non-competitive NMDAR antagonist, essentially trapping the receptor in its “open” configuration and thus preventing excessive glutamergic stimulation. In the current treatment regimen it is the only drug indicated for mild to moderate AD and is used in combination with donepezil in severe AD. It also has off label use in other dementias. Clinically memantine has limited efficacy as it does not prevent neuronal loss, dementia or disease progression (Graham, *et al.*, 2017).

Riluzole (Rilutek<sup>®</sup> developed by Sanofi) (Figure 2.13) is another agent currently in Phase III trials under investigation as the next drug in this class. It displays the ability to enhance glutamate transport activity and decrease glutamate release which can potentially be applicable in AD treatment (Hung & Fu, 2017).

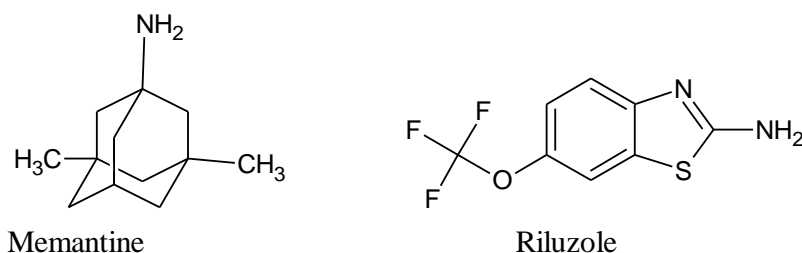


**Figure 2.13:** Structures of NMDAR antagonists explored in AD.

### 2.4.3 Other treatment options

The lack of a definitive and effective treatment regime coupled with the multifactorial nature of AD has led researchers to investigate and hypothesise a number of alternate treatment strategies incorporating our understanding of the diseases' pathology. These include; anti-tau protein strategies, antagonism of the 5HT-6 receptor, inhibition of oxidative stress and the use of multi-target directed ligands.

#### 2.4.3.1 Anti-tau protein strategies

As mentioned previously, the presence of NFTs and phosphorylated tau is one of the classic biomarkers of AD and is associated with neuronal decline. Therefore, stopping formation for these tangles is being investigated to potentially improve AD symptoms. Figure 2.14 shows the main targets involved in the tangle formation timeline.

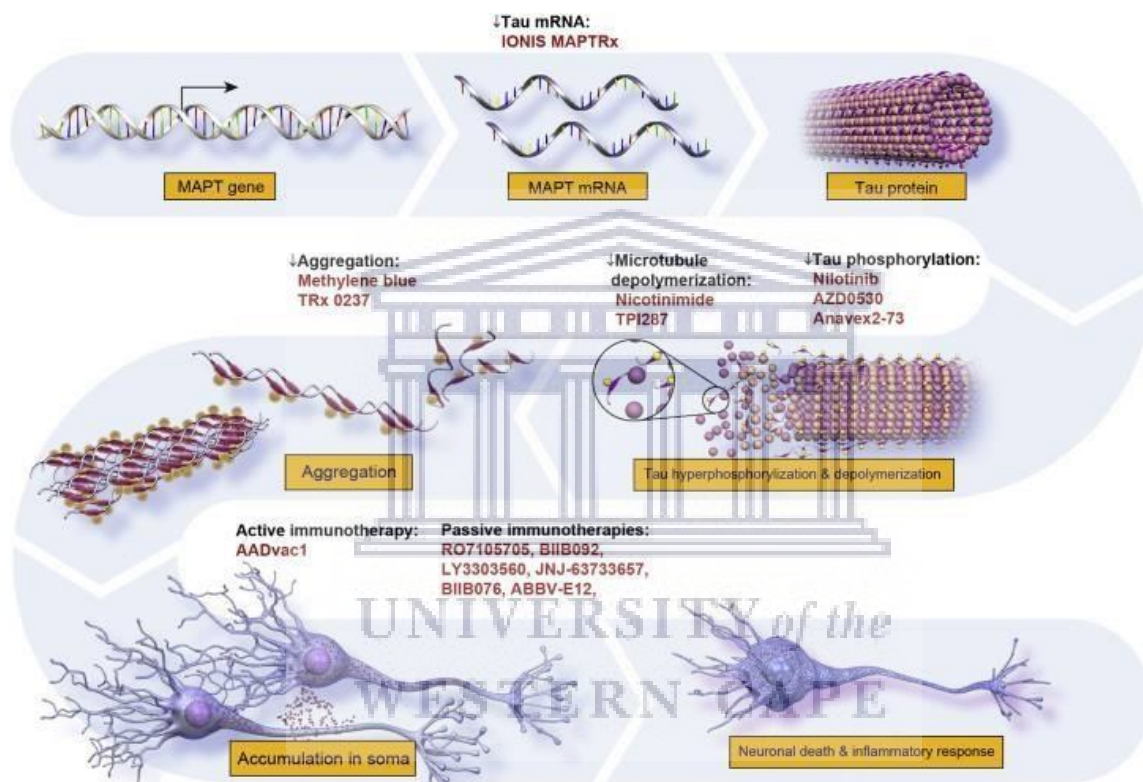


**Figure 2.14:** Formation of NFTs and the proposed sites of action for anti-tau treatments (Cummings, *et al.*, 2018).

The three most viable anti-tau strategies are:

- **Prevention of phosphorylation:** via targeting of the glycogen synthase kinase-3 enzyme responsible for phosphorylation processes in neurons with enzyme inhibitors. The most promising of these agents are ANAVEX 2-73 and tideglusib (Figure 2.15 a-b) which are in phase II clinical trials (del Ser, *et al.*, 2012; Zhang, Xu, Zhu, & Xu, 2019).
- **Anti tau aggregation:** agents such as methylene blue (Figure 2.15c) reduce covalent attractions between tau polymer units and thus decrease the chances of oligomer formation and precipitation of NFTs (Cisek, *et al.*, 2014).
- **Vaccination therapy:** both active and passive forms of immunization are in development which promote the body's immunological clearance of tau (Rosenmann, 2013).



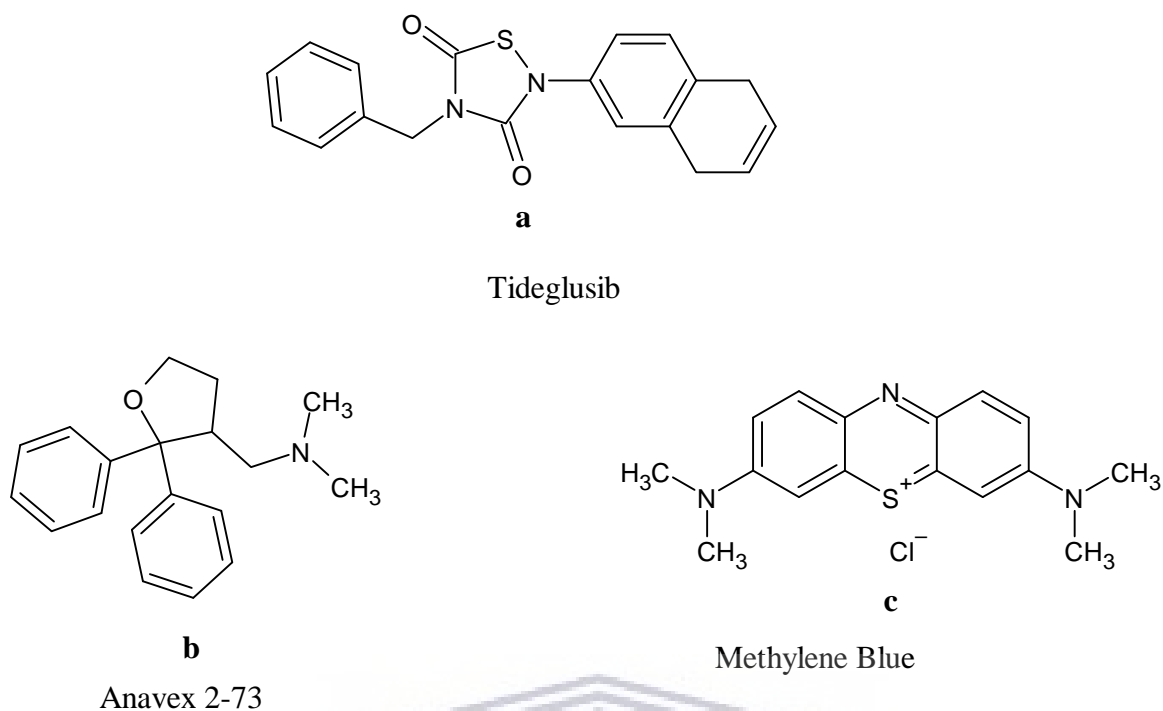


**Figure 2.15:** Various anti-tau drug therapies undergoing clinical trials for AD.

#### 2.4.3.2 5-HT-6 receptor antagonists

The 5-HT-6 receptor forms part of the larger serotonin receptor group and is expressed predominantly in the cortex and hippocampus. In addition to its primary role in the serotonergic system of regulating mood and emotion, it is closely implicated in cholinergic neurotransmission with regard to memory and learning (Ramírez, 2013; Ferrero, Solas, Francis, & Ramirez, 2016).

5-HT-6 receptors are shown to modulate ACh release, with blockage of 5-HT receptor inducing ACh release and alleviating memory deficits. This has interested researchers particularly because these agents can be used in conjunction with existing AChEIs to increase and prolong their cholinergic functions with the added benefit of alleviating behavioural and mood disorders associated with AD such as anxiety, depression and schizophrenia (Andrews, *et al.*, 2018). Intepirdine and SUVN-502 are 5-HT6 antagonists having gone into phase III clinical trials and have shown the ability to improve cognition in the preclinical phase and in animal models (Figure 2.16) (Khoury, Grysman, *et al.*, 2018).

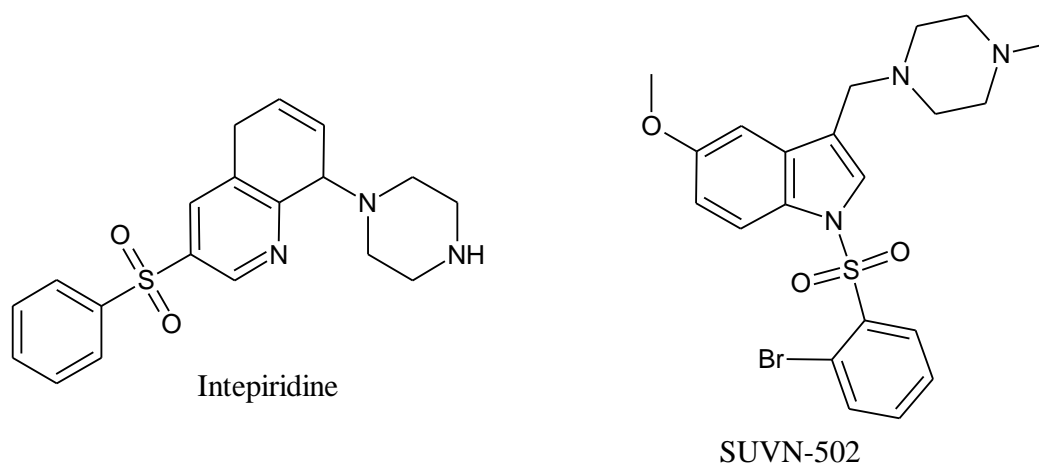


**Figure 2.16:** 5-HT-6 antagonists shown to alleviate cognitive decline in AD.

### 2.4.3.3 Antioxidants

As mentioned previously, oxidative stress is found to be part of the cascade of events that lead to neuronal cell death with numerous oxidative stress related biomarkers such as oxidated lipid and DNA species occurring in the AD affected brain. This increase in ROS may be due to reduced clearance of said species by mechanisms such as superoxide dismutase and catalase (Singh, *et al.*, 2017). In these scenarios, antioxidants have been proposed as potential treatments strategies for AD as they stop radical chain reaction and/or detoxify the  $\bullet\text{O}^2$  and  $\text{H}_2\text{O}_2$  radical species. Antioxidants can either be natural (e.g. vitamins E and C), synthetic or inorganic (Aliev, *et al.*, 2008).

A good example of antioxidants are flavonoids and their derivatives, such as baicalein (Figure 2.17), which demonstrate neuroprotective roles in cells under oxidative stress. Various models have found that the flavonoid inhibits NO production, mitochondrial ROS production and oxidative phosphorylation processes, as well as decreased A $\beta$  fibril formation and increased neurocognitive functions (de Andrade Teles, *et al.*, 2018).

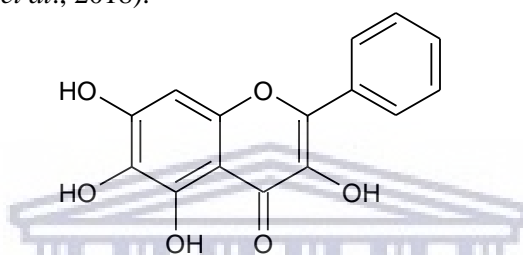


**Figure 2.17:** Structure of baicalein, a proposed flavonoid based AD treatment.

Zatta, *et al* (2003) hypothesised that oxidative stress may also arise due to excessive metal ion accumulation, with  $\text{Cu}^{2+}$ ,  $\text{Zn}^{2+}$  and  $\text{Fe}^{2+}$  in particular associated with increased ROS, peptide aggregation and neuronal damage. In this case compounds with metal chelating abilities are proposed to show benefits in AD treatment. Curcumin based compounds have shown dual ability to scavenge radicals and bind ions like  $\text{Cu}^{2+}$  and  $\text{Zn}^{2+}$  (Spinello, *et al.*, 2016).

## 2.5 Multi-Target Directed Ligands

Multi-target directed ligands (MTDLs) are drug agents which are effective at treating a disease via their high selectivity and potency to interact with multiple disease-causing targets. The concept of MTDLs was proposed by Morphy *et al* (2004) and is an evolution of the hybrid compound concept; whereby two or more known pharmacophores are covalently linked to produce a molecule with the combined pharmacological properties of said moieties. The resulting compound therefore should have the ability to act at multiple biological targets simultaneously at similar concentrations and exert a synergistic effect on the disease network that is not possible using traditional single target therapy or even polypharmacy (Korcsmáros, *et al.*, 2007). Due to this nature MTDLs are able to reduce pharmacokinetic interactions that would normally arise, avoid resistance to treatment and decrease the adverse reaction profile. Therefore, MTDLs have gained popularity as agents for treating complex conditions such as neurodegenerative diseases, cancer and malaria (Muller-Schiffmann, *et al.*, 2012).

One such MTDL available on the market is the drug ziprasidone (Figure 2.18) which is used to treat both psychosis and bipolar disorder by acting on both serotonin and dopamine receptors. This was achieved by incorporating the pharmacophores of dopamine and naphthylpiperazine, a serotonin receptor ligand. Patients treated with ziprasidone show a significantly decreased side effect profile compared to those on treatment with traditional antipsychotics such as olanzapine and risperidone (Schmidt, *et al.*, 2001; Addington, *et al.*, 2009).

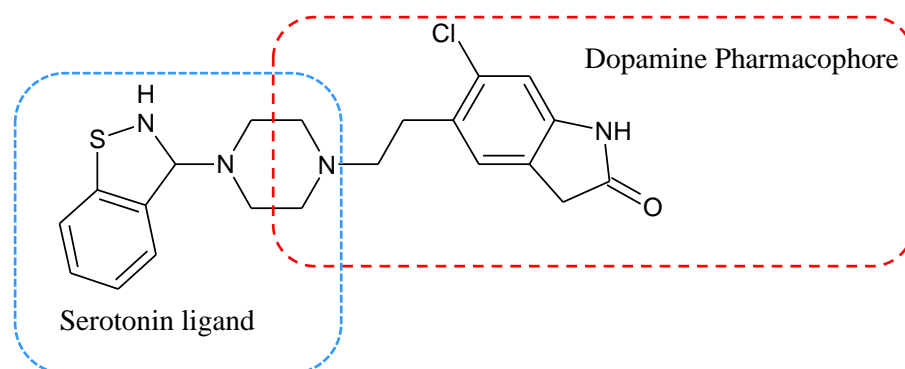


**Figure 2.18:** Ziprasidone structure displaying the hybrid molecules relevant pharmacophores.

Due to the failure of current single target treatments and complex pathology of AD, it is largely accepted that rationally designed MTDLs are the key to safe and effective treatment of AD. In current treatment the best evidence to multi-target approaching has been the combination of memantine plus a cholinesterase inhibitor typically donepezil or rivastigmine. Double blind studies show slight improvement in patients' cognitive functions in early and moderate AD compared to monotherapy, though this is not observed once the disease reaches the moderate to severe stage (Gareri, *et al.*, 2014). The multifactorial nature of AD means that there are a large number of biological targets for these MTDLs to act on. Several MTDLs have been explored for Alzheimer's with the aim of acting as both symptomatic and disease modifying agents. The main approach thus far is to target AChE in combination with one or more targets using known pharmacophores (Agatonovic-Kustrin, *et al.*, 2018).

A good example of a potential MTDL developed using this rationale is ASS234 (Figure 2.19) described by Bolea *et al* in 2013. The compound shows highly potent cholinesterase and MAO inhibitory activity in the nanomolar range and additionally has shown good neuroprotective activity. This is because the N-benzylpiperidine group from donepezil infers cholinesterase inhibition by interacting with the PAS site of ACHE, which additionally leads to decreased aggregation of A $\beta$ . The propargylamine moiety has the two-fold effect of binding to the active site of MAO and conferring neuroprotection via an unknown mechanism (Marco-Contelles, *et al.*, 2016). The compound has shown good activity *in vitro* as well as *in vivo*, rescuing memory loss and reducing synaptic dysfunction in mice models. Unlike current treatment options, ASS234 has displayed relatively low cell toxicity at high concentrations and thus it is thought to be safer than current agents (Unzeta, *et al.*, 2016).

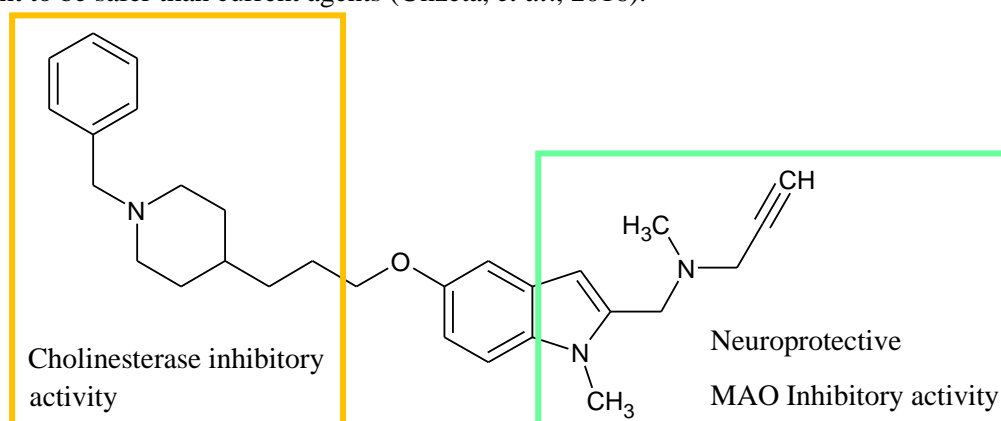


**Figure 2.19:** Structure of the promising MTDL ASS234. The benzyl-piperidine moiety (indicated in yellow) binds to the PAS of AChE whilst the indole-propargylamine portion (in green) confers MAO inhibition and neuroprotection

Another example of AChEI based MTDLs are tacrine-hydroxyquinoline hybrids (shown below in figure 2.20), which combine the scaffolds of tacrine with an 8-hydroxyquinolone derivative via a carbon linker to produce a compound whose activity greatly exceeds the sum of the parent pharmacophores. It is a more potent inhibitor of both AChE and BuChE than its tacrine parent with IC<sub>50</sub> values for both enzymes in the nanomolar and sub nanomolar range. This compound also has exceptional antioxidant activity due to its ability to not only absorb oxygen radicals, but also chelate Cu<sup>2+</sup> ions and thereby stopping ion accumulation related oxidative stress. It binds to the PAS of AChE as well and therefore decreases A $\beta$  aggregation (Fernández-Bachiller, *et al.*, 2010).

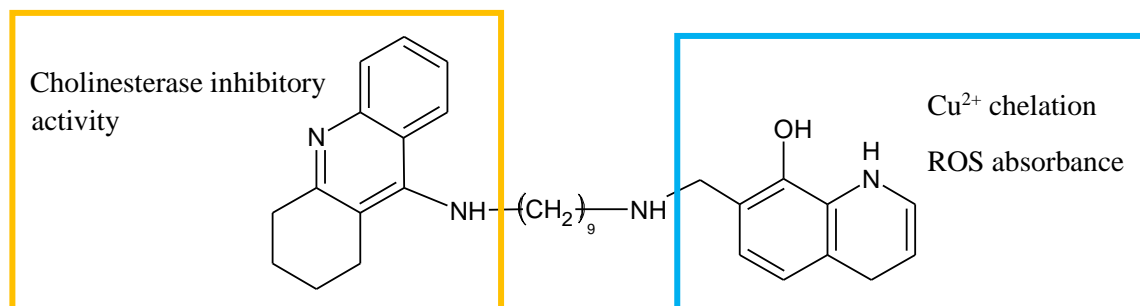


**Figure 2.20:** A tacrine-hydroxyquinoline hybrid MTDL. The tacrine moiety (in yellow) is responsible for ChE inhibitory activity was joined via a linker to an 8-hydroxyquinoline derivative (in blue) with antioxidant activity.

In development are other MTDLs which do not solely focus on the cholinergic hypothesis, but also target various other known targets that cause neurotoxicity. A good example of this is compound 12 (Figure 2.21) developed in a study by Zindo and colleagues in 2019. The compound is based on a polycyclic cage scaffold which was derived from NGP1-01, a known neuroprotective agent. This scaffold was then extensively optimised in a series of studies to develop a promising MTDL with neuroprotective capacity coupled with calcium regulatory activity and MAO inhibition (Zindo, *et al.*, 2019).

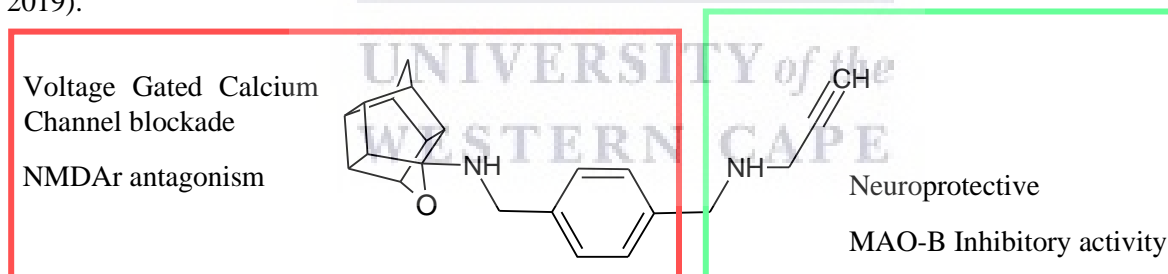


**Figure 2.21:** Polycyclic cage based compound 12 developed by Zindo *et al.* Propargylamine (green) was conjoined to the NGP1-01 derivative (in red) to enhance neuroprotective capacity to the compound

## 2.6 Coumarins

Coumarin (Figure 2.22) was originally extracted and characterised from tonka beans in 1822 by Vogel (Montagner, *et al.*, 2008). In subsequent years coumarin and coumarin derivatives have been classified as a family of compounds, also known as benzopyrones, which are of natural and synthetic origin (Murray, 2002).

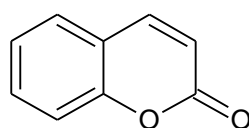


**Figure 2.22:** The coumarin scaffold.

They have a wide spectrum of pharmacological activities displaying antidepressant, antimicrobial, antitumor and antioxidant properties among others. The most prominent use of coumarins is in the anticoagulant drug warfarin, which is the mainstay blood thinner for a variety of cardiac conditions (Wu, *et al.*, 2009; Matos, *et al.*, 2015). Coumarins have also found use in psychiatric treatment in the drug ensaculin, which is a weak NMDA antagonist and 5HT<sub>1A</sub> agonist being explored for use in dementia (Hoerr & Noeldner, 2006).

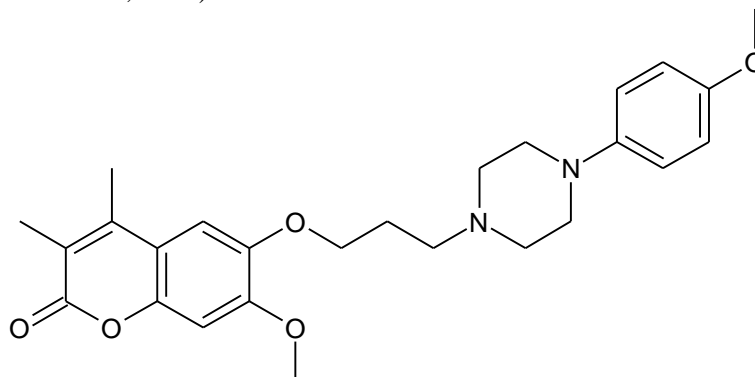


**Figure 2.23:** Ensaculin, a coumarin scaffold containing anti-dementia drug.

Coumarins and their derivatives have displayed some MAO binding affinity and are potent MAO inhibitors. Quantitative structural activity relationship studies performed on these derivatives have shown that substitutions at positions 3, 4 and/or 7 determine the activity and selectivity of the compound (Santana, *et al.*, 2008). Lipophilic groups in particular have been observed to impart great selectivity towards MAO-B inhibition due to their interactions with the hydrophobic amino acid residues surrounding the enzymes' entrance cavity (Joao Matos, *et al.*, 2012).

In addition to inhibiting MAO, coumarin derivatives have also displayed the ability to inhibit the cholinesterases. To maximise this inhibitory activity it has been found feasible to make derivatives which are long enough to be dual binding to both the CAS and PAS of the enzyme. This is achieved by substituting various spacer groups onto the scaffold which allow penetration into the gorge shaped active site (Catto, *et al.*, 2013; Yusufzai, *et al.*, 2018).

The coumarin scaffold thus has potential to be a good candidate for the development of MTDLs to treat AD. Its structure allows for versatility by allowing substitutions to occur at different positions in its structure. Figure 2.24 shows one of several MTDLs developed by combining modified coumarin scaffolds with the N-benzylpiperidine group from donepezil (Joubert, *et al.*, 2017). These compounds showed well balanced cholinesterase and MAO inhibitory activity.

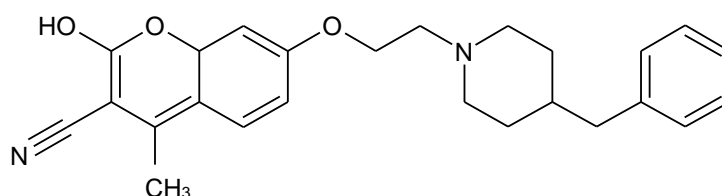


**Figure 2.24:** A coumarin based MTDL with MAO and cholinesterase inhibitory activity designed by Joubert *et al* (2017).

## 2.7 Conclusion

Alzheimer's disease belongs to a broad group of diseases termed Neurodegenerative Diseases which are on the increase due to the growing elderly population of the world. Due to the disease and its symptoms' progressive nature it continues to put a great strain on patients, caregivers and the healthcare

system. and the lack of treatment only exacerbates these problems. The complex pathophysiology underlying the disease is multifactorial with factors such as oxidative stress, tau proteins and amyloid plaques playing a role in the development of symptoms and progressive neurodegeneration. Whilst many approaches are being explored to overcome this, the utilization of MTDLs holds great promise due to their ability to target multiple disease mechanisms. Examples of MTDLs have demonstrated efficacy in treatment of other complex diseases and there are a number of MTDLs in development for AD which have shown promise for treatment. By modification of the coumarin moiety, research has demonstrated it is possible to produce MTDLs which target the causative MAO and cholinesterase enzymes. Rationally designed coumarin derivatives would thus be able to reduce oxidative stress mediated by MAO, reduce the formation of toxic A $\beta$  plaques and offer neuroprotection and thus be viable treatment for AD.



## Chapter 3

### 3. Synthetic procedures

#### 3.1 Reagents and chemicals

All reagents used in the synthesis of the compounds were obtained from Industrial Analytical (RSA) and Sigma-Aldrich® (Steinheim, Germany). All solvents used in chromatography and reactions were acquired from various commercial sources and were used without further purification unless specified.

#### 3.2 Instrumentation

##### Nuclear magnetic resonance spectroscopy (NMR):

<sup>1</sup>H and <sup>13</sup>C NMR spectra were obtained using a Bruker 400MHz Avance IIIHD Nanobay spectrometer (Rheinstetten, Germany) equipped with a 5 mm BBO probe at 333 K using standard 1D NMR pulse sequence. The internal standard used in the experiments was tetramethylsilane (TMS) and all chemical shifts are reported relative to its signal ( $\delta = 0$ ) in parts per million (ppm) in either deuterated dimethyl sulphoxide (DMSO-d<sub>6</sub>) or deuterated chloroform (CDCl<sub>3</sub>). The following abbreviations are used to describe the multiplicity of signals:

- s - singlet
- d - doublet
- dd - doublet of doublets
- t - triplet
- dt – doublet of triplets
- q - quartet
- m - multiplet



##### Infrared spectroscopy (IR):

The IR data were obtained by using a Perkin Elmer Spectrum 400 spectrometer (Waltham, USA) fitted with a diamond attenuated total reflectance (ATR) attachment linked to a computer system.

##### Mass spectroscopy (MS):

The MS data of the samples were obtained using Waters Synapt G2 MS Spectrometer (Wilmslow, UK) with an ESI probe attached in ESI Positive mode, with a cone voltage of 15 V, infused in methanol. The instrument was set to a tolerance of 50 ppm.

The data from the IR, MS and NMR are attached in the annexure.

##### Melting point determination (MP):

MPs were determined using a Stuart Melting Point SMP 20 (Staffordshire, UK) apparatus and with the compound being tested contained in glass capillary tubes. The data obtained was for the purified solid form of the compounds.

##### Microwave synthesis:

All experiment involving the use of microwave assisted methods were performed using a CEM Discover™ closed vessel system (Buckingham, UK). The settings used were custom and specific for each synthetic experiment.

### 3.3 Chromatographic techniques

A number of chromatography techniques were used for the identification compounds and purification of compounds as well as tracking reaction progress:

#### Thin Layer Chromatography

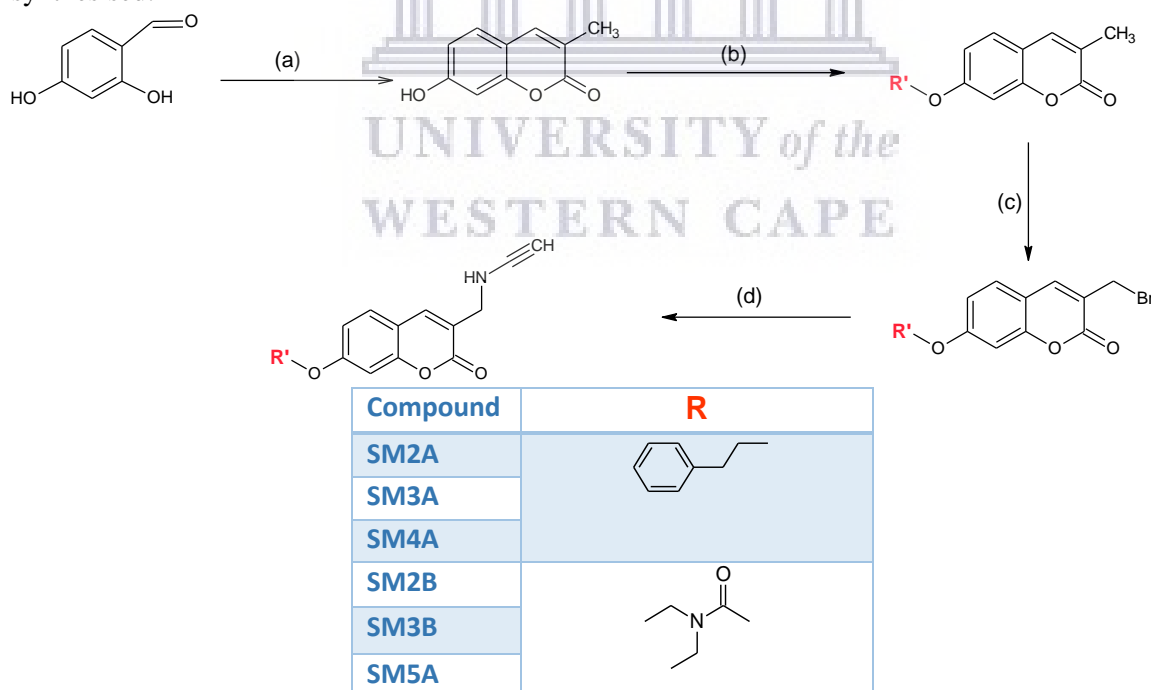
The stationary phase used were sheets of 0.20 mm thick aluminium silica gel (TLC Silica gel 60 F245 Merck KGaA) which were spotted *via* glass pipettes and placed in TLC tanks. Various mobile phases were prepared using volume:volume ratios and once the plates were developed the spots were visualised using UV light (254 nm and 366 nm) or in an iodine crystal tank.

#### Column chromatography

Purification of the specified compounds was performed in glass columns filled with appropriate amounts of silica gel (0.063 - 0.200 mm/70 - 230 mesh ASTM, Macherey - Nagel, Duren, Germany) as the stationary phase. The mobile phases used for each compound are indicated.

### 3.4 General Synthetic Procedure

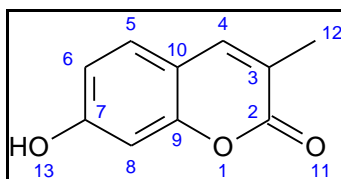
The synthesis of the proposed compounds (Scheme 3.1) began with a Pechman condensation reaction of a benzaldehyde to obtain 7-hydroxy-3-methyl-coumarin which would serve as the base scaffold. Following this, two different series of compounds were obtained which were grouped depending on whether an ethyl benzene or diethyl carbamate moiety is substituted at position 7 of the scaffold. Addition of the moiety was done *via* a microwave assisted  $S_N2$  substitution, followed by an  $\alpha$ -bromination of the  $CH_3$  at position 3 to obtain a halogenated methyl group ( $CH_2Br$ ) and finally a further  $S_N2$  substitution reaction with a propargylamine functional group. A total of seven compounds were synthesised.



**Scheme 3.1:** *Reagents and conditions:* (a) Sodium propionate, propionic anhydride, piperidine, reflux, 6 Hr; (b) 2-bromoethylbenzene, NaH, acetonitrile, MW @ 150 W, 80 °C, 5 Hr (for SM2A) or diethyl carbamoyl chloride,  $K_2CO_3$ , Acetonitrile MW @ 150 W, 80 °C, 2.5 Hr (for SM2B); (c) *N*-bromosuccinimide, benzoyl peroxide,  $CCl_4$ , stir at room temperature, 7 Hr (for SM3A) or reflux, 15 Hrs (for SM3B); (d) Propargylamine,  $K_2CO_3$ , dry THF, stir for 48 Hrs.



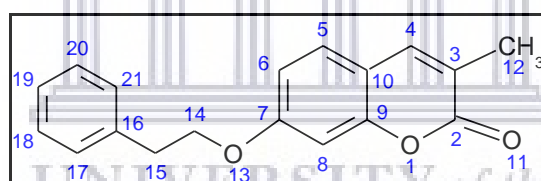
## 3.4.1 7-Hydroxy-3-methyl-2H-1-benzopyran-2-one (SM1)



**Synthesis:** A mixture of 2,4-dihydroxybenzaldehyde (7.2 mmol, 1.0 g), propionic anhydride (19.4 mmol, 2.5 mL), piperidine (1 mmol, 0.1 mL) and sodium propionate (15.6 mmol, 1.5 g) was refluxed for 6 hours. The mixture was then poured onto ice and made acidic with 20 ml of a 0.1 N solution of HCl. This yielded a precipitate that was filtered and treated under stirring with concentrated H<sub>2</sub>SO<sub>4</sub> (2 mL). The resulting mixture was poured onto ice again to afford a red brown precipitate of the desired product.

**Physical Properties:** C<sub>10</sub>H<sub>8</sub>O<sub>3</sub> ; **mass:** 764 mg ; **yield:** 60% ; **mp:** 165 °C ; **<sup>1</sup>H NMR** (400 MHz, DMSO-d<sub>6</sub>) δH (Spectrum 1) : 7.72 (s, 1 H, H – 4), 7.42 - 7.40 (d, 1 H, *J* = 8.5 Hz, H – 5), 6.76 – 6.73 (dd, 1 H, *J* = 2.2, 8.4 Hz, H – 8), 6.69 – 6.68 (d, 1 H, *J* = 2.1 Hz, H – 6), 2.02 (s, 3 H, H – 12); **<sup>13</sup>C NMR** (100 MHz, DMSO-d<sub>6</sub>) (Spectrum 2) : 161.77, 160.18, 154.51, 140.14, 128.73, 120.00, 113.04, 111.83, 101.91, 16.49; **HR-ESI [M+H]<sup>+</sup>** (Spectrum 3) : calc. 175.0395, exp. 175.0398; **IR** (FT-IR, cm<sup>-1</sup>) (Spectrum 4) : 3234, 2934, 1739, 1675, 1451.

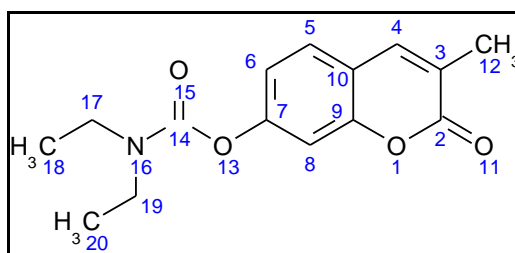
## 3.4.2 3-Methyl-7-(2-phenylethoxy)-2H-1-benzopyran-2-one (SM2A)



**Synthesis:** A microwave compatible glass-vessel was charged with 200 mg of 7-hydroxy-3-methyl-2H-1-benzopyran-2-one (SM1) and 68 mg of NaH (80% dispersion in oil) and dissolved in 10 ml of acetonitrile. To this mixture, 570 µl of 2-bromoethylbenzene was added dropwise and subsequently stirred at 80 °C for 5 hours under microwave irradiation (maximum power = 150 W). The solvent was removed *in vacuo* and the resulting crude mixture was washed with 30 ml ethyl acetate and 15 ml water. The organic layer was washed with 15 ml of 1 M KOH and then 15 ml of brine, thereafter the solvent was removed *in vacuo*. The crude product was then purified using column chromatography (Mobile Phase; hexane: ethyl acetate 3:1).

**Physical Properties:** C<sub>18</sub>H<sub>16</sub>O<sub>3</sub>; **mass:** 116 mg; **yield:** 37% ; **mp:** 89-92 °C ; **<sup>1</sup>H NMR** (400 MHz, CDCl<sub>3</sub>) δH (Spectrum 5) : 7.39 (s, 1 H, H – 4), 7.31 – 7.22 (m, 6 H, H – 5, 17, 18, 19, 20, 21), 6.78 – 6.59 (m, 2 H, H – 6, 8), 4.17 (t, 2 – H, *J* = 7.0, H – 14), 3.10 – 3.06 (t, 2 – H, *J* = 7.1, H – 15), 2.13 (s, 3 H, H – 12); **<sup>13</sup>C NMR** (100 MHz, CDCl<sub>3</sub>) (Spectrum 6) : 162.57, 160.90, 154.80, 139.33, 137.71, 128.96, 128.57, 127.76, 126.67, 122.12, 113.23, 112.69, 101.16, 69.08, 35.50, 16.94; **HR-ESI [M+H]<sup>+</sup>** (Spectrum 7) : calc. 281.1178, exp. 281.1171; **IR** (FT-IR, cm<sup>-1</sup>) (Spectrum 8) : 3026, 2850, 1612, 1284, 1247.

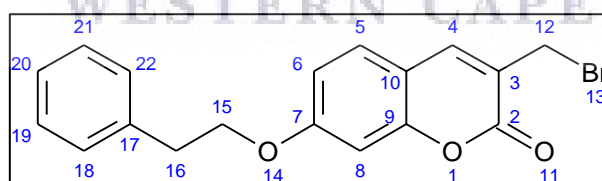
## 3.4.3 3-Methyl-2-oxo-2H-1-benzopyran-7-yl-diethylcarbamate (SM2B)



**Synthesis:** A microwave compatible glass-vessel was charged with 250 mg of 7-hydroxy-3-methyl-2H-1-benzopyran-2-one (SM1), 295 mg of  $K_2CO_3$  and a catalytic amount of TBA  $HSO_4$  and dissolved in 10 ml of acetonitrile. Following this, 385 mg of diethyl carbamoyl chloride was added dropwise and stirred at 100 °C for 2.5 hours under microwave irradiation (maximum power = 150 W). Once the reaction was complete,  $K_2CO_3$  was filtered out and the solvent was removed *in vacuo*. The crude mixture was dissolved in 30 ml ethyl acetate and 15 ml water and transferred to a separatory funnel. The layers were separated and the organic layer was washed with 15 ml of 1 M KOH and then 15 ml of water. The combined aqueous layers were extracted with ethyl acetate (3 x 20 ml). The combined organic layers were then washed with brine and concentrated under reduced pressure. The crude product was obtained as an amber coloured oil.

**Physical Properties:**  $C_{15}H_{17}NO_4$ ; **mass:** 254 mg; **yield:** 65%; **mp:** wax ;  $^1H$  NMR (400 MHz,  $DMSO-d_6$ )  $\delta$ H (Spectrum 17) : 7.85 (s, 1 H, H – 4), 7.62 – 7.60 (d, 1 H,  $J = 8.4$  Hz, H – 5), 7.20 – 7.19 (d, 1 H,  $J = 2.1$  Hz, H – 8), 7.11 – 7.09 (dd, 1 H,  $J = 2.2, 8.5$  Hz, H – 6), 3.42 – 3.37 (q, 2 H,  $J = 6.53$  Hz, H – 17), 3.36 – 3.28 (q, 2 H,  $J = 7.4$  Hz, H – 19), 2.08 (s, 3 H, H – 12), 1.21 – 1.10 (dt, 6 H,  $J = 6.6, 31.3$  Hz, H – 18, 20);  $^{13}C$  NMR (100 MHz,  $CDCl_3$ ) (Spectrum 18) : 161.94, 153.59, 153.24, 153.00, 138.79, 127.26, 124.48, 118.32, 116.64, 109.78, 42.29, 41.91, 29.57, 16.98, 14.13, 13.19; **HR-ESI**  $[M+H]^+$  (Spectrum 19) : calc. 276.1236, exp. 276.1235; **IR** (FT – IR,  $cm^{-1}$ ) (Spectrum 20) : 2920, 1708, 1471, 1316, 1240.

## 3.4.4 3-(Bromomethyl)-7-(2-phenylethoxy)-2H-1-benzopyran-2-one (SM3A)

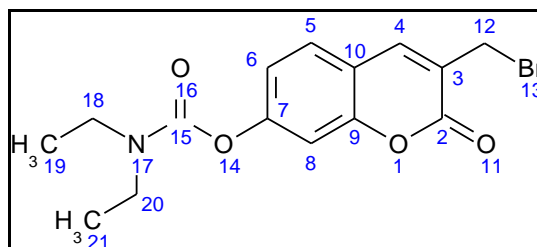


**Synthesis:** A mixture of 114 mg of N-bromosuccinimide, 150 mg of 3-methyl-7-(2-phenylethoxy)-2H-1-benzopyran-2-one (SM2A) and 33 mg of benzoyl peroxide (75%) were dissolved in 7 ml  $CCl_4$ . The reaction vessel was stirred at room temperature for 7 hours and once the reaction was complete the succinimide residue was filtered out. The solvent was removed *in vacuo* and the crude product was purified via flash column chromatography (Mobile Phase; hexane: ethyl acetate: chloroform, 4:4:1). An orange solid was obtained.

**Physical Properties:**  $C_{18}H_{15}BrO_3$ ; **mass:** 116 mg; **yield:** 43%; **mp:** 101-105 °C;  $^1H$  NMR (400MHz,  $CDCl_3$ )  $\delta$ H (Spectrum 9): 7.70 (s, 1 H, H – 4), 7.43 – 7.27 (m, 6 H, H – 5, 17, 18, 19, 20, 21), 6.86 – 6.83 (dd, 1 H,  $J = 2.33, 8.58$  Hz, H – 8), 6.81 – 6.80 (d, 1 H,  $J = 2.1$  Hz, H – 6), 4.41 (s, 2 H, H – 12), 4.25 – 4.21 (t, 2 H,  $J = 7.0$ , H – 15), 3.14 – 3.11 (t, 2 H,  $J = 7.1$ , H – 16);  $^{13}C$  NMR (100 MHz,  $CDCl_3$ )

(Spectrum 10) : 142.17, 129.02, 128.97, 128.92, 128.62, 128.58, 127.84, 126.76, 121.73, 113.39, 112.71, 101.27, 101.18, 69.27, 69.09, 35.51, 35.45, 28.166; **HR-ESI [M+H]<sup>+</sup>** (Spectrum 11) : calc. 359.0283, exp. 359.0298; **IR** (FT – IR, cm<sup>-1</sup>) (Spectrum 12): 3029, 2918, 1707 1158, 698.

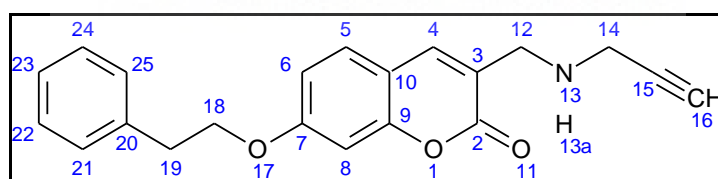
### 3.4.5 3-(Bromomethyl)-2-oxo-2H-1-benzopyran-7-yl diethylcarbamate (SM3B)



**Synthesis:** N-Bromosuccinimide (323 mg) was added to a suspension of 250 mg 3-methyl-2-oxo-2H-1-benzopyran-7-yl diethylcarbamate (SM2B) in 9 ml CCl<sub>4</sub>. Next, 192 mg of benzoyl peroxide (75%) was added to the mixture. After heating at reflux for 15 hours, the hot reaction mixture was filtered to remove the succinimide by-product. The solvent was removed *in vacuo* and the crude product was purified *via* flash column chromatography (Mobile Phase; DCM: hexane: ethyl acetate, 4:3:1) to obtain a white solid.

**Physical properties:** C<sub>15</sub>H<sub>16</sub>BrNO<sub>4</sub>; **mass:** 47 mg; **yield:** 15%; **mp:** 84-88 °C <sup>1</sup>H NMR (400 MHz, CDCl<sub>3</sub>) δH (Spectrum 21) : 7.83 (s, 1 H, H – 4), 7.48 – 7.46 (d, 1 H, *J* = 8.6 Hz, H – 5), 7.15 (d, 1 H, *J* = 1.9 Hz, H – 8), 7.13 – 7.10 (dd, 1 H, *J* = 2.1, 8.5 Hz, H – 6), 4.42 (s, 2 H, H – 12), 3.45 – 3.38 (m, 4 H, H – 18, 20), 1.28 – 1.19 (m, 6 H, H – 19, 21); <sup>13</sup>C NMR (100 MHz, CDCl<sub>3</sub>) (Spectrum 22) : 154.57, 154.39, 141.60, 128.52, 124.30, 118.95, 116.00, 110.16, 42.48, 42.08, 40.64, 35.28, 28.95, 27.66, 14.27, 13.30; **HR-ESI [M+H]<sup>+</sup>** (Spectrum 23) : calc. 354.0341, exp. 354.0344; **IR** (FT – IR, cm<sup>-1</sup>) (Spectrum 24) : 2979, 2920, 1615, 1246, 1147.

### 3.4.6 7-(2-Phenylethoxy)-3-{[(prop-2-yn-1-yl)amino]methyl}-2H-1-benzopyran-2-one (SM4A)

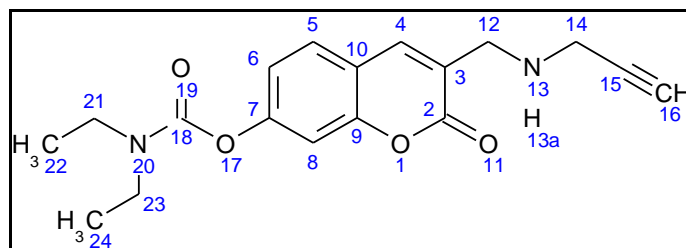


**Synthesis:** A mixture of 115 mg of 3-(bromomethyl)-7-(2-phenylethoxy)-2H-1-benzopyran-2-one (SM3A) and 441 mg of K<sub>2</sub>CO<sub>3</sub> was dissolved in 5 ml dried THF. Propargylamine (44 mg) was added dropwise and the mixture was stirred at room temperature for 48 hours. The K<sub>2</sub>CO<sub>3</sub> was filtered off and the solvent was removed under reduced pressure. The resulting crude product was purified using column chromatography (Mobile phase; hexane: ethyl acetate 2:1) and the product was obtained as a waxy amber solid.

**Physical Properties:** C<sub>21</sub>H<sub>19</sub>NO<sub>3</sub>; **mass:** 32 mg; **yield:** 30%; **mp:** wax; <sup>1</sup>H NMR (400 MHz, CDCl<sub>3</sub>) δH (Spectrum 13) : 7.70 (t, 1 H, *J* = 11.8 Hz, H – 4), 7.36 – 7.27 (m, 6 H, H – 5, 21, 22, 23, 24, 25), 6.84 – 6.81 (dd, 1 H, *J* = 2.4, 8.4 Hz, H – 8), 6.80 – 6.78 (d, 1 H, *J* = 2.2 Hz, H – 6), 4.23- 4.20 (t, 2 H, *J* = 6.9 Hz, H – 18), 3.82 (s, 2 H, H – 12), 3.52 (d, 2 H, *J* = 2.4, H – 14), 3.14 – 3.1 (t, 2 H, *J* = 7 Hz, H – 19), 2.28 (t, 1 H, *J* = 2.4 Hz, H- 16); <sup>13</sup>C NMR (100 MHz, CDCl<sub>3</sub>) (Spectrum 14): 161.81, 161.65,

155.06, 140.53, 137.63, 128.97, 128.66, 128.59, 126.71, 122.21, 113.05, 112.74, 101.17, 80.83, 72.52, 69.17, 47.67, 3.44, 35.47; **HR-ESI [M+H]<sup>+</sup>** (Spectrum 15) : calc. 334.1443, exp. 334.1450; **IR** (FT – IR, cm<sup>-1</sup>) (Spectrum 16) : 3284, 3027, 2922, 2853, 1706, 1237.

### 3.4.7 2-Oxo-3-[[prop-2-yn-1-yl]amino]methyl - 2H-1-benzopyran-7-yl diethylcarbamate (SM5A)



**Synthesis:** 3-(Bromomethyl)-2-oxo-2H-1-benzopyran-7-yl diethylcarbamate (120 mg, 0.34 mmol) was dissolved in 2.5 ml of THF before adding 480 mg (3.4 mmol) of K<sub>2</sub>CO<sub>3</sub> and 38 mg (0.68 mmol) of propargylamine. The mixture was stirred at room temperature for 48 hours following which the inorganic residue was filtered off after washing with THF. The resulting solution was concentrated *in vacuo* and purified using column chromatography (Mobile phase; DCM: hexane: ethyl acetate in a 20:1:1 ratio) and an off-white solid was obtained.

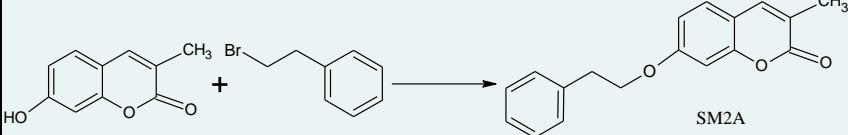
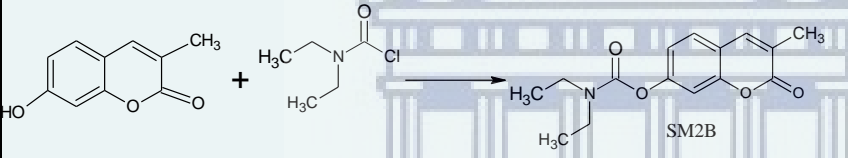
**Physical Properties:** C<sub>18</sub>H<sub>20</sub>N<sub>2</sub>O<sub>4</sub>; **mass:** 24 mg; **yield:** 21%; **mp:** 124-126 °C; **<sup>1</sup>H NMR** (400MHz, CDCl<sub>3</sub>) δH (Spectrum 25): 7.72 (s, 1 H, H – 4), 7.46 – 7.44 (m, 1 H, H – 5), 7.13 (d, 1 H, *J* = 2.0 Hz, H – 8), 7.10 – 7.07 (dd, 1 H, *J* = 2.2, 8.4 Hz, H – 6), 3.83 (s, 2 H, H – 12), 3.50 (s, 2 H, H – 14), 3.45 – 3.38 (m, 4 H, H – 21,23), 2.26 – 2.25 (t, 1 H, *J* = 2.1 Hz, H – 16), 1.28 – 1.19 (m, 8 H, H – 22, 24); **<sup>13</sup>C NMR** (100 MHz, CDCl<sub>3</sub>) (Spectrum 26) : 161.21, 153.94, 153.83, 153.29, 140.67, 128.44, 124.06, 118.65, 116.46, 109.94, 77.83, 74.45, 52.50, 42.86, 42.43, 42.04, 29.71, 14.26, 13.32; **HR-ESI [M+H]<sup>+</sup>** (Spectrum 27): calc. 330.3364, exp. 329.1495; **IR** (FT – IR, cm<sup>-1</sup>) (Spectrum 28): 2921, 2851, 1634, 1616, 1245.

### 3.5 Challenges and optimisation of synthesis

The S<sub>N</sub>2 conjugation reactions performed to add substituents to SM1 (see Scheme 3.1) were initially unsuccessful, thus modifications and optimisations had to be performed to the methods reported in the literature (see Table 3.1). For SM2A, the TLC plates for the initial reactions (performed with ethanol as a solvent at room temperature) indicated that there was no product forming from the reaction. Subsequent attempts were done with a change to acetonitrile as solvent (which is aprotic rather than protic, like ethanol) and a switch to microwave assisted synthesis, which resulted in a successful reaction with reasonable yield.

SM2B's reaction followed a similar trend with initially low yields, which likewise increased after switching to acetonitrile as the reaction solvent and the use of microwave conditions. The most significant observation was a near doubling in the yield following the addition of catalytic amounts of tetrabutylammonium hydrogensulphate (TBAHSO<sub>4</sub>). TBAHSO<sub>4</sub> acts as a phase transfer catalyst and not only increased the yield, but significantly cut down the overall reaction time.

**Table 3.1** Optimization of conjugation reactions occurring at position 7

Reaction	Conditions	Yield
	Ethanol NaH Stir @ room temp for 11hrs	<b>0%</b>
	Acetonitrile NaH MW @ 150 W, 80 °C, 5 Hr	<b>37%</b>
	DME K <sub>2</sub> CO <sub>3</sub> Stir @ room temp overnight	<b>0%</b>
	DME K <sub>2</sub> CO <sub>3</sub> Reflux for 12 hrs	<b>9%</b>
	Acetonitrile K <sub>2</sub> CO <sub>3</sub> MW @ 150 W, 100 °C, 6Hr	<b>27%</b>
	Acetonitrile K <sub>2</sub> CO <sub>3</sub> cat. TBAHSO <sub>4</sub> MW @ 150 W, 100 °C, 2.5Hr	<b>65%</b>

### 3.6 Conclusion

Seven compounds were successfully synthesised. The compounds' structures were confirmed using the analytical techniques as described in the instrumentation section and the results of the spectroscopies corroborated with their characteristics and expected values. Next, the compounds were analysed for *in vitro* biological activity as per the objectives of this study and the results are discussed in Chapter 4.

## Chapter 4

### 4. Biological Evaluation

#### 4.1 Introduction

Following the successful synthesis of the seven test compounds described in the last chapter, the compounds were evaluated using a number of *in vitro* assays in order to assess their potential as MTDLs. It is hypothesised that the compounds would show inhibitory activity towards AChE, BuChE as well as selective MAO-B inhibition. *In silico* modelling was also performed in order to simulate and elucidate the nature of the interactions these compounds could have with the aforementioned enzymes.

#### 4.2 Cholinesterases activity

Cholinesterase activity is determined using a colorimetric method first described by Ellman *et al* (1961). The assay is based on the principle that AChE and BuChE catalyse acetylthiocholine and butyrylthiocholine respectively, which are sulphur containing analogues of their natural substrates. Upon catalysis, thiocholine is cleaved off and reacts with 5,5-dithiobis-2-nitrobenzoate (DTNB) to form 5-thio-2-nitrobenzoate, which produces a yellow colour and is measured at a wavelength of 405 nm (Pohanka, *et al.*, 2011). The enzymes' activity is directly proportional to the formation and intensity of 5-thio-2-nitrobenzoate. The inhibitory activity of a compound can therefore be derived from the difference in the absorbance readings between a blank reaction mixture with no inhibitor and a run with the test compound. Using this percentage inhibition data over a range of concentrations, dose-response curves can be constructed to determine the IC<sub>50</sub> values of the test compounds.

##### 4.2.1 Consumables and instrumentation

All chemicals and reagents were obtained from Sigma-Aldrich® (Steinheim, Germany). The intensity of colour change and absorbance readings were obtained using a Rayto 2100C microplate reader (Shenzhen, China) set at an absorbance wavelength of 405 nm. The data obtained was analysed using Microsoft Excel® and GraphPad Prism software.

##### 4.2.2 Experimental procedures

The test compounds and positive control (donepezil) were dissolved in DMSO to prepare 10 mM stock solutions. The stock was then further diluted by factors of ten to produce solutions of 1 mM, 100 µM, 10 µM, 1 µM and 0.1 µM which would correspond to concentrations of 100 µM, 10 µM, 1 µM, 0.1 µM and 0.01 µM in the final reaction mixture. The test concentrations were stored in the refrigerator until the day of the assay.

Tris-HCl buffer (50 mM, adjusted to a pH 8 using 2 N NaOH) was prepared as the buffer and used to prepare enzyme stock solution (22 U/ml for *Electrophorus electricus* AChE and 12 U/ml BuChE from equine serum), 15 mM acetylthiocholine iodide, 15 mM S-butyrylthiocholine iodide and 1.5 mM DTNB (Ellman's reagent). The enzyme stock solution was stabilised for storage with 1% bovine serum albumin and stored in aliquots at -80 °C until the assay was performed.

The assay was performed in a clear, flat bottom 96 well plate, with each row consisting of wells for the positive control, the seven test compounds and the negative control. Each concentration was performed in triplicate. Prior to the assay the background absorbance for each compound at the different test concentrations was measured and accounted for when reading the final absorbance.

Before performing the assay, the enzyme was diluted to 0.88 units/ml for AChE and 0.48 units/ml for BuChE. In each individual well 148 µL DTNB, 50 µL of the enzyme and 2 µL of the test compound or

control (donepezil in the positive control and DMSO in the negative control well) were added and incubated at 25 °C for 10 minutes. Following this, 30 µL of the substrate was added to each well simultaneously using a multipipette. The plate was then placed in a Rayto® RT-2100C microplate reader and the absorbances were measured every 60 seconds over a 20-minute period. The data obtained was used to calculate the maximum inhibition over the 20-minute period and this was used to plot a dose-response graph, which subsequently could be used to extrapolate the IC<sub>50</sub> values of the compounds. A one sample t-test was performed by comparing the mean values of the compounds' data against the mean for the negative control. The concentration of DMSO was kept constant at less than 1% in order not to interfere with the assay results.

### 4.2.3 AChE assay results and discussion

In general, the designed compounds were expected to have good AChE inhibitory capacity. The starting scaffold, SM1, is expected to have the least activity and activity of the compounds is predicted to increase once substitutions are performed on positions 3 and/or 7 of the scaffold. This increase in activity should arise from the fact that the resultant molecules should become large enough to span the length of the active site gorge and interact with both the CAS and PAS (Catto, *et al.*, 2006). The nature of the substitutions could also affect the inhibitory activity, with series B's carbamate containing compounds expected to have superior activity compared to series A's compounds (Ma, *et al.*, 2010; Colovic, *et al.*, 2013). The propargylamine containing compounds SM4A and SM5A were expected to have greater activity due to the length of the compounds resulting in dual site binding (Stefanachi, *et al.*, 2018).

The results of the assay were analysed and a one-way t-test was performed using GraphPad Prism to determine that all values were statistically significant, with p-values less than 0.05. Percentage inhibition of the compounds was measured relative to the negative control, which is assumed to represent the enzyme's uninfluenced activity. The results of the assay showed that in general the compounds had low inhibitory activity against AChE. Figure 4.1 below summarises the percentage AChE inhibition observed at the highest concentration (100 µM) used for this assay. It can be observed that compounds SM1, SM2A and SM2B exhibited the least inhibitory activity, all displaying less than 15% enzyme inhibition at a 100 µM concentration. Compounds SM3A, SM4A and SM5A performed slightly better as they displayed 25-30% inhibition at this concentration. Compound SM3B displayed the best inhibitory activity with 49% inhibition, and the data was plotted onto a dose response curve which shows that its IC<sub>50</sub> value lies at around 108 µM (Figure 4.2).

The results demonstrate that substitutions with the carbamate or benzyloxy moieties at position 7 do not solely confer significant AChE inhibitory activity to the scaffold, as SM2A and SM2B have similar activity to SM1. However, α-bromination of the methyl at position 3 to produce -CH<sub>2</sub>Br appears to enhance the molecules inhibitory effect. This can be observed by the increase in inhibition observed with SM3A and SM3B as compared to SM2A and SM2B and these 3-bromomethyl derivatives had the highest inhibition in both series. With the exception of SM3B, the compounds with the carbamate moiety did not display superior activity as expected based on the literature.

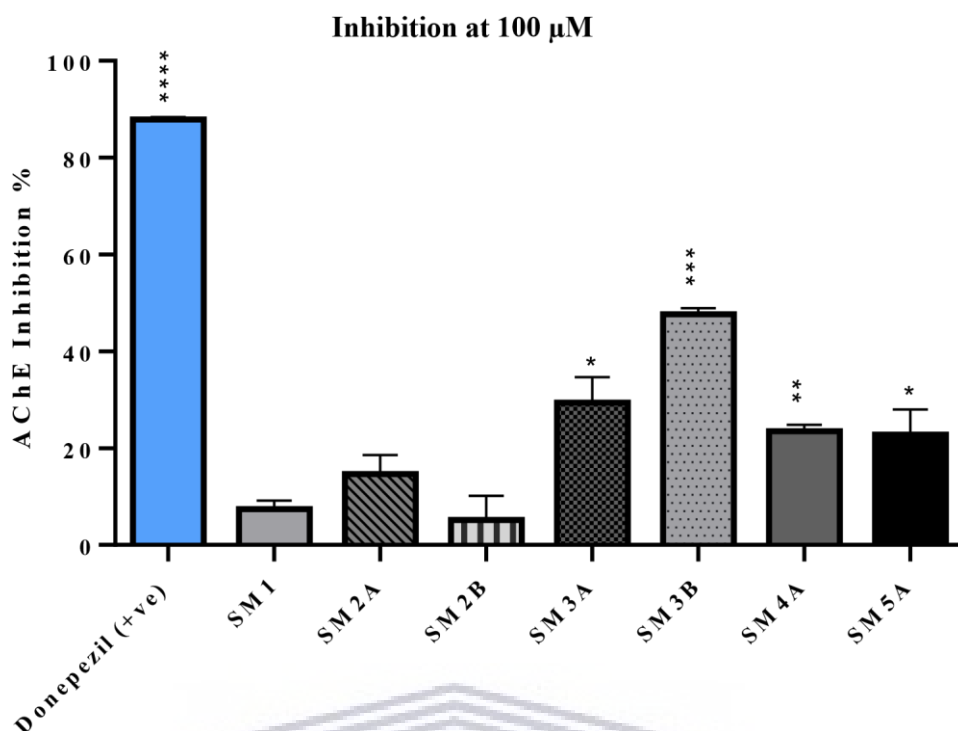


**Figure 4.1:** AChE inhibition for each test compound at 100  $\mu$ M. Data was performed in triplicate with each bar representing the mean percentage inhibition  $\pm$  standard deviation. A one sample t test was used to compare the compounds data to the -ve control. The asterisks indicate the statistical significance of each data set (\*,  $p < 0.05$ ; \*\*,  $p < 0.005$ ; \*\*\*,  $p < 0.001$  and \*\*\*\*,  $p < 0.0001$ ).

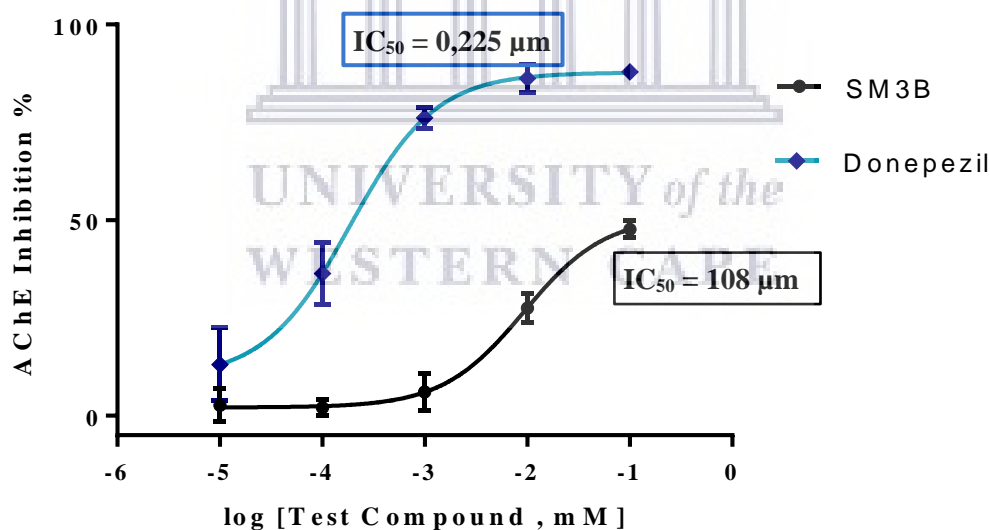


**Figure 4.2:** Non-linear dose response curves for the most active compound SM3B and donepezil indicating their  $IC_{50}$  values. Each data point is plotted indicating the mean inhibition  $\pm$  SD at each concentration.

As observed with SM4A and SM5A, the incorporation of propargylamine did not result in the expected increase in activity. These compounds were hypothesized to have the best inhibitory activity due to their length, and whilst they displayed better inhibition than SM2A and SM2B, overall this difference was not significant. Docking simulations were performed on the compounds in order to elucidate the structure activity relationships responsible for the observed weak inhibitory activity of the compounds.



### 4.2.3.1 Molecular Modelling of AChE

The AChE enzyme active site is an ellipsoid shaped gorge, consisting of 2 main sites termed the peripheral anionic site (PAS) and the choline binding site (also termed the CAS) containing the catalytic triad. The peripheral anionic site is situated at the entrance of the active site. It is made up of largely aromatic amino acids such as Trp 279 and is responsible for guiding and stabilising substrates in the active site. Towards the bottom of this gorge lies the CAS and catalytic triad, which are essential for the enzymes' catalytic capability (Sussman & Silman, 1992). In order for inhibition to take place the designed ligands were expected to form binding interactions with amino acids found in these mentioned regions, ideally interacting with both sites simultaneously. From literature it is expected that the coumarin nucleus will sit in the PAS of the enzyme and the various substituents interact with the CAS and catalytic triad (Anand & Singh, 2013).

#### 4.2.3.1.1 Molecular Modelling Methods

Molecular Operating Environment (MOE) 2018 on the Windows platform was used for the studies. The co-crystallised AChE enzyme was obtained from the PSLIO/PDB data bank co-crystallised with donepezil (Code: 1EVE). Prior to the studies the enzyme was first energy minimised and the enzyme was protonated to position hydrogens and assign ionization states in the macromolecular structure. The co-crystallised ligand was then selected to identify which binding site to use as the pocket for docking. The prepared enzyme was then saved in this state for use in docking studies.

The test ligands were drawn using the ChemSketch 2016 software, saved as MDL files (V3000) and prepared for docking by energy minimising them in MOE using the MMFF94 force field. A database of these compounds was created and docking performed. Five possible docking conformations for each compound were tested and the conformer with the lowest binding energy selected and discussed below.

#### 4.2.3.1.2 Results

The results of the docking simulations were used to correlate the structure activity relationships responsible for the results obtained in the AChE assay. Accordingly, the weak activity of SM1 can be attributed to the fact that none of its most stable conformations allow it to form significant interactions with any key residues in the AChE active site gorge (Figure 4.3)

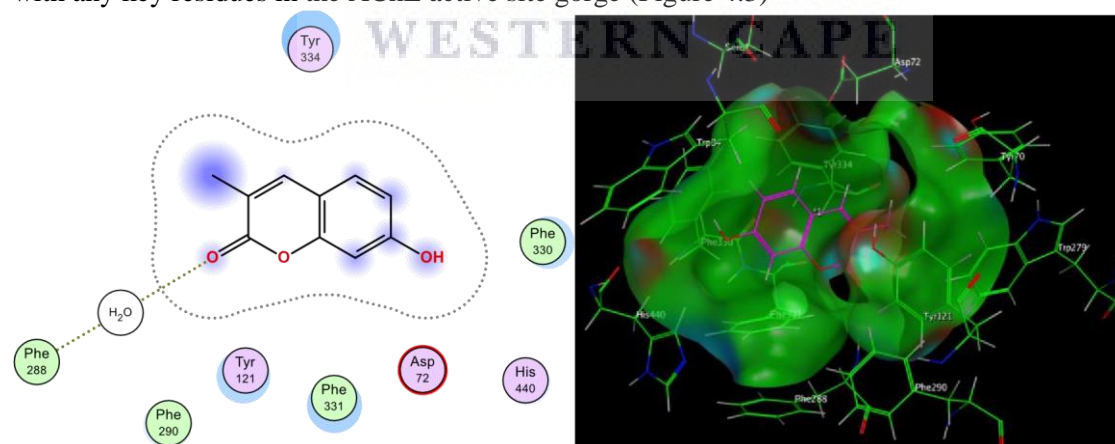


**Figure 4.3:** Diagrammatic representation of compound SM1's lack of binding interactions with AChE (left). A 3D docking simulation (right) shows SM1 indicated in pink and the active sites' amino acids indicated in green.

The addition of the substituents to position 7 done in SM2A and SM2B results in orienting the coumarin nucleus away from the PAS and towards the CAS (Figure 4.4). When the molecules are oriented in this

way, neither compound is able to form favourable interactions with amino acids in either of these regions.

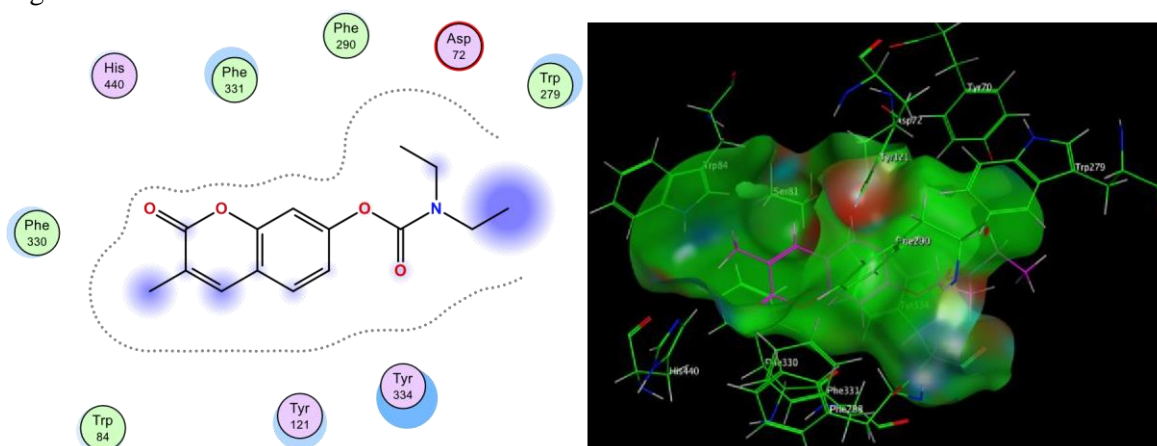


**Figure 4.4:** Diagrammatic representation of compound SM2B binding interactions with AChE (left) and docking simulation (right) with SM2B indicated in pink and amino acids indicated in green.

The improved inhibitory capacity of compounds SM3A and SM3B can be attributed to the replacement of the CH<sub>3</sub> at position 3 with -CH<sub>2</sub>Br (See Figure 4.5). The molecules appear to have similar poses as seen with SM2B in the active site, however the -CH<sub>2</sub>Br group forms  $\pi$ -H interactions with Trp 84. Additionally, there is  $\pi$ - $\pi$  stacking between the aromatic region of the coumarin and Phe 330, both of which are key residues for substrate binding in the CAS. It can be hypothesised that the electron withdrawing effect caused by bromine may have led to more stable interactions with the aromatic Trp 84 residue and was responsible for these compounds' superior inhibitory activities.

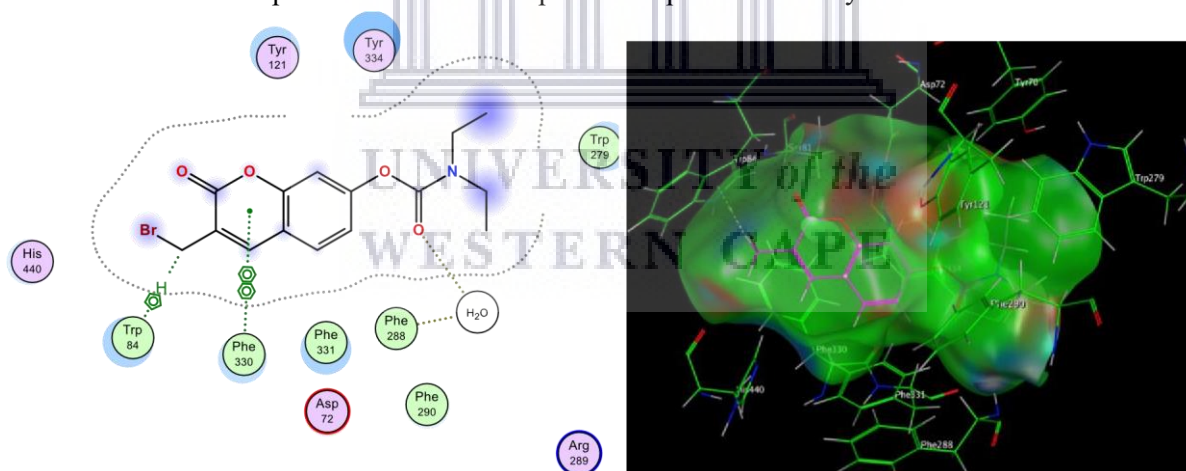


**Figure 4.5:** Diagrammatic representation of compound SM3B binding interactions with AChE (left) and docking simulation (right) with SM3B indicated in pink and amino acids indicated in green.

Figure 4.6 below shows that while the addition of the propargylamine moiety in derivatives SM4A and SM5A elongated the molecules, it did not contribute to the formation of any favourable interaction in the active site. The added length altered the conformation and disrupted the binding interactions which had been demonstrated with SM3A and SM3B.

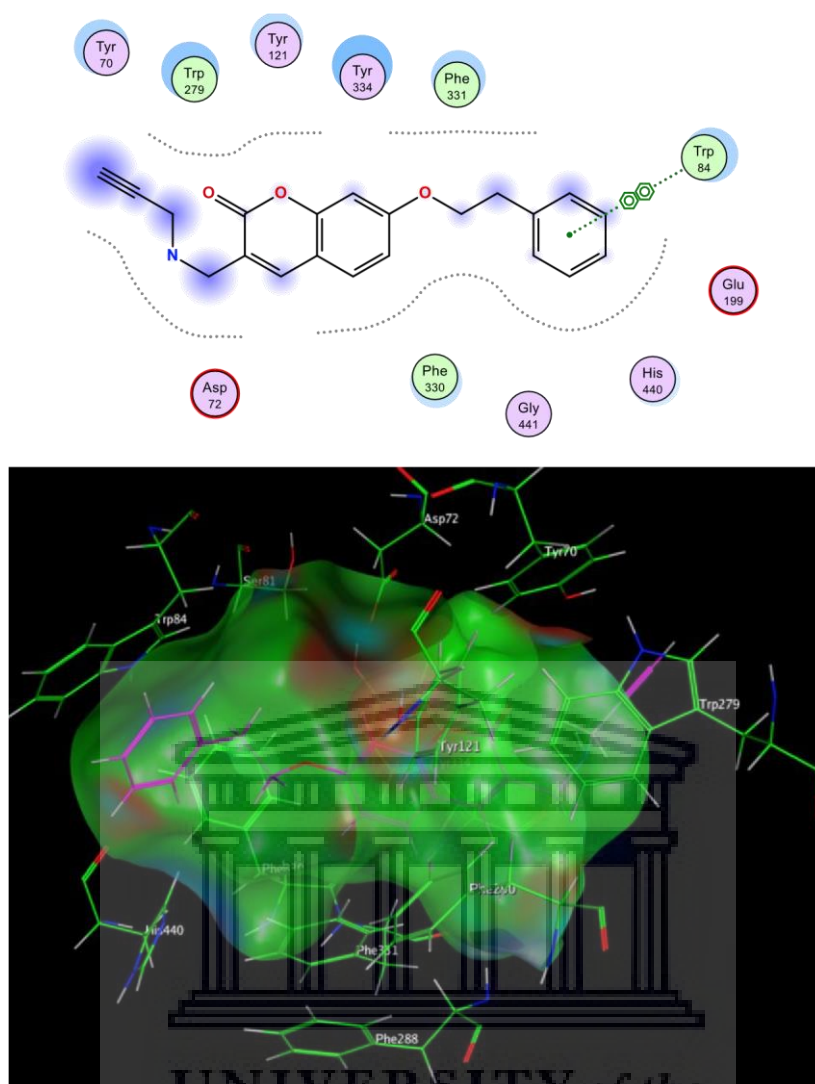


**Figure 4.6:** Diagrammatic representation of compound SM4A binding interactions with AChE (top) and docking simulation (bottom) SM4A indicated in pink and amino acids indicated in green. The propargylamine moiety lies outside of the active site.

#### 4.2.4 BuChE assay results and discussion

The compounds were also expected to have BuChE inhibitory activity in line with the objectives of this study, bearing in mind the takeover role this enzyme has in the advanced disease state. The results represented in Figure 4.6 show that in general, the compounds were more active against BuChE than AChE at the 100  $\mu$ M concentration. Each compound had a higher percentage inhibition than when tested against AChE with compounds SM2A, SM2B, SM3A and SM4A displaying 32% to 40% enzyme inhibition.

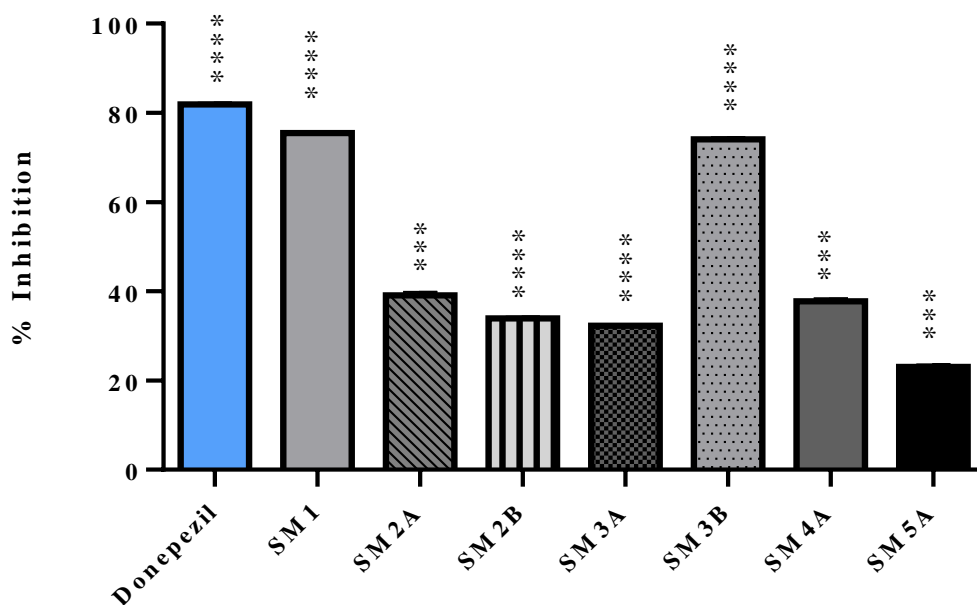


**Figure 4.7:** Percentage inhibition of BuChE at 100  $\mu\text{M}$  concentration by the test compounds. Each bar represents the mean percentage of inhibition as well as standard deviation. A one sample t test was used to compare the compounds data to the -ve control. The asterisks indicate the statistical significance of the data sets (\*\*\*,  $p < 0.001$  and \*\*\*\*,  $p < 0.0001$ ).

Compounds SM1 and SM3B were the most active inhibitors with  $\text{IC}_{50}$  values of 20.25  $\mu\text{M}$  and 23.27  $\mu\text{M}$ , respectively (Figure 4.9). These values show that whilst the compounds have good activity they are not as potent as more typical cholinesterase inhibitors such as donepezil (Figure 4.7). The base scaffold SM1 displayed the best BuChE inhibition and the trend of the results show that substitution on position 7 with either the carbamate or benzyloxy moiety leads to a decrease in activity. Whilst  $\alpha$ -bromination of the  $-\text{CH}_3$  does not affect the 7-benzyloxy derivative, this drastically improves the activity of the 7-carbamate derivative (SM3B). Replacing the  $-\text{Br}$  with the propargylamine moiety diminishes the inhibitory capacity of the 7-carbamate derivatives and does not improve the already poor activity of the 7-benzyloxy derivative.

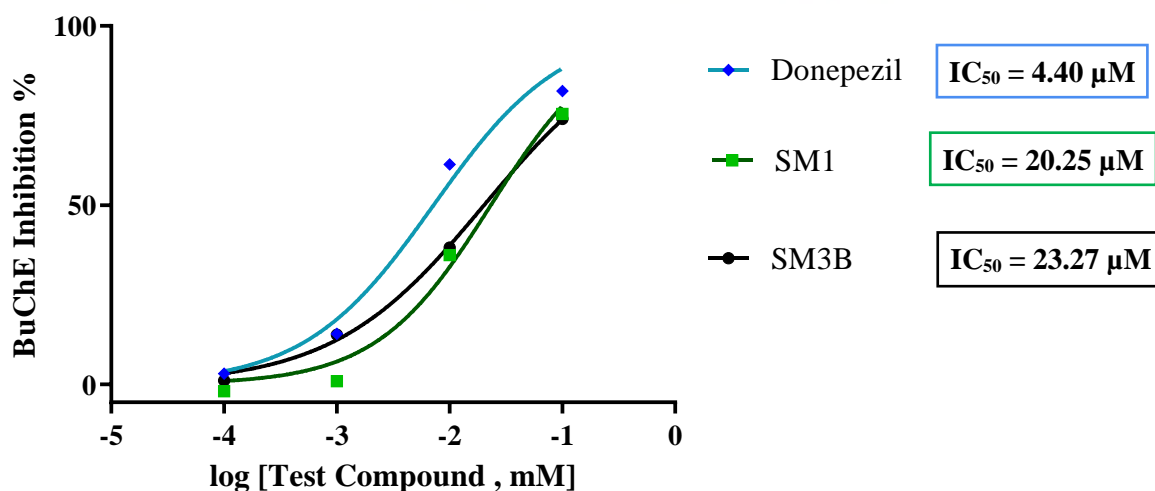


**Figure 4.8:** Non-linear dose response curves for donepezil and the most active compounds, SM1 and SM3B, with  $\text{IC}_{50}$  values indicated. Each data point is plotted indicating the mean inhibition  $\pm$  SD at each concentration.

Based on their higher percentage inhibition for BuChE, the tested compounds can be classified as weakly selective BuChE inhibitors. The compounds' selectivity may be hypothesized to them having stronger binding interactions with the higher density of hydrophobic amino acids lining the active site gorge of BuChE. The larger volume of BuChE's active site may also allow the enzyme the ability to accommodate the compounds better as compared to AChE (Shen, *et al.*, 2006).

### 4.3 MAO Assay

In order to assess the compounds for *in vitro* activity against MAO-A and MAO-B, a fluorometry based assay was performed. MAO is a known catalytic deaminator for a wide range of substances and this assay takes advantage of this by utilizing the synthetic compound kynuramine as an alternative substrate to be catalysed in place of typical substrates such as dopamine (Mazzio, *et al.*, 2012). The oxidative catalysis of kynuramine by MAO produces 4-hydroxyquinolone (4HQ), which is fluorescent and thus its formation can easily be detected using a fluorometer at an excitation wavelength of 310 nm and emission wavelength of 410 nm (See Figure 4.9 ) (Matsumoto, *et al.*, 1985).



**Figure 4.9:** Formation of the fluorophore 4HQ following catalysis of kynuramine.

The intensity of fluorescence detected can therefore be directly correlated to the enzyme activity. When the enzyme is fully active there is no interference with 4HQ production. Therefore in the presence of an inhibitor, less fluorescence is detected as less 4HQ is produced. The degree of enzyme inhibition can therefore be calculated as a function of the difference between these two fluorescence readings. The percentage inhibition across a range of concentrations was calculated and used to plot non-linear dose-response curves in order to determine the IC<sub>50</sub> values of the compounds.

#### 4.3.1 Consumables and instrumentation

All chemicals and reagents were obtained from Sigma-Aldrich® (Steinheim, Germany). The fluorescence readings were obtained using a SynergyMx Biotek spectrophotometer (Winooski, USA) with readings done at excitation and emission wavelengths of 310 nm and 410 nm respectively. The data obtained was analysed using Microsoft Excel® and Graph Pad Prism 8 software.

#### 4.3.2 Experimental procedures

The test compounds and positive control (clorgiline for MAO-A and rasagiline for MAO-B) were dissolved in DMSO to prepare 10 mM stock solutions. The stock was then further diluted by factors of ten to produce solutions of 1 mM, 100 µM, 10 µM, 1 µM and 0.1 µM which would correspond to concentrations of 100 µM, 10 µM, 1 µM, 0.1 µM and 0.01 µM in the final reaction mixture. The test concentrations were stored in the refrigerator until the day of the assay. A potassium phosphate buffer (KH<sub>2</sub>PO<sub>3</sub> 100 mM, pH 7.4, adjusted by 2N NaOH, made isotonic using 0.9 % w/v NaCl) was prepared

and refrigerated until further use. The enzyme stock solutions were prepared by dissolving 2.5 mg of enzyme in 33.33 ml of phosphate buffer to produce stock solutions of 0.075 mg/ml which were stored in 1 ml aliquots at -80 °C until the assay. Once in the final reaction mixture this enzyme solution will have a concentration of 0.0075 mg/ml. The substrate was prepared by dissolving kynuramine HBr in potassium buffer and was prepared as two separate concentrations; 750 µM for MAO-A and 500 µM for MAO-B. When placed in the reaction mixture, these solutions ended up with final concentrations of 45 µM for MAO-A and 30 µM for MAO-B respectively. Fresh substrate was prepared on the day of the assay.

The assay was carried out in 2 ml Eppendorf vials. To each vial, 207.5 µL of phosphate buffer was added followed by 2.5 µL of the respective test compound or control (positive control: clorgiline for MAO-A or rasagiline for MAO-B; control: DMSO). Following this, 25 µL of the enzyme stock was added to each vial in 10 second intervals and the vials were incubated at 37 °C for 10 minutes. After this time period 15 µL of kynuramine (750 µM for MAO-A and 500 µM for MAO-B) was added at 10 second intervals and then incubated for 20 minutes. To stop the reaction at the end of this time 150 µL of 2 N NaOH was added and the mixture was shaken. Using a micropipette 80 µL of the mixture was transferred to a well in a black flat based 96 well plate. The plate was placed in the fluorescent reader and readings taken at excitation/emission wavelength of 310 nm/410 nm. Each assay was performed in triplicate and the data was analysed using Graph Pad Prism 8 software.

#### 4.3.3 Results and discussion

Coumarin derivatives are known to be fluorophores and based on the principal of this assay this may interfere with obtained results (Donovalová, *et al.*, 2012). Accordingly, the background fluorescence of each test compound at each concentration had to be accounted for inhibition calculations. The enzyme inhibition was calculated using the formula:

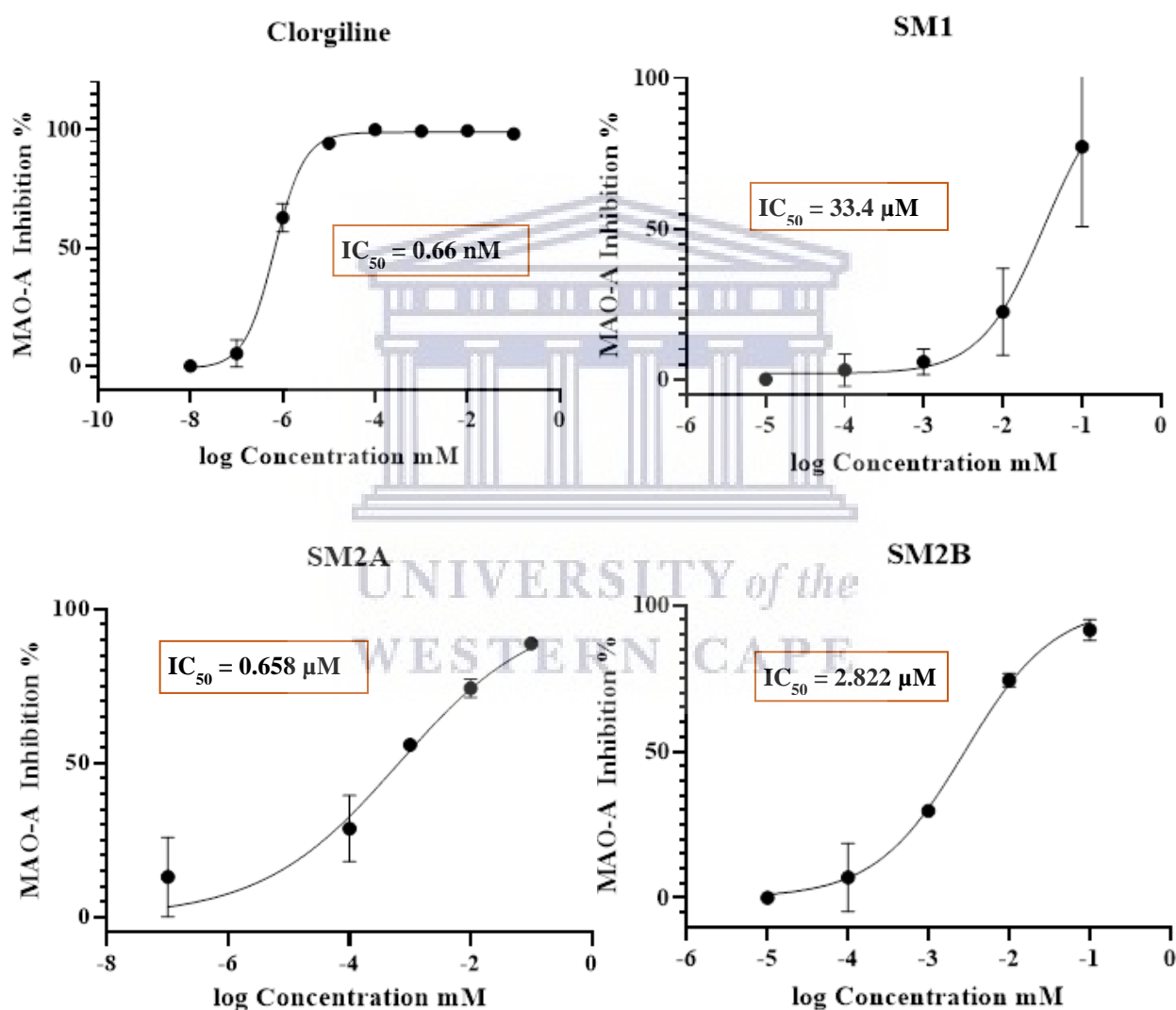
$$\text{Enzyme Inhibition \%} = \frac{\text{DMSO control fluorescence} - (\text{Test fluorescence} - \text{Background fluorescence}) \times 100}{\text{Negative Control fluorescence}}$$

It was expected that all compounds would display inhibition for both isoforms of the MAO enzyme. Based on work done by Foka *et al* (2018) and Bruhlmann *et al* (2001), it was expected that the benzyloxy substitution would impart superior MAO inhibition to the test compounds compared to the carbamate moiety. Thus, the compounds expected to perform best would be from series A. The propargylamine derivatives from each series were expected to have enhanced inhibition of both isoforms, but with selectivity towards MAO-B (Kumar, *et al.*, 2016).

##### 4.3.3.1 MAO-A

The results of the MAO-A assay demonstrated that all the tested compounds exhibited good inhibitory activity towards the enzyme. Compounds SM2A, SM3A and SM3B performed best, displaying IC<sub>50</sub> values in the mid nanomolar range, but did not perform as well as clorgiline the positive control (Figure 4.10). The results confirmed that whilst substitutions to position 7 increased the inhibitory capacity, the benzyloxy moiety confers superior inhibition as compared to the carbamate moiety. This is demonstrated with the fact that with the exception of SM3A, the compounds with this substitution have 5 to 6 times higher activity than their counterparts in series B.

Contrary to expectations for the assay, the results showed that substitution of propargylamine led to decreased activity of the compounds, with SM4A and SM5A having the lowest activities barring the unsubstituted scaffold SM1. This trend was demonstrated in both series of compounds, in the case of SM5A the activity of the compound was 8 to 60-fold less active than the other compounds in the same series. SM3A and SM3B showed the best activities with  $IC_{50}$  values of  $0.476 \mu\text{M}$  and  $0.3545 \mu\text{M}$  respectively. Replacing the  $-\text{CH}_3$  with  $-\text{CH}_2\text{Br}$  at position 3 showed a significant increase in activity of the compounds towards MAO-A.  $\alpha$ -Bromination of the methyl group introduces a large electron withdrawing group and it can be hypothesised that this allows the molecules to form stronger significant interactions with amino acids in the enzymes active site. This, among other structure activity relationships, will be explored with molecular modelling performed on these compounds later in the chapter.



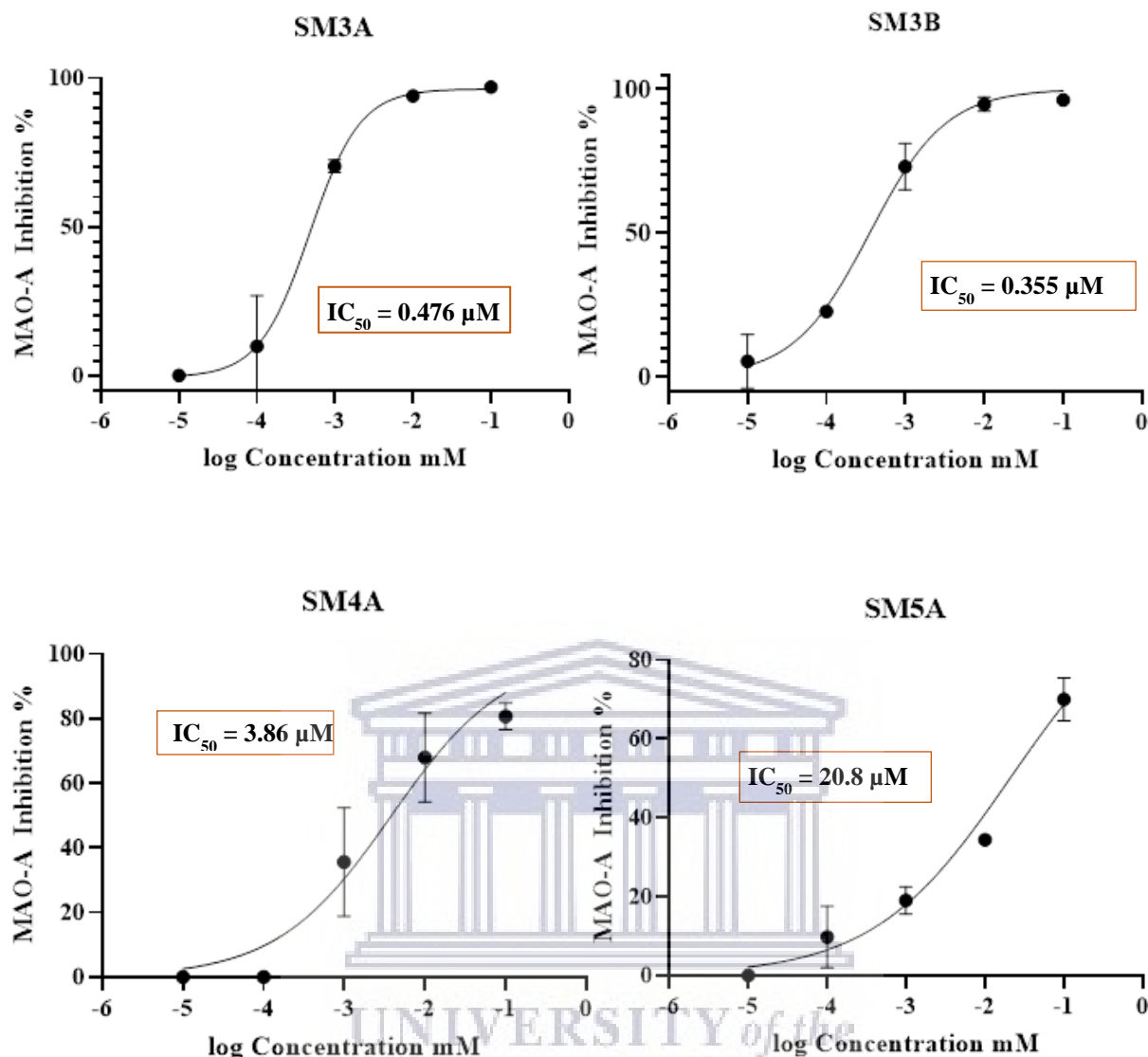


**Figure 4.10:** Dose-response curves for MAO-A inhibition with  $IC_{50}$  values displayed for the test compounds and positive control. Each data point is plotted indicating the mean inhibition  $\pm$  SD at each concentration.

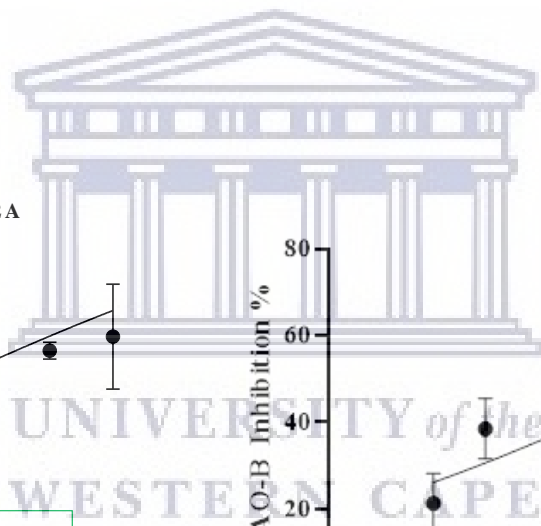
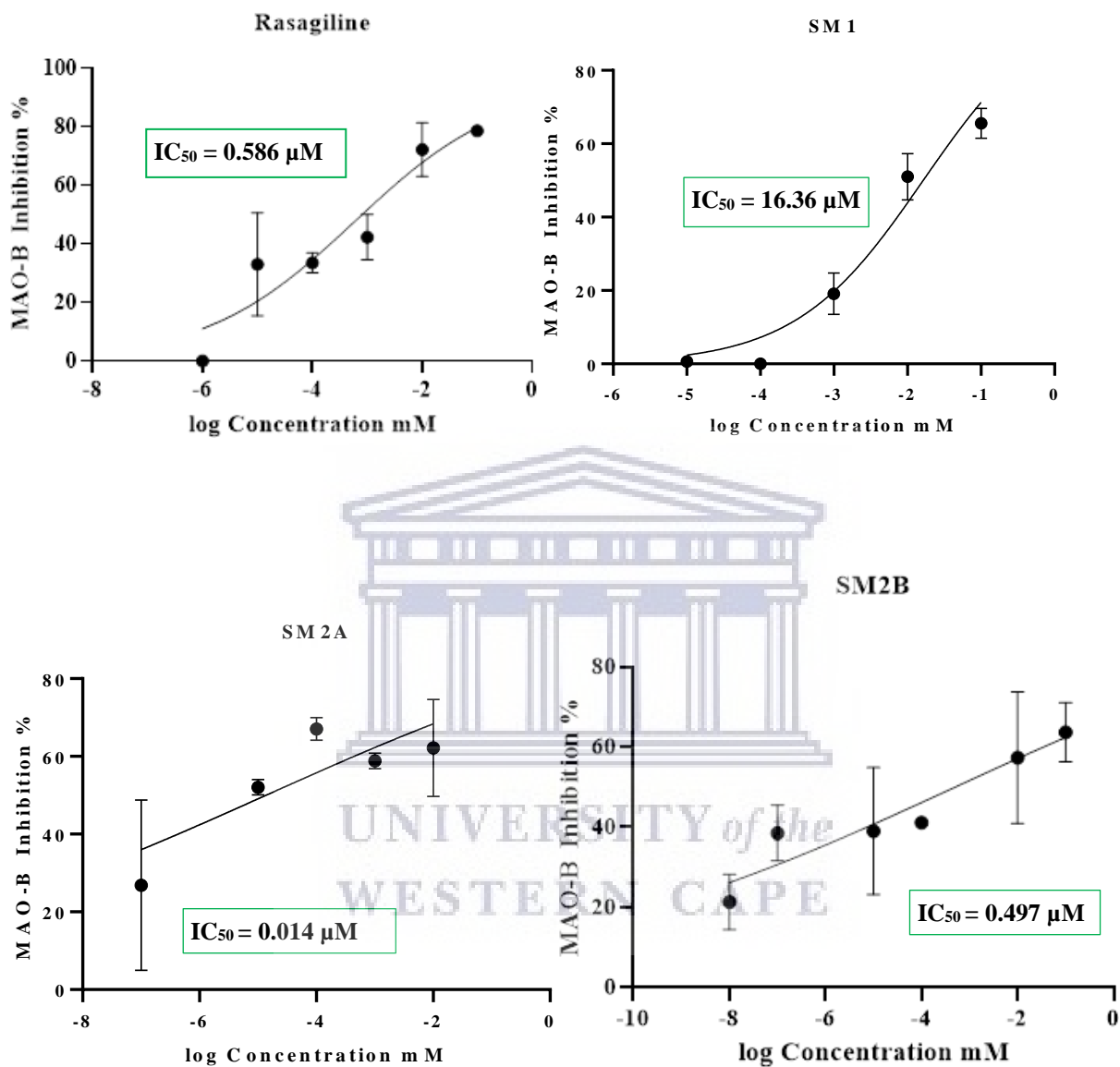
#### 4.3.3.2 MAO-B

The results of the MAO-B assay demonstrated that the majority of the tested compounds had superior inhibitory activity towards this enzyme as compared to MAO-A (Figure 4.11). This fits into the hypothesis that the compounds would have superior MAO-B activity. The exception to this was SM3A, which only exhibited 35% enzyme inhibition at the highest concentration for the assay (100  $\mu\text{M}$ ). Five of the test compounds demonstrated to be exceptionally good inhibitors of MAO-B, with nanomolar  $IC_{50}$  values. Compounds SM2A and SM4A performed best in the assay with  $IC_{50}$  values of 13 nM and 27 nM. This makes them 20 to 40 times more potent than rasagiline, an MAO-B inhibitor currently on the market indicated for PD treatment.

Similar to what was observed for MAO-A, substitution of the benzyloxy at position 7 conferred superior activity as compared to substitution of the carbamate moiety. This is observed in that the 7-benzyloxy compounds displayed better inhibition than their 7-carbamate substituted counterparts. Unlike what was



observed for MAO-A, the incorporation of the propargylamine imparts increased activity with compounds SM4A and SM5A displaying nanomolar  $IC_{50}$  values.



UNIVERSITY of the  
WESTERN CAPE

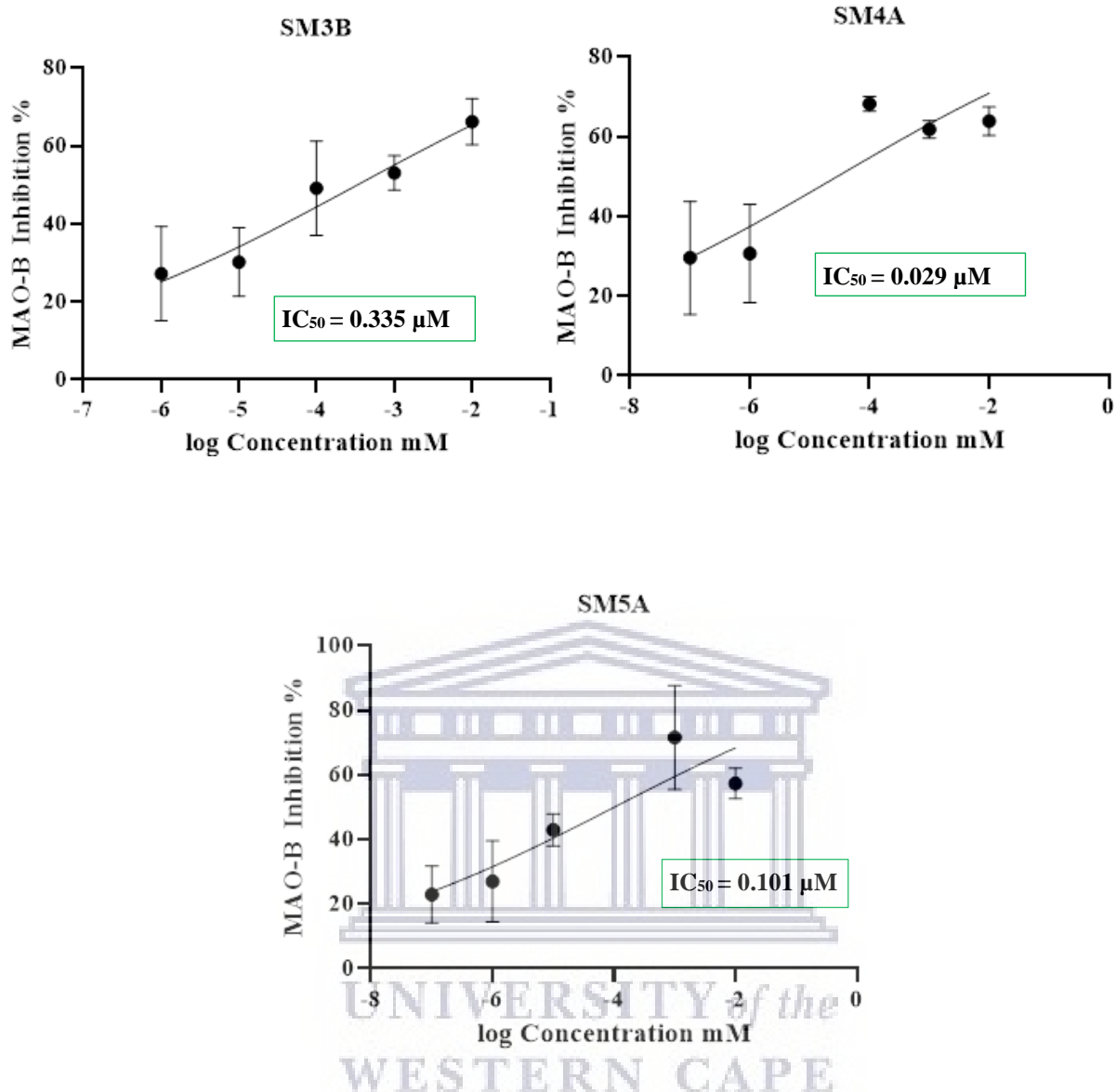


**Figure 4.11:** Dose-response curves for MAO-B inhibition with IC<sub>50</sub> values displayed for the test compounds and positive control. Each data point is plotted indicating the mean inhibition  $\pm$  SD at each concentration.

These results demonstrated that the compounds were more selective for the MAO-B isoform over the MAO-A isoform. This is desirable as this is the isoform found predominantly in the brain and avoids the potential of a tyramine induced hypertensive crisis developing as seen with non-selective inhibitors (Grady & Stahl, 2012). The selectivity index (SI) was used to calculate and quantify how much more selective the compounds are for MAO-B than MAO-A using the following formula:

$$\text{Selectivity Index} = \frac{\text{MAO-A IC}_{50}}{\text{MAO-B IC}_{50}}$$

From table 4.1 below, it can be inferred that compounds in Series A have greater selectivity for MAOB, thus it can be hypothesised that the benzyloxy moiety in position 7 imparts this desirable selectivity. It can also be observed that whilst  $\alpha$ -bromination of the methyl group at position 3 increases MAO-A

inhibitory activity (as seen for SM3B), this comes at the cost of diminishing the compounds' selectivity towards MAO-B. Incorporation of propargylamine appears to have the greatest influence on the compounds selectivity as the propargylamine derivatives SM4A and SM5A have the greatest selectivity, being 130 to 200 times more selective towards MAO-B than MAO-A.

Overall the assay results are promising as it can be observed that the synthesised compounds display good inhibitory activity towards both MAO enzyme isoforms. In addition to this, six of the compounds are selective towards MAO-B. Molecular modelling was conducted in order to determine the binding interactions responsible for the observed results.

**Table 4.1:** Summary of MAO IC<sub>50</sub> values and selectivity indices of test compounds.

Compound	MAO-A IC <sub>50</sub>	MAO-B IC <sub>50</sub>	Selectivity Index
Clorgiline (+ve)	0.66 nM	-	-
Rasagiline (+ve)	--	0.586 μM	-
SM1	33.4 μM	16.36 μM	2.04
SM2A	0.658 μM	0.014 μM	47.7
SM2B	2.822 μM	0.497 μM	5.67
SM3A	0.476 μM	-	-
SM3B	0.355 μM	0.333 μM	1.05
SM4A	3.86 μM	0.029 μM	133.2
SM5A	20.8 μM	0.101 μM	205.9

#### 4.3.4 Molecular Modelling of MAO

MAO-A and MAO-B share 70% of their amino acid sequence. Both enzymes have an entrance cavity and a substrate cavity which contains the FAD co-factor essential for enzyme function. MAO-B's active site is smaller and elongated as compared to MAO-A, whose active site is more round shaped and allows for greater substrate rotation (Medvedev, *et al.*, 2003). Whilst MAO-A crystallises as a simple monomer MAO-B crystallises as a dimer, however for the purpose of these simulations only one monomeric unit was considered. Based on the literature, it was expected that for all the compounds the coumarin moiety should fit well into the enzymes' substrate cavity and subsequently form interactions with key amino acids (Gnerre, *et al.*, 2000).

##### 4.3.4.1 Molecular modelling methods

Molecular Operating Environment (MOE) 2018 on the Windows platform was used for the studies. The co-crystallised MAO enzymes were obtained from the PSLIO/PDB data bank with MAO-A co-crystallised with clorgiline (Code: 2BXS) and MAO-B co-crystallised with safinamide (Code: 2V5Z). Prior to the studies the enzymes were energy minimised and the enzyme was protonated to position hydrogens and assign ionization states in the macromolecular structure. The co-crystallised ligand was

then selected to identify which binding site to use as the pocket for docking and the prepared enzyme was then saved in this state for use in docking studies.

The test ligands were drawn using the ChemSketch 2018 software and saved as MDL files (V3000) and energy minimised to prepare them for docking. A database of these compounds was created and docking performed. Five possible docking conformations for each compound were tested and the one with the lowest binding energy chosen and discussed below.

#### 4.3.4.2 Results

The docking results from SM1 showed that the coumarin nucleus fits well into both enzymes' active sites. However, for MAO-A while the nucleus simply enters the entrance cavity site there are no significant binding interactions occurring with amino acids in this site. Contrary to this, for MAO-B it can be observed that the coumarin moiety fits well into the entrance cavity, forming relatively stable  $\pi$ -H bonds between the aromatic ring and the amino acids Ile 199 and Leu 171 (Figure 4.13). This hydrogen bond with the Leu 171 residue on the fringe of the substrate cavity was observed and conserved for the rest of the compounds and may explain their selectivity towards MAO-B.

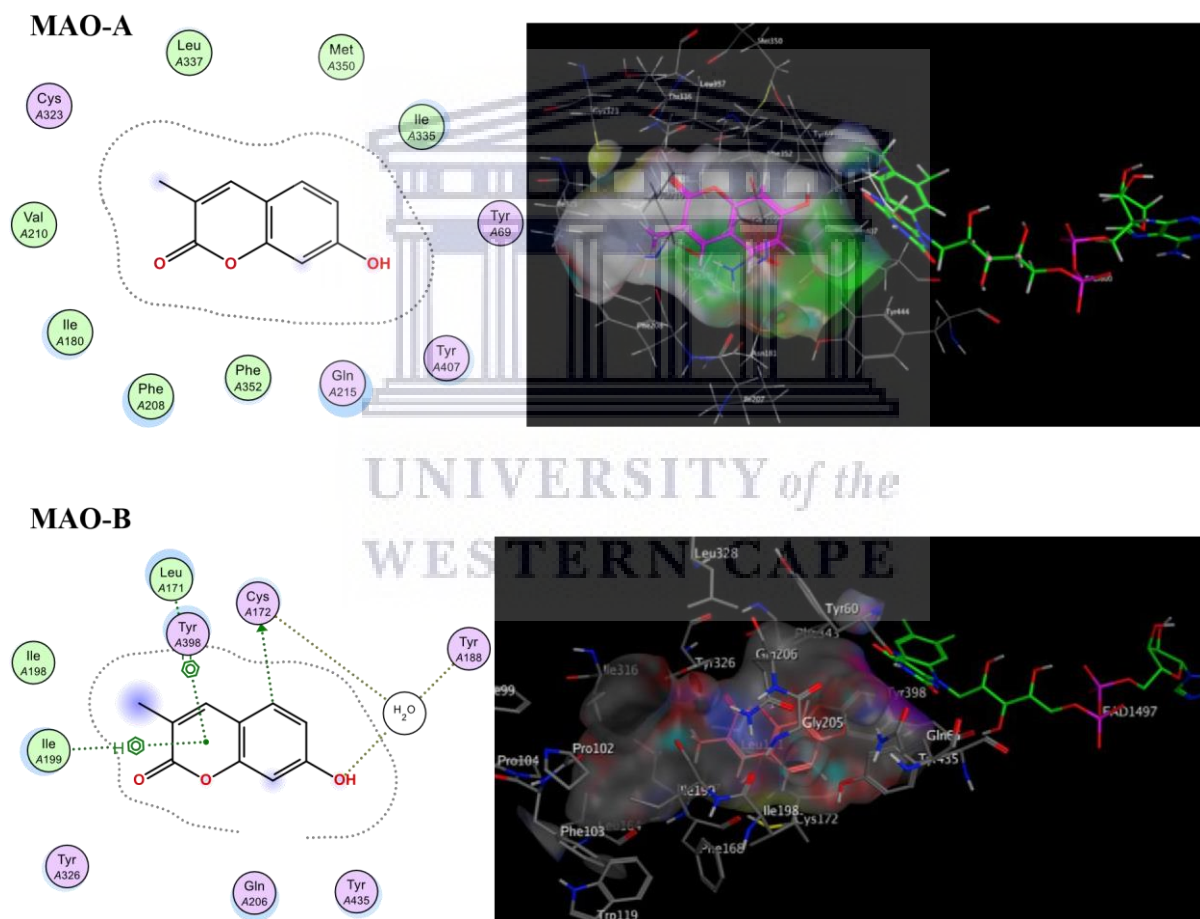


**Figure 4.13:** Diagrammatic representations of compound SM1's binding interactions with MAO-A (top) and MAO-B (bottom). The compound is indicated in pink and amino acids indicated in grey with the FAD cofactor indicated in green.

## 4.3.4.2.1 Series A

From the results of the MAO assays it was observed that series A generally displayed better inhibition than series B for both enzymes (see Table 4.1). From the docking simulations performed on MAO-A it can be seen that substitution with the benzyloxy moiety resulted in compounds SM2A and SM3A occupying MAO-A's rounder shaped substrate cavity better than SM1 did (Figure 4.14). The 7-benzyloxy substituent alters the compound's shape and conformation favourably and the resulting volume of the compounds may lead to steric blocking of the substrate from penetrating the substrate cavity. In addition to this, SM3A is able to form weaker sidechain interactions with Asn 181 in the MAO-A active site and this may explain why the compound's activity is slightly better than SM2A. With regards to MAO-B, the compounds' (particularly SM2A's) good activity and selectivity towards MAO-B can be attributed to the previously noted interactions between the coumarin moiety and Leu 171 coupled with new stable  $\pi$ -H bonds which form between the benzyloxy moiety and the Ile 199 residue. This interaction is important as the Ile 199 residue is critical in forming part of the gating mechanism which allows access to MAO-B's substrate cavity (Milczek, *et al.*, 2011).

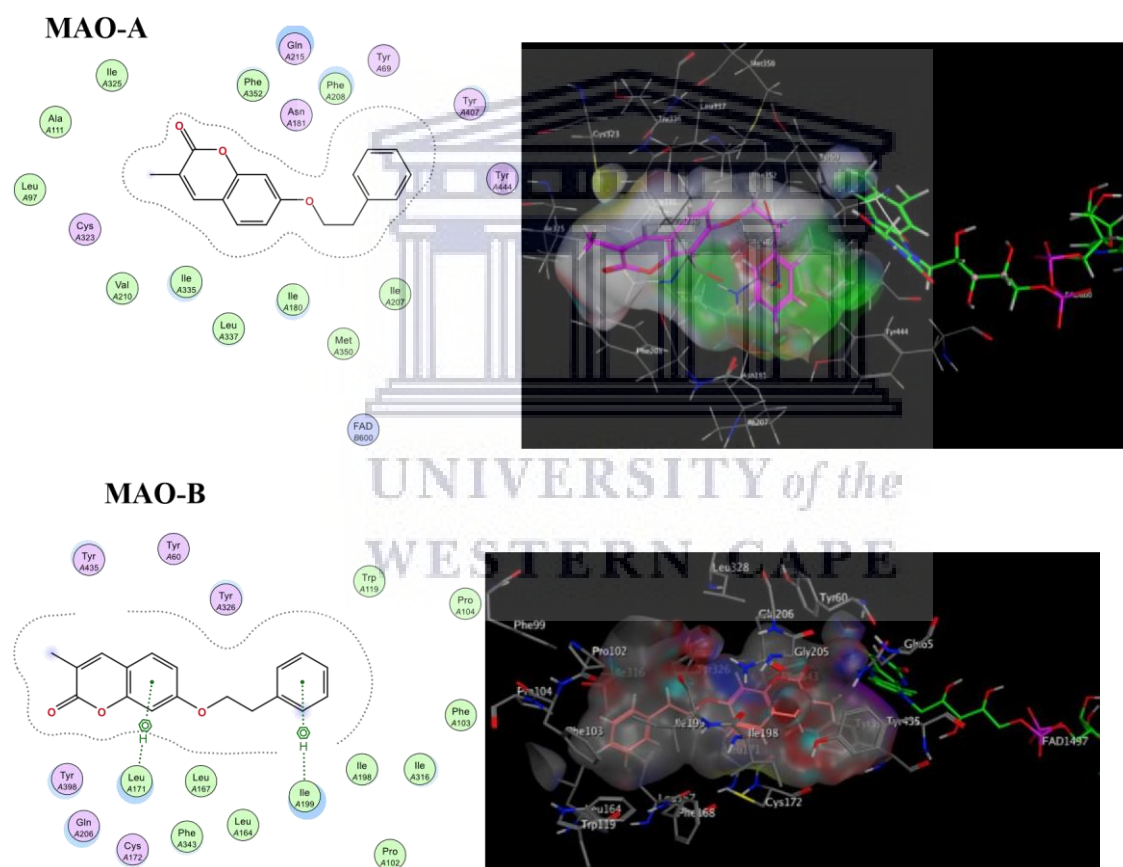


**Figure 4.14:** Diagrammatic representations of compound SM2A's binding interactions with MAO-A (top) and MAO-B (bottom). The compound is indicated in pink and amino acids indicated in grey with the FAD cofactor indicated in green.

Figure 4.15 shows that addition of the propargylamine to the 7-benzyloxy scaffold produced a molecule which is unable to fit into the active site of MAO-A. Docking conformations of compound SM4A demonstrated that the molecule lacks the flexibility to fit and subsequently interact with the active site. This is in contrast to docking in MAO-B, where it was observed that SM4A fits in the active site with the propargylamine moiety pointing towards the FAD cofactor. The FAD cofactor is essential for

substrate catalysis and thus compounds which can come into close proximity or bind to this cofactor are known to inhibit enzyme function to a greater extent (Moureau, *et al.*, 1994; Chimenti, *et al.*, 2010). In addition to being in proximity with the FAD cofactor, the molecule maintains the  $\pi$ -H bonding between Cys 172 and its coumarin nucleus. From the low nanomolar IC<sub>50</sub> the compound displayed in the assay, it can be seen that interactions such as these are important in producing a potent and highly selective inhibitor of MAO-B.

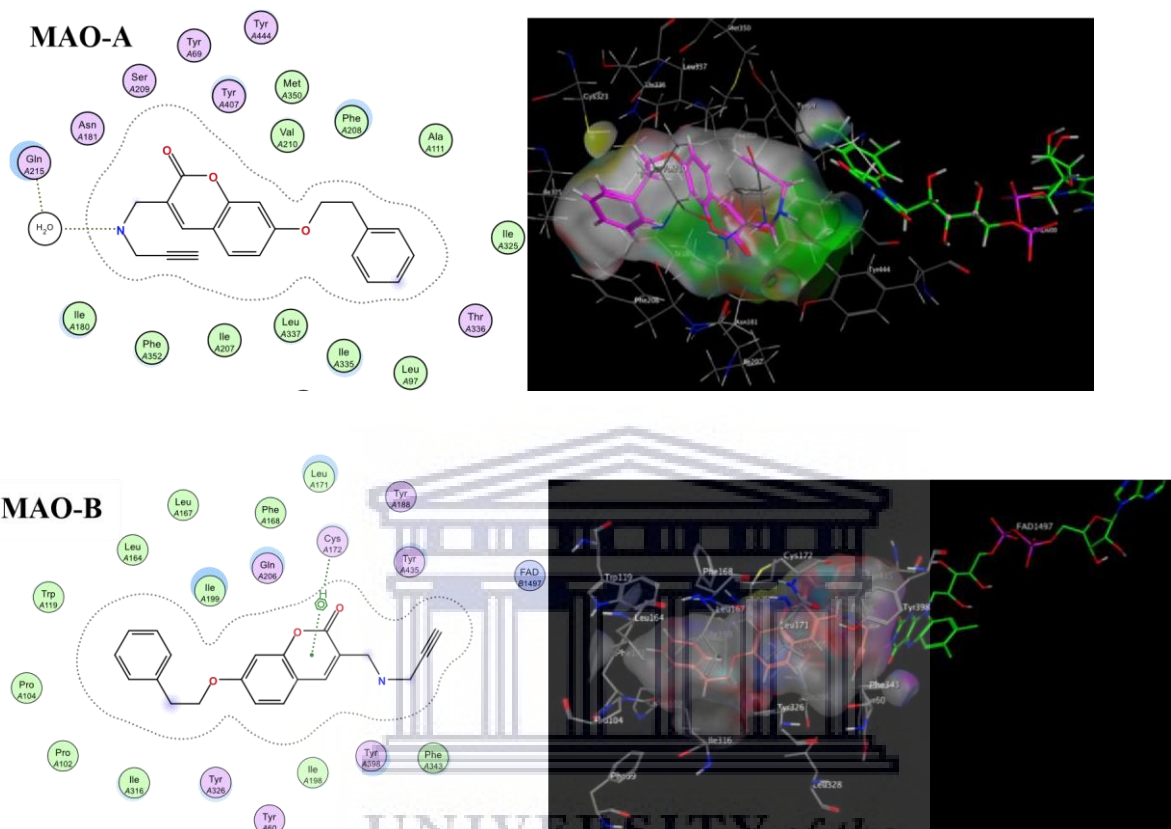


**Figure 4.15:** Diagrammatic representations of compound SM4A's binding interactions with MAO-A (top) and MAO-B (bottom). The compound is indicated in pink and amino acids indicated in grey with the FAD cofactor indicated in green.

#### 4.3.4.2.2 Series B

When docking with MAO-A compounds SM2B are seen to exhibit weak sidechain interactions between Cys 323 residue (near the entrance of the catalytic site) and the oxygen atom on the carbamate moiety. When docking with MAO-B its observed that both SM2B and SM3B retain the  $\pi$ -H interaction with Leu 171 which was first seen with SM1 (Figure 4.16). This may account for the molecule's selectivity and superior activity towards MAO-B. The compounds in this series however lack the hydrogen bond with Ile 199 and this may account for their lower activity compared to their counterparts in series A.

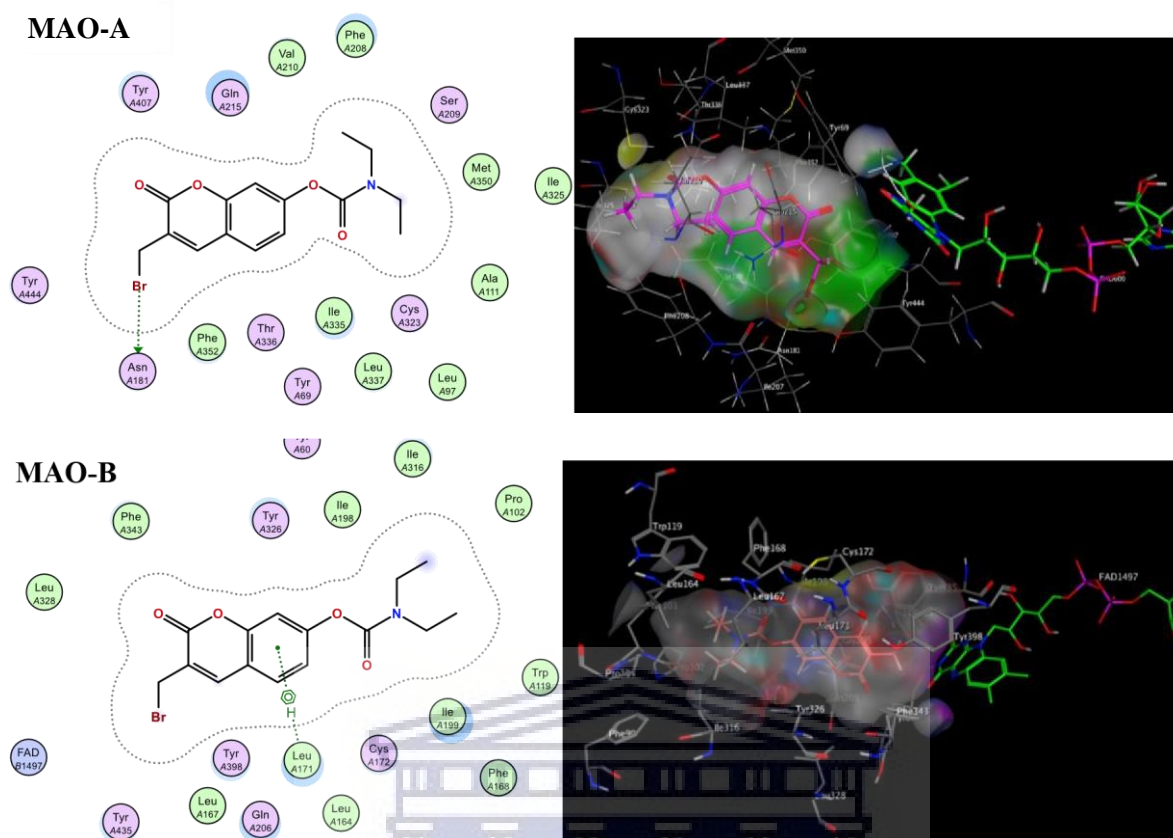


**Figure 4.16:** Diagrammatic representations of compound SM3B's binding interactions with MAO-A (top) and MAO-B (bottom). The compound is indicated in pink and amino acids indicated in grey with the FAD cofactor indicated in green.

The docking results of the propargylamine derivative SM5A showed that the majority of its docking poses could not fit well into the MAO-A active site, and as a result no significant interactions could be formed with amino acids in the cavities. This was reflected in the assay as SM5A displayed relatively low MAO-A inhibitory capacity compared to the other compounds with an  $IC_{50}$  of 20.8  $\mu\text{M}$ . On the other hand, from Figure 4.17 it can be seen the elongated nature of the MAO-B active site allows for better accommodation of the molecule within the substrate cavity. SM5A is thus able to form crucial  $\pi$ -H bonds with the enzymes' FAD cofactor via its propargylamine moiety. This demonstrates the importance of incorporating the propargylamine moiety for selective MAO-B inhibitors as the compound displayed the highest selectivity of the tested compounds, being over 200 times more selective for MAO-B than MAO-A.

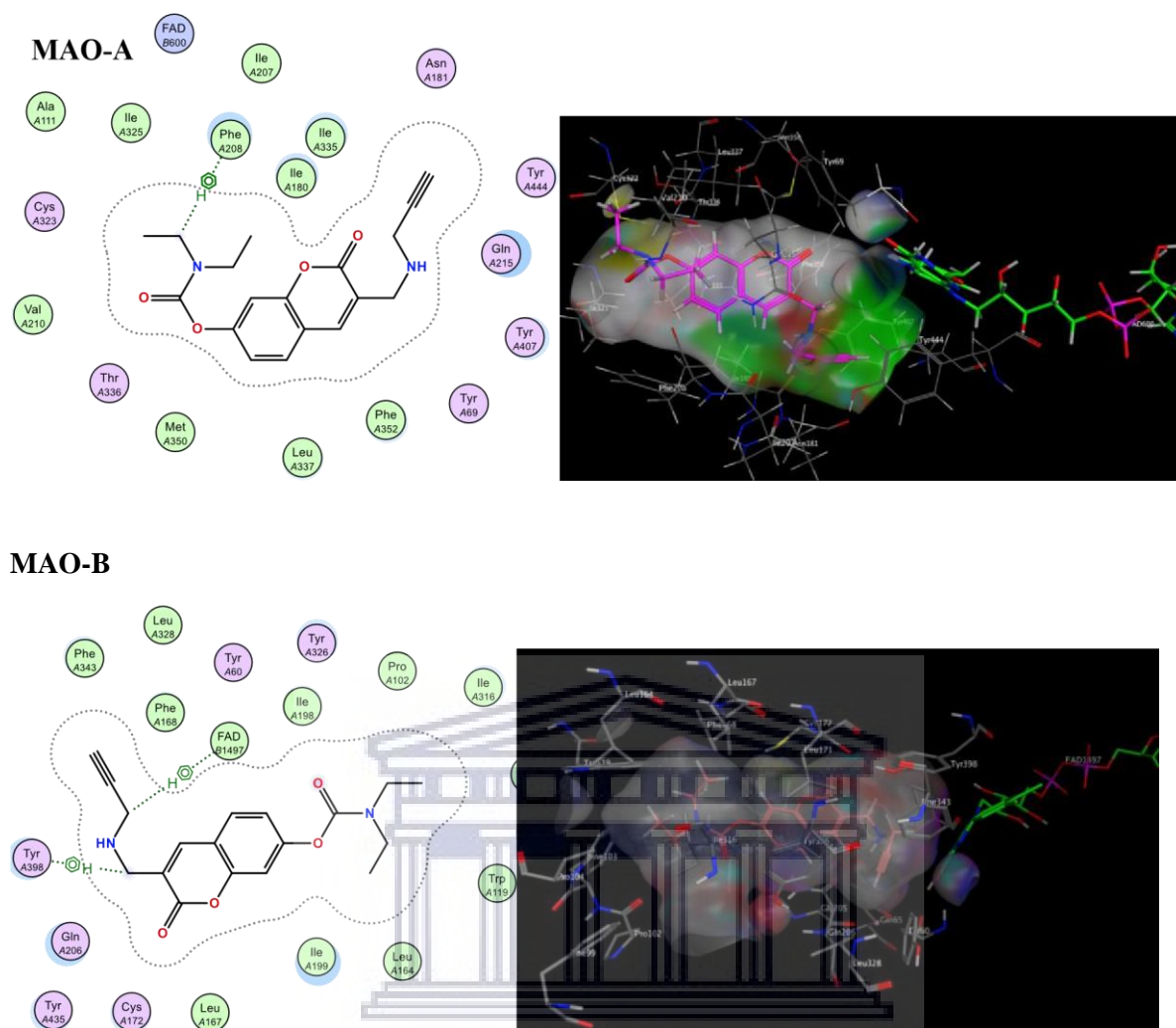


**Figure 4.17:** Diagrammatic representations of compound SM5As' binding interactions with MAO-A (top) and MAO-B (bottom). The compound is indicated in pink and amino acids indicated in grey with the FAD cofactor indicated in green.

#### 4.4 Cytotoxicity and neuroprotection studies

Cell viability and proliferation is an important indicator of cell health and cytotoxic assays provide us with a quick and accurate way to assess the toxicity of new potential drug molecules. When looking at the degenerative nature of AD it is pertinent that the compounds designed in this study are assessed for their effects on cell health and do not potentiate neuronal cell death. Cell based assays such as these are important as they provide a more holistic representation of a potential drugs' effects once in the body (McNutt, *et al.*, 2014). The compounds were thus further evaluated in *in vitro* cytotoxicity and neuroprotection studies.

##### 4.4.1 Cytotoxicity studies

Cytotoxicity of the compounds was assessed first in order to establish the toxicity of the compounds and what concentrations this occurs at. This was done using a standard 3-[4,5-dimethylthiazol-2-yl]2,5-diphenyl tetrazolium bromide (MTT) assay. MTT is a yellow salt which is reduced to form a purple formazan compound in the presence of living cells. This expected cell metabolism is indicative of cell survival and so cell viability can be determined as a function of the amount of this formazan detected spectrophotometrically (Fotakis & Timbrell, 2006). The test compounds were



compared to a vehicle control which consist of cells treated with DMSO which was used to indicate 100% cell survival.

#### 4.4.1.1 Experimental procedures

SH-SY5Y cells were plated in growth medium in flat bottom 96 well plates at a density of approximately 7,500 cells/well. The cells were allowed to adhere to the plate surface for 24 hours and following this their media was replenished with fresh media containing the test compounds at 10  $\mu\text{M}$ , 50  $\mu\text{M}$  and 100  $\mu\text{M}$  concentrations dissolved in DMSO. Vehicle control cells were treated with DMSO, at a concentration similar to that of the highest concentration of the test compounds. Following an incubation period of 48 hours, 10  $\mu\text{L}$  of MTT solution (5 mg/mL) was added to each well. This was further incubated for 4 hours and the formazan formed was solubilized with 100  $\mu\text{L}$  of DMSO. The plates were read using a BMG Labtech Omega<sup>®</sup> POLARStar (Ortenberg, Germany) plate reader spectrophotometer to determine the absorbance recorded at a wavelength of 570 nm. The percentage cell viability was calculated relative to the vehicle control using the formula below:

$$\text{Cell viability \%} = \frac{\text{Absorbance of treated well}}{\text{Absorbance of untreated well}} \times 100$$

#### 4.4.1.2 Results and discussion

The results of the assay were obtained in triplicate and subjected to ANOVA analysis for statistical significance and the data is presented in Figure 4.18. The results show that in general exposure to the test compounds led to a concentration dependent decrease in the SH-SY5Y cell counts. With the majority of the compounds this decrease in viability was not statistically significant ( $p > 0.05$ ) at the 50  $\mu\text{M}$  and 10  $\mu\text{M}$  concentrations. At 10  $\mu\text{M}$  the compounds' cytotoxic effect is diminished and can be seen to cause a favourable increase in the cell count compared to the untreated control. This increase ranges from 2% to 22%. Compound SM2B had the best cytotoxicity profile and was the only compound which displayed a dose-dependent increase in cell viability correlating with an increase in its concentration.

The 3-bromomethyl containing compounds SM3A and SM3B showed the most concentration related cytotoxicity, with significant reduction in cell count at 50  $\mu\text{M}$  and 100  $\mu\text{M}$ . SM3A's profile was significantly better with 65% and 7% survival at 50  $\mu\text{M}$  and 100  $\mu\text{M}$  compared to a 0% survival rate at the same respective concentrations for SM3B. It can be derived from this observation that the 3-bromomethyl substitution underlies this cytotoxicity and this is in agreement with previous studies describing the general cytotoxicity of halogen containing coumarin derivatives (Zhang, *et al.*, 2012). This cytotoxicity is mitigated at the lower 10  $\mu\text{M}$  concentration at which the compound caused slight increase in the cell count. Whilst the cytotoxic profile of the propargylamine derivatives in each series was better than these 3-bromomethyl derivatives, the compounds were more cytotoxic compared to SM2A and SM2B.

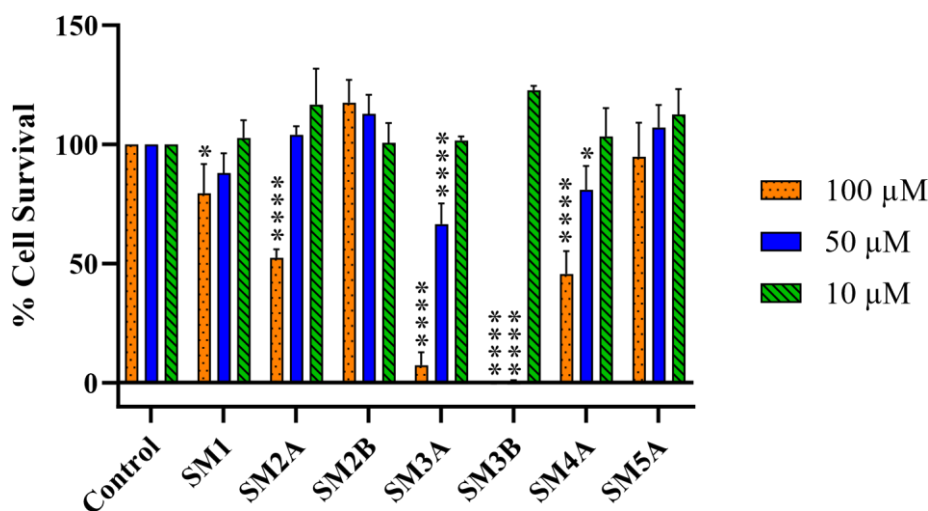


**Figure 4.18:** Percentage cell viability of test compounds relative to a control of untreated viable cells. Each bar represents the mean percentage survival and SD. An ANOVA analysis determined the statistical significance (\*,  $p < 0.05$  and \*\*\*\*,  $p < 0.0001$ ) when comparing the compounds data to the positive control.

Bearing in mind the results of the previous enzyme inhibitory assays, it is noteworthy that the compounds' MAO-B  $IC_{50}$  values ( $\leq 18 \mu\text{M}$ ) are significantly lower than the concentrations where significant cell loss is observed. This gives an indication that the compounds can safely be used within the range of their MAO inhibitory activity without causing significant harm to the cells they are administered to. For compound SM1 this extends to its BuChE  $IC_{50}$  ( $20.8 \mu\text{M}$ ) as significant cytotoxicity was recorded at  $100 \mu\text{M}$ . For compound SM3B this assay would have to be performed at more concentrations between  $50 \mu\text{M}$  and  $10 \mu\text{M}$  to investigate whether it is significantly cytotoxic around  $25 \mu\text{M}$  which is the concentration of its BuChE  $IC_{50}$  value.

Based on the results of SH-SY5Y cytotoxicity analysis it was confirmed that the compounds can be tested for MPP<sup>+</sup> induced neuroprotection studies. These assays could be conducted at compound concentrations between  $1 \mu\text{M}$  and  $10 \mu\text{M}$  as these would not negatively affect the viability of the cells.

#### 4.4.2 Neuroprotection

The neurotoxin 1-methyl-4-phenyl pyridinium (MPP<sup>+</sup>) is widely known to induce an apoptotic cascade in neurons and is thus used to induce neurodegeneration in a variety of *in vitro* and *in vivo* assays and models for NDs (Zeng, *et al.*, 2006; Santos, *et al.*, 2015). The induced apoptosis takes place via a variety of mechanisms including the formation of free radicals and targeting of the mitochondria, leading to depletion of ATP in the cell (Fonck & Baudry, 2003). Thus this assay can demonstrate the neuroprotective nature of multifunctional compounds such as the test compounds, based on their ability to rescue the cells from MPP<sup>+</sup> neurotoxicity. In this assay, SH-SY5Y cell lines were incubated with the test compounds following which they are challenged with  $2000 \mu\text{M}$  of MPP<sup>+</sup>. Following further incubation, a spectrophotometric assay is performed to assess cell viability. The percentage of cells which survived is calculated relative to a negative control consisting of untreated cells. A positive control of cells challenged with the same  $2000 \mu\text{M}$  MPP<sup>+</sup> but with no compound is conducted as well in order to establish a baseline of the negative effect of the neurotoxin on the cell line.

##### 4.4.2.1 Experimental procedures

SH-SY5Y cells were seeded onto a 96-well plate in growth medium at a density of 7,500 cells/well.

Different concentrations (1  $\mu\text{M}$ , 5  $\mu\text{M}$ , 10  $\mu\text{M}$ ) of test compounds were administered to the cells and following a two hour incubation period the cells were treated with 2000  $\mu\text{M}$  MPP<sup>+</sup> and incubated for a further 48 hours to induce cytotoxicity. Afterwards, an MTT colorimetric assay was used to measure cell viability relative to an untreated control. To determine the data's statistical significance, a Turkey's multiple comparison test was conducted on all experimental replicates using GraphPad Prism<sup>®</sup> 8.

#### 4.4.2.2 Results and discussion

Each experiment was performed in triplicate and tested for statistical significance. As illustrated in figure 4.19, the cell survival of untreated cells exposed to the MPP<sup>+</sup> for 48 hours, declined significantly to around 56%.

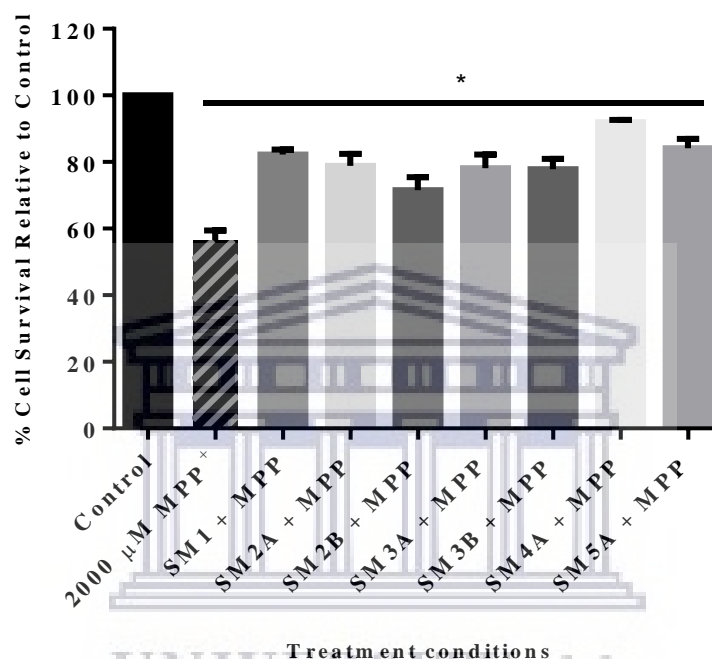


**Figure 4.19:** Bar graph comparing the effect of the test compounds on MPP<sup>+</sup>-induced toxicity in SHSY5Y cells. The viability count of the untreated control was defined as 100%. Error bars represent the standard deviation of the mean data. Statistical significance (\*,  $p < 0.05$ ) when compared to the control is indicated.

Subsequently, all the cell lines treated with the test compounds displayed higher survival counts compared to the untreated control cell line. This indicates that the compounds provided neuroprotection to the cells. Compared to the untreated cells, the cells exposed to the test compounds resulted in between 70% and 90% of cells surviving. The nature of the substitution at position 7 does not seem to influence this neuroprotection greatly, as there is no significant trend observed in the difference in neuroprotection across the two series. However, as expected from literature, the propargylamine derivatives exhibited the highest neuroprotective capability, with cells treated with compounds SM4A and SM5A having 92% and 85% survival rates respectively, further demonstrating the moiety's significance in neuroprotection.

The general neuroprotective profile of the compounds may also suggest that this neuroprotection is independent of their enzyme inhibitory capabilities, as all compounds performed fairly similarly despite having different enzyme inhibitory profiles. As described in literature, coumarin derivatives may possess inherent anti-inflammatory, anti-apoptotic and antioxidant effect and these coupled with the test compounds MAO inhibition may synergistically counter the MPP<sup>+</sup> induced apoptosis (Kapp, *et al.*, 2017)

The results from the cytotoxicity and neurotoxicity studies show in general that at a concentration of below 10  $\mu\text{M}$ , the compounds will exhibit good neuroprotective capacity. This gives an indication that the compounds would be tolerated well by neurons and most importantly ameliorate the neurodegeneration underlying progression of AD to some extent.

#### 4.5 Conclusion

In accordance with the aims of this study the ability of the test compounds to act as multifunctional ligands for AD was assessed successfully. The results obtained throughout this chapter are summarised in Table 4.2 below and provide valuable insights into which compounds would serve as the best MTDLs.

**Table 4.3:** Summarised results of the test compounds activity in the relevant biological assays. Compounds SM3B and SM4A are highlighted as displaying the best activity.

Compound	AChE IC <sub>50</sub>	BuChE IC <sub>50</sub>	MAO-A IC <sub>50</sub>	MAO-B IC <sub>50</sub>	MPP <sup>+</sup> neuroprotection
SM1	>100 $\mu\text{M}$	20.25 $\mu\text{M}$	33.4 $\mu\text{M}$	16.36 $\mu\text{M}$	82.24 %
SM2A	>100 $\mu\text{M}$	>100 $\mu\text{M}$	0.658 $\mu\text{M}$	0.014 $\mu\text{M}$	78.85 %
SM2B	>100 $\mu\text{M}$	>100 $\mu\text{M}$	2.822 $\mu\text{M}$	0.498 $\mu\text{M}$	71.59 %
SM3A	>100 $\mu\text{M}$	>100 $\mu\text{M}$	0.476 $\mu\text{M}$	>100 $\mu\text{M}$	78.11 %
SM3B	108 $\mu\text{M}$	23.27 $\mu\text{M}$	0.355 $\mu\text{M}$	0.333 $\mu\text{M}$	77.86 %
SM4A	>100 $\mu\text{M}$	>100 $\mu\text{M}$	3.86 $\mu\text{M}$	0.029 $\mu\text{M}$	91.96 %
SM5A	>100 $\mu\text{M}$	>100 $\mu\text{M}$	20.8 $\mu\text{M}$	0.101 $\mu\text{M}$	84.19 %

From these results it can be surmised that the compounds produced in this study display potent selective MAO-B inhibition as well as excellent neuroprotective ability. Overall, the best compound with regards to this was SM4A. The compound has a selectivity index of 133 towards MAO-B, with an IC<sub>50</sub> of 29 nM making it 20 times the potency of rasagiline. This compound also exhibited exceptional neuroprotection with 92% cell viability. SM4A highlights the trend of the 7-benzyloxy derivatives of series A having better activity than their counterparts in series B. In silico modelling of the compounds showed that this is because the compounds can form favourable interactions with the key Ile 199 residue in MAO-Bs entrance cavity. In addition, the propargylamine moiety (present in SM4A and SM5A) was shown to impart significant neuroprotection and MAO-B selectivity to the 7-substituted coumarin scaffold and this reaffirms its importance in developing MTDLs for AD.

Whilst the compounds lacked the desired activity towards AChE, they were more selective towards BuChE and so further optimization studies would need to be performed in order to improve their cholinesterase inhibitory profile. Compound SM3B displayed the best activity towards the cholinesterase and thus can also be highlighted as a promising potential MTDL. The compound displays selective BuChE inhibition and non-selective MAO inhibition at sub millimolar concentrations (AChE IC<sub>50</sub> = 108  $\mu\text{M}$ , BuChE IC<sub>50</sub> = 23  $\mu\text{M}$ , MAO-A IC<sub>50</sub> = 0.355  $\mu\text{M}$ , MAO-B IC<sub>50</sub> = 0.333  $\mu\text{M}$ ).

## Chapter 5

### 5. Summary and conclusion

#### 5.1 Introduction

Neurodegenerative Diseases (NDs) are a group of cognitive and movement related disorders resulting from neuronal loss in the brain. There is no singular cause or process that is responsible for this cell death, but instead it is the result of different interlinked mechanisms, underpinned by genetic and environmental factors (Lanctôt, *et al.*, 2009; Gabbianelli & Damiani, 2018).

Alzheimer's Disease (AD) was first classified over a century ago and is the most prevalent ND as well as form of dementia, with over 30 million diagnosed patients worldwide (Takeda, 2019). Its symptoms are progressive, initially characterised by recurring short term memory loss. As the disease progresses, higher cognitive and executive functions such as decision making and language are affected (East, 2017). As with other NDs the complex pathophysiology of AD has made treatment difficult and only symptomatic relief is provided by the drugs available on the market. Nevertheless, theories such as the role of oxidative stress and the cholinergic hypothesis have gained momentum in explaining the disease's pathology and in guiding treatment options (Tönnies & Trushina, 2017). By inhibiting the activity of the causative MAO and cholinesterase enzymes, it becomes possible to not only improve cognitive functions, but also to achieve neuroprotection and subsequently halt disease progression (Yanez & Vina, 2013; Wang, *et al.*, 2015).

By developing multitarget directed ligands (MTDLs) it is possible to simultaneously target both of these targets and achieve a synergistic therapeutic effect whilst avoiding the pitfalls of polypharmacy (Morphy, *et al.*, 2004). The coumarin scaffold has many intrinsic pharmacological properties and coumarin derivatives have shown promise as a starting point for MTDL design strategies due to ease of functionalisation and inherent ChE and MAO inhibitory capacity (Stefanachi, *et al.*, 2018).

This study therefore aimed to further explore the potential of coumarin derivatives as MTDLs by designing and synthesising 2 series of compounds which have substitutions of moieties known to enhance inhibition of MAO and cholinesterases. Propargylamine is one such moiety known for its capacity to confer neuroprotection and increase MAO inhibition (Naoi, *et al.*, 2003). These molecules could have the potential to relieve the symptoms of AD, slow down disease progression and ultimately reduce the burden of the disease.

#### 5.2 Synthesis

The designed compounds were successfully synthesised using a multiple step process. Initially, a Pechmann condensation reaction was performed to produce SM1, which acted as the starting scaffold. From this compound (SM1), SM2A and SM2B were then synthesised via microwave assisted S<sub>N</sub>2 reactions. These methods were employed as necessary optimisations to this reaction step, following low-yields produced when using conventional methods such as refluxing. The microwave assisted methods resulted in a two to three-fold increase in yield, as well as considerably reducing reaction times. Following this step, the 7-substituted coumarins were  $\alpha$ -brominated at position 3 using N-bromosuccinimide to produce the intermediates SM3A and SM3B. These intermediates then allowed for the final step consisting of a further S<sub>N</sub>2 substitution to incorporate propargylamine on position 3, producing SM4A and SM5A.

A total of 7 compounds were synthesised with yields ranging from 15% to 65%. The low yields arose as a result of incomplete reactions, which did not use up all of the available starting materials. This then necessitated purification of the reaction mixtures via column chromatography at each step, which

in turn led to further product loss. The potential MTDLs were structurally elucidated using NMR, MS and IR techniques and evaluated for biological activity.

### 5.3 Biological Evaluation

The compounds were evaluated for biological activity through *in vitro* cell and enzyme based assays. Activity against the cholinesterase enzymes was assessed using a modified colorimetric Ellman's assay against *Electrophorus electricus* AChE and equine BuChE (Ellman, *et al.*, 1961; Denya, *et al.*, 2018).

The results of the assay showed that the compounds lacked significant inhibition towards AChE; they exhibited only 10% to 30% inhibition of enzyme activity at a 100  $\mu\text{M}$  concentration with the 3-bromoethyl derivatives SM3A and SM3B having the best activities. Molecular modelling showed that this was because the compounds could not form substantive interactions with amino acids in AChE's active site. By contrast the compounds displayed higher percentage inhibition towards BuChE (Figure 5.1) and thus can be classified, in general, as weak selective BuChE inhibitors.

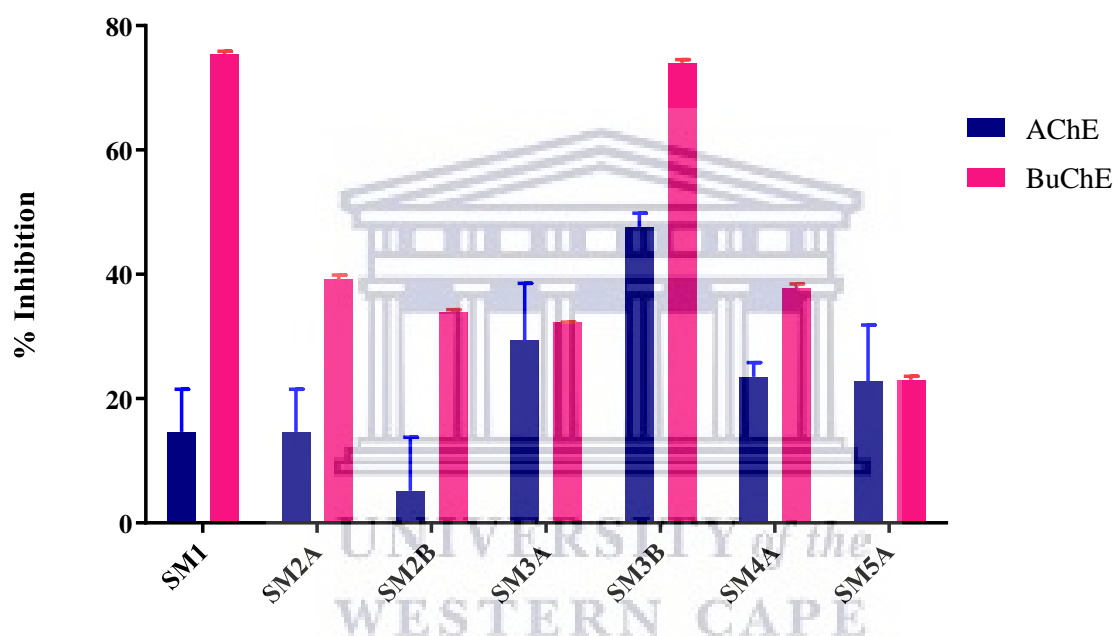


**Figure 5.1:** Comparative inhibitions of the cholinesterase enzymes with error bars shown, highlighting the BuChE selectivity of the test compounds. Data is represented as mean % inhibition and SD.

The compounds were also assessed for their MAO inhibitory activity using a fluorometric assay with recombinant human MAO-A and human MAO-B (Matsumoto, *et al.*, 1985). The compounds demonstrated good inhibition of both MAO isoforms. They display potent MAO-B inhibition with  $\text{IC}_{50}$  values ranging from low micromolar to nanomolar values. Five of the compounds displayed lower  $\text{IC}_{50}$  values (0.497  $\mu\text{M}$  to 0.029  $\mu\text{M}$ ) than those of rasagiline (0.586  $\mu\text{M}$ ). The 7-benzyloxy derivatives had greater inhibition than their 7-carbamate counterparts whilst the propargylamine derivatives had exceptional selectivity towards MAO-B. Molecular modelling attributed the compounds' activity to their ability to sterically block the entrance cavity and additionally form interactions in the substrate cavity. MAO-B selectivity resulted from the compounds ability to form interactions with Leu 171, an important amino acid residue for MAO-B catalytic activity.

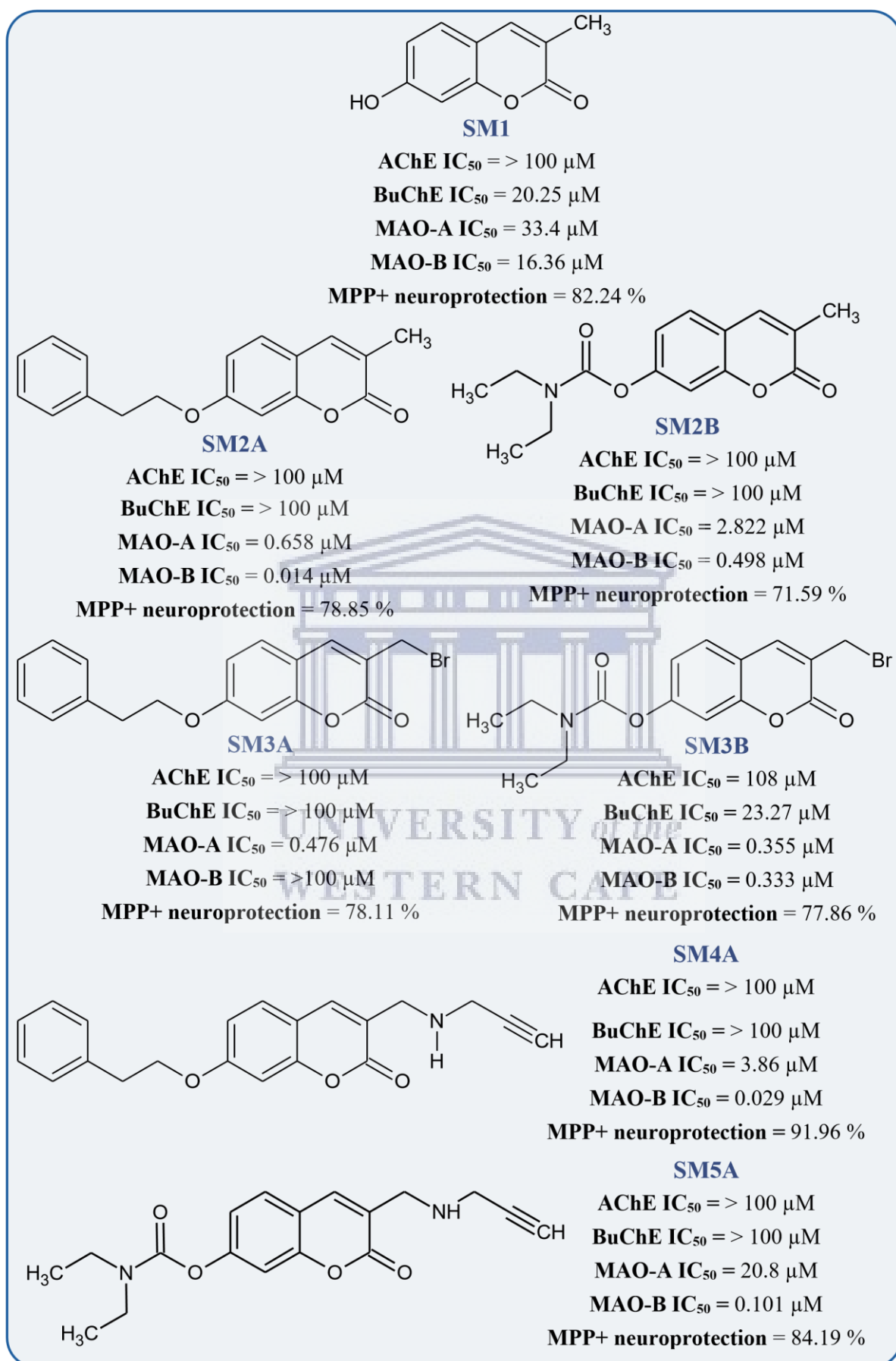


**Figure 5.2:** Coumarin derivatives synthesised with a summary of their relevant biological activity.

Cytotoxicity studies showed that the compounds were not toxic to neuroblastoma cells, particularly at concentrations within their range of IC<sub>50</sub> values. Subsequent neuroprotective studies demonstrated that the compounds significantly increase the survival rate of human neuroblastoma cells which have been compromised with MPP<sup>+</sup>. The propargylamine derivatives displayed the best neuroprotection, which is in line with our hypothesis and as described in previous studies. The results are summarised in figure 5.2 above.

### 5.4 Conclusion

With the growing threat that is arising from the lack of AD treatment, continual research is paramount in overcoming these shortcomings. MTDLs provide a viable solution to overcome the current AD treatment failures and continued research may provide the answer to combat this and similar multifactorial diseases.

The objectives of this study were to synthesise a number of neuroprotective coumarin derivatives with cholinesterase and MAO inhibition. Seven novel compounds were successfully synthesised and biological evaluations showed that despite their lack of cholinesterase inhibitory activities, they are potent inhibitors of MAO and offer excellent neuroprotection. Therefore, substitution of the benzyloxy, carbamate and propargylamine moieties to the coumarin scaffold have great potential in developing compounds which can reduce neurodegeneration in AD patients from MAO mediated oxidative stress. Compounds SM3B and SM4A displayed the best activities and embody these properties the best.

Although the aims of the study were achieved to varying extents, there were limitations which provide the opportunity for further work to be done. Further structure activity investigations could be performed by incorporating known moieties such as tacrine which confer additional ChE inhibitory activity. Similarly, methylation of the 3-propargylamine compounds could be performed to produce 3-methylpropargylamine derivatives, as studies have found methyl propargylamine to be a potentially more neuroprotective moiety (Naoi, *et al.*, 2003). It is also necessary to investigate the compounds' druggability such as their ability to cross the BBB, scavenge free radicals and inhibit A $\beta$  plaque formation. Future work is also needed to optimise these structures in order to be sufficiently active against the cholinesterase enzymes and therefore alleviate the PAS mediated amyloidosis and cognitive decline associated with the cholinergic system. Based on the observations in this study elongation of the molecules may allow them to span the AChE gorge and form interactions within the active site which would inhibit AChE activity.



---

## References

1. Abdshahzadeh, H. *et al.*, 2019. 3-Aryl Coumarin Derivatives Bearing Aminoalkoxy Moiety as Multi-Target-Directed Ligands against Alzheimer's Disease. *Chemistry & Biodiversity*, 16(5), p. e1800436.
2. Adams, K. B., 2007. Specific effects of caring for a spouse with dementia: differences in depressive symptoms between caregiver and non-caregiver spouses. *International Psychogeriatrics*, 20(3), pp. 508-520.
3. Addington, D. E. *et al.*, 2009. A Comparison of Ziprasidone and Risperidone in the Long-Term Treatment of Schizophrenia: A 44-Week, Double-Blind, Continuation Study. *The Canadian Journal of Psychiatry*, 54(1), pp. 46-54.
4. Agatonovic-Kustrin, S., Kettle, C. & Morton, D. W., 2018. A molecular approach in drug development for Alzheimer's disease. *Biomedicine & Pharmacotherapy*, Volume 106, pp. 553-565.
5. Alberdi, E., MV, S.-G. & F, C., 2010. Amyloid beta oligomers induce Ca<sup>2+</sup> dysregulation and neuronal death through activation of ionotropic glutamate receptors.. *Cell Calcium*, 47(3), pp. 264-272.
6. Aliev, G. *et al.*, 2008. Antioxidant Therapy in Alzheimer's Disease: Theory and Practice. *MiniReviews in Medicinal Chemistry*, 8(13), pp. 1395-1406.
7. Allegri, R. F., 2006. Economic impact of dementia in developing countries: an evaluation of costs of Alzheimer-type dementia in Argentina. *International Psychogeriatrics*, 19(4), pp. 705-718.
8. Alvarez, A. *et al.*, 1998. Stable Complexes Involving Acetylcholinesterase and Amyloid- $\beta$  Peptide Change the Biochemical Properties of the Enzyme and Increase the Neurotoxicity of Alzheimer's Fibrils. *The Journal of Neuroscience*, 18(9), pp. 3213-3223.
9. Alzheimer's Association, 2019. Alzheimer's disease facts and figures. *Alzheimer's & Dementia*, pp. 321-387.
10. Anand, P. & Singh, B., 2013. A review on cholinesterase inhibitors for Alzheimer's disease. *Archives of Pharmacal Research*, 36(4), pp. 375-399.
11. Andrews, M., Tousi, B. & Sabbagh, M. N., 2018. 5HT<sub>6</sub> Antagonists in the Treatment of Alzheimer's Dementia: Current Progress. *Neurology and Therapy*, 7(1), pp. 51-58.
12. Anglister, L., Haesaert, B. & McMahan, U. J., 1994. Globular and asymmetric acetylcholinesterase in the synaptic basal lamina of skeletal muscle. *The Journal of Cell Biology*, 125(1), pp. 183-196.
13. Apostolova, L. G., 2016. Alzheimer Disease. *CONTINUUM: Lifelong Learning in Neurology*, 22(2), pp. 419-434.
14. Auld, D. S., Kar, S. & Quirion, R., 1998.  $\beta$ -Amyloid peptides as direct cholinergic neuromodulators: a missing link?. *Trends in Neurosciences*, 21(1), pp. 43-49.
15. Bartus, R., Dean, R., Beer, B. & Lippa, A., 1982. The cholinergic hypothesis of geriatric memory dysfunction. *Science*, 217(4558), pp. 408-414.

16. Binda, C. *et al.*, 2003. Insights into the mode of inhibition of human mitochondrial monoamine oxidase B from high-resolution crystal structures. *Proceedings of the National Academy of Sciences*, 100(17), pp. 9750-9755.
17. Bird, T., 2015. *Alzheimer Disease Overview*. [Online] Available at: <https://www.ncbi.nlm.nih.gov/books/NBK1161/>
18. Blennow, K. *et al.*, 2015. Amyloid biomarkers in Alzheimer's disease. *Trends in Pharmacological Sciences*, 36(5), pp. 297-309.
19. Blennow, K. & Zetterberg, H., 2018. Biomarkers for Alzheimer's disease: current status and prospects for the future. *Journal of Internal Medicine*, 284(6), pp. 643-663.
20. Bolea, I. *et al.*, 2013. Multipotent, Permeable Drug ASS234 Inhibits A $\beta$  Aggregation, Possesses Antioxidant Properties and Protects from A $\beta$ -induced Apoptosis In Vitro. *Current Alzheimer Research*, 10(8), pp. 797-808.
21. Bourne, Y., 2003. Structural insights into ligand interactions at the acetylcholinesterase peripheral anionic site. *The EMBO Journal*, 22(1), pp. 1-12.
22. Bowen, D. M., Smith, C. B., White, P. & Davison, A. N., 1976. Neurotransmitter-related enzymes and indices of hypoxia in senile dementia and other abiotrophies. *Brain*, Volume 99, pp. 459-496.
23. Brothers, H. M., Gosztyla, M. L. & Robinson, S. R., 2018. The Physiological Roles of Amyloid- $\beta$  Peptide Hint at New Ways to Treat Alzheimer's Disease. *Frontiers in Aging Neuroscience*, 10(118).
24. Brühlmann, C. *et al.*, 2001. Coumarins Derivatives as Dual Inhibitors of Acetylcholinesterase and Monoamine Oxidase. *Journal of Medicinal Chemistry*, 44(19), pp. 3195-3198.
25. Brunnström, H. R. & Englund, E., 2009. Cause of death in patients with dementia disorders. *European Journal of Neurology*, 16(4), pp. 488-492.
26. Burghaus, L. *et al.*, 2000. Quantitative assessment of nicotinic acetylcholine receptor proteins in the cerebral cortex of Alzheimer patients. *Molecular Brain Research*, 76(2), pp. 385-388.
27. Cacquevel, M., Aeschbach, L., Houacine, J. & Fraering, P. C., 2012. Alzheimer's Disease-Linked Mutations in Presenilin-1 Result in a Drastic Loss of Activity in Purified  $\gamma$ -Secretase Complexes. *PLoS ONE*, 7(4), p. e35133.
28. Cai, Z., 2014. Monoamine oxidase inhibitors: Promising therapeutic agents for Alzheimer's disease (Review). *Molecular Medicine Reports*, 9(5), pp. 1533-1541.
29. Carvajal, F. J. & Inestrosa, N. C., 2011. Interactions of AChE with A $\beta$  aggregates in Alzheimer's brain: therapeutic relevance of IDN 5706. *Frontiers in Molecular Neuroscience*, Volume 4, p. 19.
30. Catto, M. *et al.*, 2006. Structural Insights into Monoamine Oxidase Inhibitory Potency and Selectivity of 7-Substituted Coumarins from Ligand- and Target-Based Approaches. *Journal of Medicinal Chemistry*, 49(16), pp. 4912-4925.

31. Catto, M. *et al.*, 2013. Design, synthesis and biological evaluation of coumarin alkylamines as potent and selective dual binding site inhibitors of acetylcholinesterase. *Bioorganic & Medicinal Chemistry*, 21(1), pp. 146-152.
32. Cavalli, A. *et al.*, 2008. Multi-target-Directed Ligands To Combat Neurodegenerative Diseases. *Journal of Medicinal Chemistry*, 51(3), pp. 347-372.
33. Chang, P., 2014. *Neurodegenerative Disease List and Tips to Prevent It*. [Online]. Available at: <http://energyfanatics.com/2014/08/15/neurodegenerative-disease-list-tips-prevent-it/>
34. Chen, 2017. Amyloid beta: structure, biology and structure-based therapeutic development. *Acta Pharmacologica Sinica*, Volume 38. pp. 1205-1235.
35. Chen, X., Fang, L., Liu, J. & Zhan, C.-G., 2011. Reaction Pathway and Free Energy Profile for Butyrylcholinesterase-Catalyzed Hydrolysis of Acetylcholine. *The Journal of Physical Chemistry B*, 115(5), pp. 1315-1322.
36. Chimenti, F. *et al.*, 2010. Investigations on the 2-thiazolyldiazine scaffold: Synthesis and molecular modeling of selective human monoamine oxidase inhibitors. *Bioorganic & Medicinal Chemistry*, 18(15), pp. 5715-5723.
37. Chin-Chan, M., Navarro-Yepes, J. & Betzabet, Q.-V., 2015. Environmental pollutants as risk factors for neurodegenerative disorders: Alzheimer and Parkinson diseases. *Frontiers in Cellular Neuroscience*, Volume 9, p. 124.
38. Chiou, S.-Y., Huang, C.-F., Hwang, M.-T. & Lin, G., 2009. Comparison of active sites of butyrylcholinesterase and acetylcholinesterase based on inhibition by geometric isomers of benzene-di-N-substituted carbamates. *Journal of Biochemical and Molecular Toxicology*, 23(5), pp. 303-308.
39. Cisek, K., Cooper, G., Huseby, C. & Kuret, J., 2014. Structure and Mechanism of Action of Tau Aggregation Inhibitors. *Current Alzheimer Research*, 11(10), pp. 918-927.
40. Çokuğraş, A. N., 2003. Butyrylcholinesterase: Structure and Physiological. [*Turkish Journal of Biochemistry*, 28(2), pp. 54-61.
41. Colovic, M. B. *et al.*, 2013. Acetylcholinesterase Inhibitors: Pharmacology and Toxicology. *Current Neuropharmacology*, 11(3), pp. 315-335.
42. Cummings, J., Lee, G., Ritter, A. & Zhong, K., 2018. Alzheimer's disease drug development pipeline: 2018. *Alzheimer's & Dementia: Translational Research & Clinical Interventions*, Volume 4, pp. 195-214.
43. Czajkowski, C., Kaufmann, C., & Karlin, A. (1993). Negatively charged amino acid residues in the nicotinic receptor delta subunit that contribute to the binding of acetylcholine. *Proceedings of the National Academy of Sciences of the United States of America*, 90(13), pp. 6285–6289

44. Daniele, S., Giacomelli, C. & Martini, C., 2018. Brain ageing and neurodegenerative disease: The role of cellular waste management.. *Biochemical Pharmacology*, Volume 158, pp. 207-276.
45. Danysz, W. *et al.*, 2000. Neuroprotective and symptomatological action of memantine relevant for alzheimer's disease — a unified glutamatergic hypothesis on the mechanism of action. *Neurotoxicity Research*, 2(2-3), pp. 85-97.
46. Darvesh, S. *et al.*, 2008. Carbamates with Differential Mechanism of Inhibition Toward Acetylcholinesterase and Butyrylcholinesterase *Journal of Medicinal Chemistry*, 51(14), pp. 4200-4212.
47. Davies, P. & Maloney, A., 1976. SELECTIVE LOSS OF CENTRAL CHOLINERGIC NEURONS IN ALZHEIMER'S DISEASE. *The Lancet*, 308(8000), p. 1403.
48. Davis, L. & Britten, J., 1997. Cholinesterase Its significance in anaesthetic practice. *Anaesthesia*, Volume 52, pp. 244-260.
49. de Andrade Teles, R. B. *et al.*, 2018. Flavonoids as Therapeutic Agents in Alzheimer's and Parkinson's Diseases: A Systematic Review of Preclinical Evidences. *Oxidative Medicine and Cellular Longevity*, Volume. 2018, pp. 1-21.
50. de Jager, C. A., Msemburi, W., Pepper, K. & Combrinck, M. I., 2017. Dementia Prevalence in a Rural Region of South Africa: A Cross-Sectional Community Study. *Journal of Alzheimer's Disease*, 60(3), pp. 1087-1096.
51. del Ser, T. *et al.*, 2012. Treatment of Alzheimer's Disease with the GSK-3 Inhibitor Tideglusib: A Pilot Study. *Journal of Alzheimer's Disease*, 33(1), pp. 205–215.
52. Denya , I. *et al.*, 2018. Design, synthesis and evaluation of indole derivatives as multifunctional agents against Alzheimer's disease. *MedChemComm*, 9(2), pp. 357-370.
53. Donovalová, J. *et al.*, 2012. Spectral Properties of Substituted Coumarins in Solution and Polymer Matrices. *Molecules*, 17(3), pp. 3259-3276.
54. Dorszewska, J. *et al.*, 2016. Molecular Basis of Familial and Sporadic Alzheimer's Disease. *Current Alzheimer Research*, 13(9), pp. 952-963.
55. Drachman, D. A., 1974. Human Memory and the Cholinergic System. *Archives of Neurology*, 30(2), pp. 113-121.
56. Durães, F. & Pinto, M., 2018. Old Drugs as New Treatments for Neurodegenerative Diseases. *Pharmaceuticals*, 11(2), p. 44.
57. Dvir, H. *et al.*, 2010. Acetylcholinesterase: From 3D structure to function. *Chemico-Biological Interactions*, 187(1-3), pp. 10-22.
58. East, A., 2017. *Taking the Worry Out of Hiring In-Home and 24/7 Alzheimer's Care*. [Online] Available at: <https://caringpeopleinc.com/blog/taking-worry-hiring-home-247-dementiaalzheimers-care/> [Accessed 7 July 2019].
59. Edmondson, D. E. *et al.*, 2004. Structure and Mechanism of Monoamine Oxidase. *Current Medicinal Chemistry*, 11(15), pp. 1983-1993.

60. Edwards, F., 2019. A Unifying Hypothesis for Alzheimer's. *Trends in Neurosciences*, 42(5), pp. 310-322.
61. Ellman, G. L., Courtney, K., Andres, V. & Featherstone, R. M., 1961. A new and rapid colorimetric determination of acetylcholinesterase activity. *Biochemical Pharmacology*, 7(2), pp. 88-95.
62. Erasmus, H., Fauvel, B. & Jaeg, T., 2009. *Human Acetylcholinesterase - Proteopedia, life in 3D*. [Online] Available at: [https://proteopedia.org/wiki/index.php/Human\\_Acetylcholinesterase](https://proteopedia.org/wiki/index.php/Human_Acetylcholinesterase)
63. Erkinen, M. G. & Mee-Ohk, K., 2017. Clinical Neurology and Epidemiology of the Major Neurodegenerative Diseases. *Cold Spring Harbor Perspectives in Biology*, 10(4), a033118.
64. Eslami, M., Hashemianzadeh, S. M., Bagherzadeh, K. & Seyed Sajadi, S. A., 2015. Molecular perception of interactions between bis(7)tacrine and cystamine-tacrine dimer with cholinesterases as the promising proposed agents for the treatment of Alzheimer's disease. *Journal of Biomolecular Structure and Dynamics*, 34(4), pp. 855-869.
65. Farina, R. *et al.*, 2015. Structure-Based Design and Optimization of Multitarget-Directed 2HChromen-2-one Derivatives as Potent Inhibitors of Monoamine Oxidase B and Cholinesterases. *Journal of Medicinal Chemistry*, 58(14), pp. 5561-5578.
66. Farlow, M. R., 2003. Clinical Pharmacokinetics of Galantamine. *Clinical Pharmacokinetics*, 42(15), pp. 1383-1392.
67. Fernández-Bachiller, M. I. *et al.*, 2010. Novel Tacrine-8-Hydroxyquinoline Hybrids as Multifunctional Agents for the Treatment of Alzheimer's Disease, with Neuroprotective, Cholinergic, Antioxidant, and Copper-Complexing Properties. *Journal of Medicinal Chemistry*, 53(13), pp. 4927-4937.
68. Ferrante, R., 2016. *The Stages Of Alzheimer's Disease - Home Care Services*. [Online] Available at: <http://www.homecaresantaclarita.com/stages-alzheimers-look-loved-one/>
69. Ferreira-Vieira, T. H., Guimaraes, I. M., Silva, F. R. & Ribeiro, F. M., 2016. Alzheimer's disease: Targeting the Cholinergic System. *Current Neuropharmacology*, 14(1), pp. 101-115.
70. Ferrero, H., Solas, M., Francis, P. T. & Ramirez, M. J., 2016. Serotonin 5-HT<sub>6</sub> Receptor Antagonists in Alzheimer's Disease: Therapeutic Rationale and Current Development Status. *CNS Drugs*, 31(1), pp. 19-32.
71. Finberg, J. P., 2014. Update on the pharmacology of selective inhibitors of MAO-A and MAO-B: Focus on modulation of CNS monoamine neurotransmitter release. *Pharmacology & Therapeutics*, 143(2), pp. 133-152.
72. Finberg, J. P. & Gillman, K., 2011. Selective inhibitors of monoamine oxidase type B and the "cheese effect". *International Review of Neurobiology*, Volume 100, pp. 169-190.

73. Fonck, C. & Baudry, M., 2003. Rapid reduction of ATP synthesis and lack of free radical formation by MPP<sup>+</sup> in rat brain synaptosomes and mitochondria. *Brain Research*, 975(1-2), pp. 214-221.
74. Förstl, H. & Kurz, A., 1999. Clinical features of Alzheimer's disease. *European Archives of Psychiatry and Clinical Neuroscience*, Volume 249, pp. 288-290.
75. Fotakis, G. & Timbrell, J. A., 2006. In vitro cytotoxicity assays: Comparison of LDH, neutral red, MTT and protein assay in hepatoma cell lines following exposure to cadmium chloride. *Toxicology Letters*, 160(2), pp. 171-177.
76. Fowler, J. S. *et al.*, 2015. Monoamine oxidase: radiotracer chemistry and human studies. *Journal of Labelled Compounds and Radiopharmaceuticals*, 58(3), pp. 51-64.
77. Francis, P. T., 2005. The Interplay of Neurotransmitters in Alzheimer's Disease. *CNS Spectrums*, 10(S18), pp. 6-9.
78. Frozza, R. L., Lourenco, M. V. & De Felice, F. G., 2018. Challenges for Alzheimer's Disease Therapy: Insights from Novel Mechanisms Beyond Memory Defects. *Frontiers in Neuroscience*, Volume 12.
79. Gabbianelli, R. & Damiani, E., 2018. Epigenetics and neurodegeneration: role of early-life nutrition. *The Journal of Nutritional Biochemistry*, Volume 57, pp. 1-13.
80. García-Ayllón, M.-S. *et al.*, 2010. Altered Levels of Acetylcholinesterase in Alzheimer Plasma. *PLoS ONE*, 5(1), p. e8701.
81. Gareri, P. *et al.*, 2014. Retrospective Study on the Benefits of Combined Memantine and cholinesterase inhibitor treatment in aged Patients affected with Alzheimer's Disease: The MEMAGE Study. *Journal of Alzheimer's Disease*, 41(2), pp. 633-640.
82. Gatz, M., Reynolds, C. A. & Fratiglioni, L., 2006. Role of Genes and Environments for Explaining Alzheimer Disease. *Archives of General Psychiatry*, 63(2), pp. 168-174.
83. Gaweska, H. & Fitzpatrick, P. F., 2011. Structures and mechanism of the monoamine oxidase family. *BioMolecular Concepts*, 2(5), pp. 365–377.
84. Giacobini, E., 2003. Cholinesterases: New Roles in Brain Function and in Alzheimer's Disease. *Neurochemical Research*, 28(3-4), pp. 515-522.
85. Gnerre, C. *et al.*, 2000. Inhibition of Monoamine Oxidases by Functionalized Coumarin Derivatives: Biological Activities, QSARs, and 3D-QSARs. *Journal of Medicinal Chemistry*, 43(25), pp. 4747-4758.
86. Grady, M. M. & Stahl, S. M., 2012. Practical guide for prescribing MAOIs: debunking myths and removing barriers. *CNS Spectrums*, 17(1), pp. 2-10.
87. Graham, W. V., Bonito-Oliva, A. & Sakmar, T. P., 2017. Update on Alzheimer's Disease Therapy and Prevention Strategies. *Annual Review of Medicine*, 68(1), pp. 413-430.

88. Greig, N., Reale, M. & Tata, A., 2013. New Pharmacological Approaches to the Cholinergic System: An Overview on Muscarinic Receptor Ligands and Cholinesterase Inhibitors. *Recent Patents on CNS Drug Discovery*, 8(2), pp. 123-141.
89. Hangya, B., Ranade, S., Lorenc, M. & Kepecs, A., 2015. Central Cholinergic Neurons Are Rapidly Recruited by Reinforcement Feedback. *Cell*, 162(5), pp. 1155-1168.
90. Hebb, C. O. & Whittaker, V. P., 1958. Intracellular distributions of acetylcholine and choline acetylase. *The Journal of Physiology*, 142(1), pp. 187-196.
91. Hoerr, R. & Noeldner, M., 2006. Ensaculin (KA-672. HCl): A Multitransmitter Approach to Dementia Treatment. *CNS Drug Reviews*, 8(2), pp. 143-158.
92. Hung, S.-Y. & Fu, W.-M., 2017. Drug candidates in clinical trials for Alzheimer's disease. *Journal of Biomedical Science*, 24(1), p.47.
93. IKEDA, E. *et al.*, 2000. Reduction of vesicular acetylcholine transporter in beta-amyloid proteininfused rats with memory impairment. *Nuclear Medicine Communications*, 21(10), pp. 933-937.
94. Jacobson, S. A. & Sabbagh, M. N., 2008. Donepezil: potential neuroprotective and diseasemodifying effects. *Expert Opinion on Drug Metabolism & Toxicology*, 4(10), pp. 1363-1369.
95. Jain, P. & Joshi, H., 2012. Coumarin: Chemical and Pharmacological Profil. *Journal of Applied Pharmaceutical Science*, 2(6), pp. 236-240.
96. Joao Matos, M. *et al.*, 2012. Focusing on New Monoamine Oxidase Inhibitors: Differently Substituted Coumarins As An Interesting Scaffold. *Current Topics in Medicinal Chemistry*, 12(20), pp. 2210-2239.
97. Jockers, 2019. *20 Ways to Beat Alzheimer's Disease - DrJockers.com*. [Online] Available at: <https://drjockers.com/alzheimers-disease/>
98. Johnell, K. & Fastbom, J., 2008. Concurrent Use of Anticholinergic Drugs and Cholinesterase Inhibitors. *Drugs & Aging*, 25(10), pp. 871-877.
99. Johnson, G. & Moore, S., 2006. The Peripheral Anionic Site of Acetylcholinesterase: Structure, Functions and Potential Role in Rational Drug Design. *Current Pharmaceutical Design*, 12(2), pp. 217-225.
100. Johnson, G. & Moore, S. W., 2012. Why has butyrylcholinesterase been retained? Structural and functional diversification in a duplicated gene. *Neurochemistry International*, 61(5), pp. 783-797.
101. Joubert, J. *et al.*, 2017. Synthesis and evaluation of 7-substituted coumarin derivatives as multimodal monoamine oxidase-B and cholinesterase inhibitors for the treatment of Alzheimer's disease. *European Journal of Medicinal Chemistry*, Volume 125, pp. 853-864.

102. Kadernani, Y. E. *et al.*, 2014. Adamantane amine derivatives as dual acting NMDA receptor and voltage-gated calcium channel inhibitors for neuroprotection. *Med. Chem. Commun.*, 5(11), pp. 1678-1684.
103. Kapp, E. *et al.*, 2017. Versatility of 7-Substituted Coumarin Molecules as Antimycobacterial Agents, Neuronal Enzyme Inhibitors and Neuroprotective Agents. *Molecules*, 22(10), p. 1644.
104. Kasper, J. D., 2015. The Disproportionate Impact Of Dementia On Family And Unpaid Caregiving To Older Adults. *Health Affairs*, 34(10), pp. 1642-1649.
105. Khoury, R. *et al.*, 2018. The role of 5 HT6-receptor antagonists in Alzheimer's disease: an update. *Expert Opinion on Investigational Drugs*, 27(6), pp. 523-533.
106. Korcsmáros, T. *et al.*, 2007. How to design multi-target drugs. *Expert Opinion on Drug Discovery*, 2(6), pp. 799-808.
107. Kretschmer, B. D., Kratzer, U. & Schmidt, W. J., 1998. Riluzole, a glutamate release inhibitor, and motor behavior. *Naunyn-Schmiedeberg's Archives of Pharmacology*, 358(2), pp. 181-190.
108. Kumar, B., Sheetal, S., Mantha, A. K. & Kumar, V., 2016. Recent developments on the structure–activity relationship studies of MAO inhibitors and their role in different neurological disorders. *RSC Advances*, 6(48), pp. 42660-42683.
109. Lanctôt, K. L., Rajaram, R. D. & Herrmann, N., 2009. Review: Therapy for Alzheimer's disease: how effective are current treatments?. *Therapeutic Advances in Neurological Disorders*, 2(3), pp. 163-180.
110. Linton, A., 2005. The Benefits of Cholinesterase Inhibitors: Managing the Behavioral and Neuropsychiatric Symptoms of Alzheimer's Disease. *Journal of Gerontological Nursing*, 31(12), pp. 4-9.
111. Li, Q., Yang, H., Chen, Y. & Sun, H., 2017. Recent progress in the identification of selective butyrylcholinesterase inhibitors for Alzheimer's disease. *European Journal of Medicinal Chemistry*, Volume 132, pp. 249-309.
112. Lockridge, O., 2015. Review of human butyrylcholinesterase structure, function, genetic variants, history of use in the clinic, and potential therapeutic uses. *Pharmacology & Therapeutics*, Volume 148, pp. 34-46.
113. Lyketsos, C. G. *et al.*, 2011. Neuropsychiatric symptoms in Alzheimer's disease. *Alzheimer's & Dementia*, 7(5), pp. 532-539.
114. Ma, H.-J. *et al.*, 2010. Synthesis and Insecticidal Activity of Novel Carbamate Derivatives as Potential Dual-Binding Site Acetylcholinesterase Inhibitors. *Journal of Agricultural and Food Chemistry*, 58(24), pp. 12817-12821.
115. Marco-Contelles, J. *et al.*, 2016. ASS234, As a New Multi-Target Directed Propargylamine for Alzheimer's Disease Therapy. *Frontiers in Neuroscience*, Volume 10, p. 294.
116. Massoulié, J., 1980. The polymorphism of cholinesterases and its physiological significance. *Trends in Biochemical Sciences*, 5(6), pp. 160-164.



117. Matos, M. J. et al., 2015. Coumarins — An Important Class of Phytochemicals. In: A. Venket Rao & L. G. Rao, eds. *Phytochemicals - Isolation, Characterisation and Role in Human Health*.
118. Matsumoto, T. *et al.*, 1985. A sensitive fluorometric assay for serum monoamine oxidase with kynuramine as substrate. *Clinical Biochemistry*, 18(2), pp. 126-129.
119. McNutt, P., Beske, P., Thirunavukkarsu, N. & Singh, B. R., 2014. Cell-Based Assays for Neurotoxins.. In: *Biological Toxins and Bioterrorism*. Dordrecht: Springer, Dordrecht, pp. 247271.
120. Medvedev, A. E., Ivanov, A. S. & Veselovsky, A. V., 2003. Computer visualisation of the active site of monoamine oxidase-A by means of selective inhibitors. *InflammoPharmacology*, 11(2), pp. 135-143.
121. Mehta, M., Adem, A. & Sabbagh, M., 2012. New Acetylcholinesterase Inhibitors for Alzheimer's Disease. *International Journal of Alzheimer's Disease*, Volume 2012, pp. 1-8.
122. Michel, C. H. *et al.*, 2013. Extracellular Monomeric Tau Protein Is Sufficient to Initiate the Spread of Tau Protein Pathology. *Journal of Biological Chemistry*, 289(2), pp. 956-967.
123. Milczek, E. M. *et al.*, 2011. The 'gating' residues Ile199 and Tyr326 in human monoamine oxidase B function in substrate and inhibitor recognition. *FEBS Journal*, 278(24), pp. 4860-4869.
124. Montagner, C. *et al.*, 2008. Antifungal Activity of Coumarins. *Zeitschrift für Naturforschung C*, 63(1-2), pp. 21-28.
125. Morphy, R., Kay, C. & Rankovic, Z., 2004. From magic bullets to designed multiple ligands. *Drug Discovery Today*, 9(15), pp. 641-651.
126. Moureau, F. *et al.*, 1994. A reversible monoamine oxidase inhibitor, toloxatone: spectrophotometric and molecular orbital studies of the interaction with flavin adenine dinucleotide (FAD). *European Journal of Medicinal Chemistry*, 29(4), pp. 269-277.
127. Mufson, E. J., Counts, S. E., Perez, S. E. & Ginsberg, S. D., 2008. Cholinergic system during the progression of Alzheimer's disease: therapeutic implications. *Expert Review of Neurotherapeutics*, 8(11), pp. 1703-1718.
128. Muller-Schiffmann, A., Sticht H & Korth, C., 2012. Hybrid compounds: from simple combinations to nanomachines.. *BioDrugs*, 26(1), pp. 21-31.
129. Murphy, D. L. *et al.*, 1990. Marked Amine and Amine Metabolite Changes in Norrie Disease Patients with an X-Chromosomal Deletion Affecting Monoamine Oxidase. *Journal of Neurochemistry*, 54(1), pp. 242-247.
130. Murray, R., 2002. The Naturally Occurring Coumarins. In: W. Herz, H. Falk, G. Kirby & R. Moore , eds. *Fortschritte der Chemie organischer Naturstoffe / Progress in the Chemistry of Organic Natural Products.*, pp. 1-619
131. Naoi, M. *et al.*, 2003. Anti-apoptotic function of propargylamine inhibitors of type-B monoamine oxidase. *InflammoPharmacology*, 11(2), pp. 175-181.

132. Nichols, E. *et al.*, 2019. Global, regional, and national burden of Alzheimer's disease and other dementias, 1990–2016: a systematic analysis for the Global Burden of Disease Study 2016. *The Lancet Neurology*, 18(1), pp. 88-106.
133. Niikura, T., Tajima, H. & Kita, Y., 2006. Neuronal Cell Death in Alzheimer's Disease and a Neuroprotective Factor, Humanin. *Current Neuropharmacology*, 4(2), pp. 139-147.
134. Nunan, J. & Small, D., 2000. Regulation of APP cleavage by  $\alpha$ -,  $\beta$ - and  $\gamma$ -secretases. *FEBS Letters*, 483(1), pp. 6-10.
135. Orhan, I. & Gulcan, H., 2015. Coumarins: Auspicious Cholinesterase and Monoamine Oxidase Inhibitors. *Current Topics in Medicinal Chemistry*, 15(17), pp. 1673-1682.
136. Patil, P. O. & Bari, S. B., 2013. A comprehensive review on synthesis and designing aspects of coumarin derivatives as monoamine oxidase inhibitors for depression and Alzheimer's disease. *Bioorganic & Medicinal Chemistry*, 21(9), pp. 2434-2450.
137. Paul Murphy, M. & Levine, H., 2010. Alzheimer's Disease and the Amyloid- $\beta$  Peptide. *Journal of Alzheimer's Disease*, 19(1), pp. 311-323.
138. Pérez, V., Marco, J. L., Fernández-Álvarez, E. & Unzeta, M., 1999. Relevance of benzyloxy group in 2-indolyl methylamines in the selective MAO-B inhibition. *British Journal of Pharmacology*, 127(4), pp. 869-876.
139. Pietsch, M. *et al.*, 2009. Kinetics of inhibition of acetylcholinesterase in the presence of acetonitrile. *FEBS Journal*, 276(8), pp. 2292-2307.
140. Pohanka, M., Hrabínová, M., Kuca, K. & Simonato, J.-P., 2011. Assessment of Acetylcholinesterase Activity Using Indoxylacetate and Comparison with the Standard Ellman's Method. *International Journal of Molecular Sciences*, 12(4), pp. 2631-2640.
141. Prado, V. F., Janickova, H., Al-Onaizi, M. A. & Prado, M. A., 2017. Cholinergic circuits in cognitive flexibility. *Neuroscience*, Volume 345, pp. 130-141.
142. Radić, Z. & Taylor, P., 2001. Peripheral site ligands accelerate inhibition of acetylcholinesterase by neutral organophosphates. *Journal of Applied Toxicology*, 21(S1), pp. S13-S14.
143. Ramírez, M. J., 2013. 5-HT<sub>6</sub> receptors and Alzheimer's disease. *Alzheimer's research & therapy*, 5(2), p. 15.
144. Rees, T. & Brimijoin, S., 2003. The role of acetylcholinesterase in the pathogenesis of Alzheimer's disease. *Drugs of Today*, 39(1), p. 75.
145. Riederer, P., 2004. Monoamine Oxidase-B Inhibition in Alzheimer's Disease. *NeuroToxicology*, 25(1-2), pp. 271-277.
146. Rinne, J. O., 2003. Brain acetylcholinesterase activity in mild cognitive impairment and early Alzheimer's disease. *Journal of Neurology, Neurosurgery & Psychiatry*, 74(1), pp. 113-115.
147. Rochais, C., Lecoutey, C., Gaven, F. & Giannoni, P., 2015. Novel Multitarget-Directed Ligands (MTDLs) with Acetylcholinesterase (AChE) Inhibitory and Serotonergic Subtype 4

- Receptor (5-HT<sub>4</sub>R) Agonist Activities As Potential Agents against Alzheimer's Disease: The Design of Donecopride. *Journal of Medicinal Chemistry*, 58(7), pp. 3172-3187.
148. Rosenmann, H., 2013. Immunotherapy for Targeting Tau Pathology in Alzheimer's Disease and Tauopathies. *Current Alzheimer Research*, 10(3), pp. 217-228.
149. Santana, L. *et al.*, 2008. Quantitative Structure–Activity Relationship and Complex Network Approach to Monoamine Oxidase A and B Inhibitors. *Journal of Medicinal Chemistry*, 51(21), pp. 6740-6751.
150. Santos, N. A. G. *et al.*, 2015. The neuroprotection of cannabidiol against MPP + -induced toxicity in PC12 cells involves trkA receptors, upregulation of axonal and synaptic proteins, neuritogenesis, and might be relevant to Parkinson's disease. *Toxicology in Vitro*, 30(1), pp. 231240.
151. Sashidhara, K. & Modukuri, R. K., 2014. Discovery of 3-Arylcoumarin-tetracyclic Tacrine Hybrids as Multifunctional Agents against Parkinson's Disease. *ACS Medicinal Chemistry Letters*, 5(10), pp. 1099-1103.
152. Saxena, A. *et al.*, 1999. Differences in active-site gorge dimensions of cholinesterases revealed by binding of inhibitors to human butyrylcholinesterase. *Chemico-Biological Interactions*, Volume 119-120, pp. 61-69.
153. Schedin-Weiss, S. *et al.*, 2017. Monoamine oxidase B is elevated in Alzheimer disease neurons, is associated with  $\gamma$ -secretase and regulates neuronal amyloid  $\beta$ -peptide levels. *Alzheimer's Research & Therapy*, 9(1), p.57.
154. Schliebs, R. & Arendt, T., 2006. The significance of the cholinergic system in the brain during aging and in Alzheimer's disease. *Journal of Neural Transmission*, 113(11), pp. 1625-1644.
155. Schmidt, A. W., Lebel, L. A., Howard, H. R. & Zorn, S. H., 2001. Ziprasidone: a novel antipsychotic agent with a unique human receptor binding profile. *European Journal of Pharmacology*, 425(3), pp. 197-201.
156. Schneider, L. S. *et al.*, 2019. Low-dose ladostigil for mild cognitive impairment. *Neurology*, 93(15), e1474–e1484.
157. Seeley, W. *et al.*, 2009. Neurodegenerative diseases target large-scale human brain networks.. *Neuron*, 62(1), pp. 42-52..
158. Shen, Q. *et al.*, 2006. Synthesis and Biological Evaluation of Functionalized Coumarins as Acetylcholinesterase Inhibitors.. *ChemInform*, 37(18), pp. 1307-1315.
159. Silman, I. & Sussman, J. L., 2008. Acetylcholinesterase: How is structure related to function?. *Chemico-Biological Interactions*, 175(1-3), pp. 3-10.
160. Singh, M. *et al.*, 2013. Acetylcholinesterase inhibitors as Alzheimer therapy: From nerve toxins to neuroprotection. *European Journal of Medicinal Chemistry*, Volume 70, pp. 165-188.

161. Singh, S. K., Srikrishna, S., Castellani, R. J. & Perry, G., 2017. Antioxidants in the Prevention and Treatment of Alzheimer's Disease. *Nutritional Antioxidant Therapies: Treatments and Perspectives*, pp. 523-553.
162. Skovronsky, D. M., Lee, V. M.-Y. & Trojanowski, J. Q., 2006. NEURODEGENERATIVE DISEASES: New Concepts of Pathogenesis and Their Therapeutic Implications. *Annual Review of Pathology: Mechanisms of Disease*, 1(1), pp. 151-170. Snider, B. J. *et al.*, 2009. Cerebrospinal Fluid Biomarkers and Rate of Cognitive Decline in Very Mild Dementia of the Alzheimer Type. *Archives of Neurology*, 5(66), pp. 638-645.
163. Son, S.-Y. *et al.*, 2008. Structure of human monoamine oxidase A at 2.2-Å resolution: The control of opening the entry for substrates/inhibitors. *Proceedings of the National Academy of Sciences*, 105(15), pp. 5739-5744.
164. Soto-Ortega, D. D. *et al.*, 2011. Inhibition of amyloid- $\beta$  aggregation by coumarin analogs can be manipulated by functionalization of the aromatic center. *Bioorganic & Medicinal Chemistry*, 19(8), pp. 2596-2602.
165. Spangenberg, E. *et al.*, 2016. Eliminating microglia in Alzheimer's mice prevents neuronal loss without modulating amyloid- $\beta$  pathology. *Brain*, 139(4), pp. 1265-1281.
166. Spinello, A. *et al.*, 2016. Metal Ions and Metal Complexes in Alzheimer's Disease. *Current Pharmaceutical Design*, 22(26), pp. 3996-4010.
167. Spires-Jones, T. *et al.*, 2009. Tau pathophysiology in neurodegeneration: a tangled issue.. *Trends in Neurosciences*, 32(3), pp. 150-159.
168. Stefanachi, A. *et al.*, 2018. Coumarin: A Natural, Privileged and Versatile Scaffold for Bioactive Compounds. *Molecules*, 23(2), p. 250.
169. Sussman, J. L. & Silman, I., 1992. Acetylcholinesterase: Structure and use as a model for specific cation-protein interactions. *Current Biology*, 2(5), p. 612.
170. Swerdlow, R., 2007. Pathogenesis of Alzheimer's disease. *Clinical interventions in aging*, 2(3), pp. 347-359.
171. Takeda, S., 2019. Progression of Alzheimer's disease, tau propagation, and its modifiable risk factors. *Neuroscience Research*, Volume 141, pp. 16-42.
172. Talevi, A., 2015. Multi-target pharmacology: possibilities and limitations of the "skeleton key approach" from a medicinal chemist perspective. *Frontiers in Pharmacology*, Volume 6, p. 205.
173. Tanzi, R. E. & Bertram, L., 2005. Twenty Years of the Alzheimer's Disease Amyloid Hypothesis: A Genetic Perspective. *Cell*, 120(4), pp. 545-555.
174. Terry, A. & Buccafusco, J. J., 2003. The Cholinergic Hypothesis of Age and Alzheimer's Disease-Related Cognitive Deficits: Recent Challenges and Their Implications for Novel Drug Development. *Journal of Pharmacology and Experimental Therapeutics*, 306(3), pp. 821-827.
175. Texidó, L. *et al.*, 2011. Amyloid  $\beta$  peptide oligomers directly activate NMDA receptors. *Cell Calcium*, 49(3), pp. 184-190.

176. Tong, J. *et al.*, 2013. Distribution of Monoamine Oxidase Proteins in Human Brain: Implications for Brain Imaging Studies. *Journal of Cerebral Blood Flow & Metabolism*, 33(6), pp. 863-871.
177. Tönnies, E. & Trushina, E., 2017. Oxidative Stress, Synaptic Dysfunction, and Alzheimer's Disease. *Journal of Alzheimer's Disease*, 57(4), pp. 1105-1121.
178. Touchon, J. *et al.*, 2013. The impact of memantine in combination with acetylcholinesterase inhibitors on admission of patients with Alzheimer's disease to nursing homes: cost-effectiveness analysis in France. *The European Journal of Health Economics*, 15(8), pp. 791-800.
179. Unzeta, M. *et al.*, 2016. Multi-Target Directed Donepezil-Like Ligands for Alzheimer's Disease. *Frontiers in Neuroscience*, Volume 10, p. 205.
180. Vajda, F., 2004. Neuroprotection and Neurodegenerative Disease. In: *Alzheimer's Disease. Current Clinical Neurology*. Totowa, NJ: Humana Press, pp. 235-243.
181. Van der Schyf, C. J., 2011. The use of multi-target drugs in the treatment of neurodegenerative diseases. *Expert Review of Clinical Pharmacology*, 4(3), pp. 293-298.
182. Van der Schyf, C. J., 2011. The use of multi-target drugs in the treatment of neurodegenerative diseases. *Expert Review of Clinical Pharmacology*, 4(3), pp. 293-298.
183. Wang, R. & Reddy, P. H., 2017. Role of Glutamate and NMDA Receptors in Alzheimer's Disease. *Journal of Alzheimer's Disease*, 57(4), pp. 1041-1048.
184. Wang, Y. *et al.*, 2015. Dual functional cholinesterase and MAO inhibitors for the treatment of Alzheimer's disease: synthesis, pharmacological analysis and molecular modeling of homoisoflavonoid derivatives. *Journal of Enzyme Inhibition and Medicinal Chemistry*, 31(3), pp. 1-9.
185. Weinreb, O., Amit, T., Bar-Am, O. & Youdim, M. B., 2010. Rasagiline: A novel antiParkinsonian monoamine oxidase-B inhibitor with neuroprotective activity. *Progress in Neurobiology*, 92(3), pp. 330-344.
186. Westfall, T., 2009. Cholinergic Neurotransmission in the Autonomic and Somatic Motor Nervous System. *Encyclopedia of Neuroscience*, pp. 827-834.
187. Wiemerslage, L., Schultz, B. J., Ganguly, A. & Lee, D., 2013. Selective degeneration of dopaminergic neurons by MPP<sup>+</sup> and its rescue by D2 autoreceptors in *Drosophila* primary culture. *Journal of Neurochemistry*, 126(4), pp. 529-540.
188. Wu, L. *et al.*, 2009. The Structure and Pharmacological Functions of Coumarins and Their Derivatives. *Current Medicinal Chemistry*, 16(32), pp. 4236-4260.
189. Xu, T.-H. *et al.*, 2016. Alzheimer's disease-associated mutations increase amyloid precursor protein resistance to  $\gamma$ -secretase cleavage and the A $\beta$ 42/A $\beta$ 40 ratio. *Cell Discovery*, 2(1), pp. 16026.
190. Xu, Y. *et al.*, 2008. Flexibility of Aromatic Residues in the Active-Site Gorge of

- Acetylcholinesterase: X-ray versus Molecular Dynamics. *Biophysical Journal*, 95(5), pp. 2500-2511.
191. Yanez, M. & Vina, D., 2013. Dual Inhibitors of Monoamine Oxidase and Cholinesterase for the Treatment of Alzheimer Disease. *Current Topics in Medicinal Chemistry*, 13(14), pp. 1692-1706.
192. Yiannopoulou, K. G. & Papageorgiou, S. G., 2012. Current and future treatments for Alzheimer's disease. *Therapeutic Advances in Neurological Disorders*, 6(1), pp. 19-33.
193. Yuan, P. & Grutzendler, J., 2016. Attenuation of  $\beta$ -Amyloid Deposition and Neurotoxicity by Chemogenetic Modulation of Neural Activity. *Journal of Neuroscience*, 36(2), pp. 632-641.
194. Yusufzai, S. K. *et al.*, 2018. Molecular docking studies of coumarin hybrids as potential acetylcholinesterase, butyrylcholinesterase, monoamine oxidase A/B and  $\beta$ -amyloid inhibitors for Alzheimer's disease. *Chemistry Central Journal*, 12(1), pp. 128.
195. Zatta, P., Lucchini, R., van Rensburg, S. J. & Taylor, A., 2003. The role of metals in neurodegenerative processes: aluminum, manganese, and zinc. *Brain Research Bulletin*, 62(1), pp. 15-28.
196. Zhang, P., Xu, S., Zhu, Z. & Xu, J., 2019. Multi-target design strategies for the improved treatment of Alzheimer's disease. *European Journal of Medicinal Chemistry*, Volume 176, pp. 228-247.
197. Zhang, Y., Kua, J. & McCammon, J. A., 2002. Role of the Catalytic Triad and Oxyanion Hole in Acetylcholinesterase Catalysis: An ab initio QM/MM Study. *Journal of the American Chemical Society*, 124(35), pp. 10572-10577.
198. Zindo, F. T., Joubert, J. & Malan, S. F., 2015. Propargylamine as functional moiety in the design of multifunctional drugs for neurodegenerative disorders: MAO inhibition and beyond. *Future Medicinal Chemistry*, 7(5), pp. 609-629.
199. Zindo, F. T. *et al.*, 2019. Design, synthesis and evaluation of pentacycloundecane and hexacycloundecane propargylamine derivatives as multifunctional neuroprotective agents. *European Journal of Medicinal Chemistry*, Volume 163, pp. 83-94.

# Annexure: Spectral Data

$^1\text{H}$  NMR,  $^{13}\text{C}$  NMR, MS and IR  
Spectra

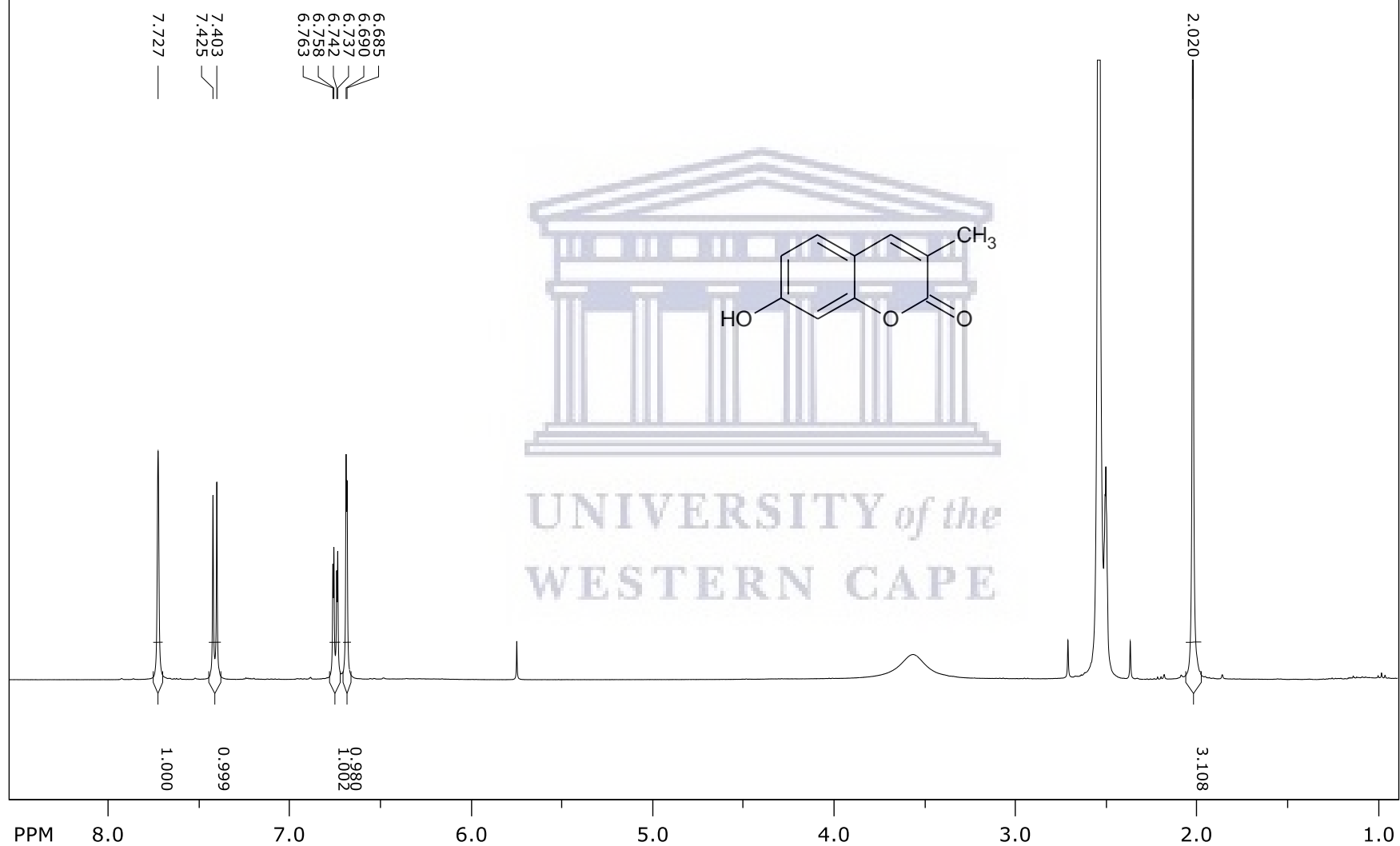


UNIVERSITY *of the*  
WESTERN CAPE

Spectrum 1:  $^1\text{H}$  NMR COMPOUND SM1

SpinWorks 4:

PROTON DMSO {C:\Bruker\TopSpin3.2} JJ-SheunopaMzezewa 19

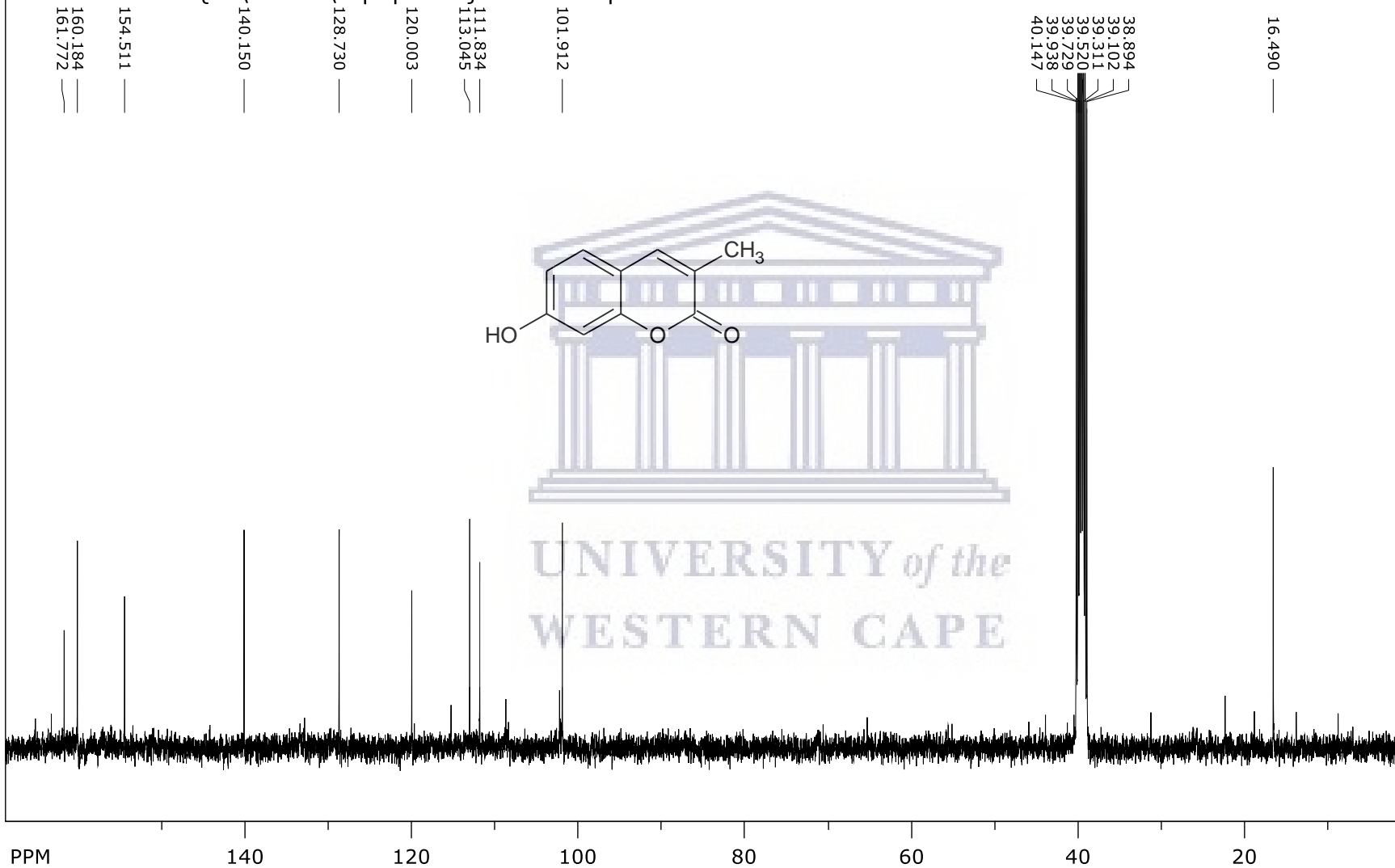




SpinWorks 4:

Spectrum 2:  $^{13}\text{C}$  NMR COMPOUND SM1

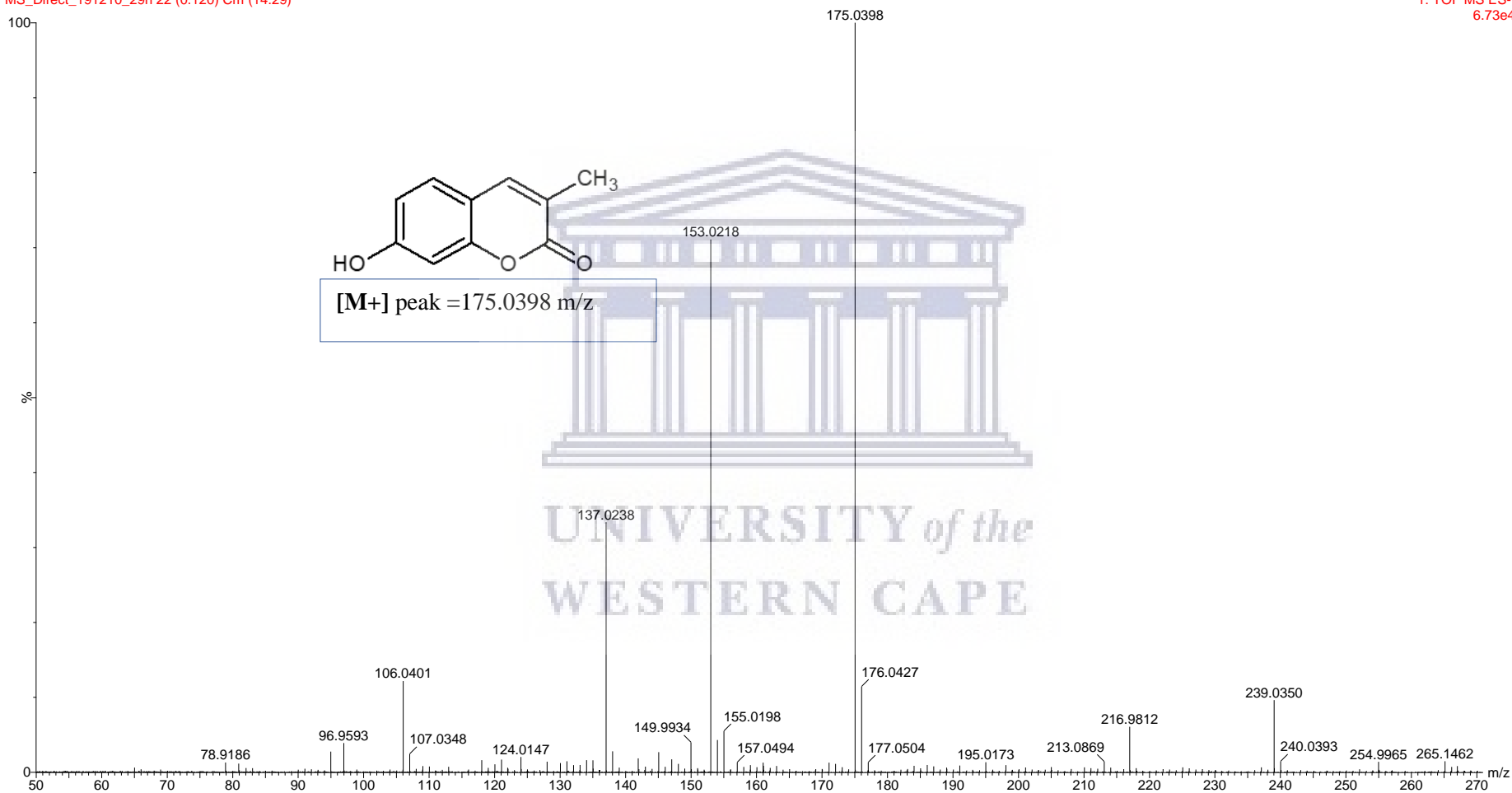
C13CPD DMSO {C:\Bruker\TopSpin3.2} JJ-SheunopaMzezewa 19



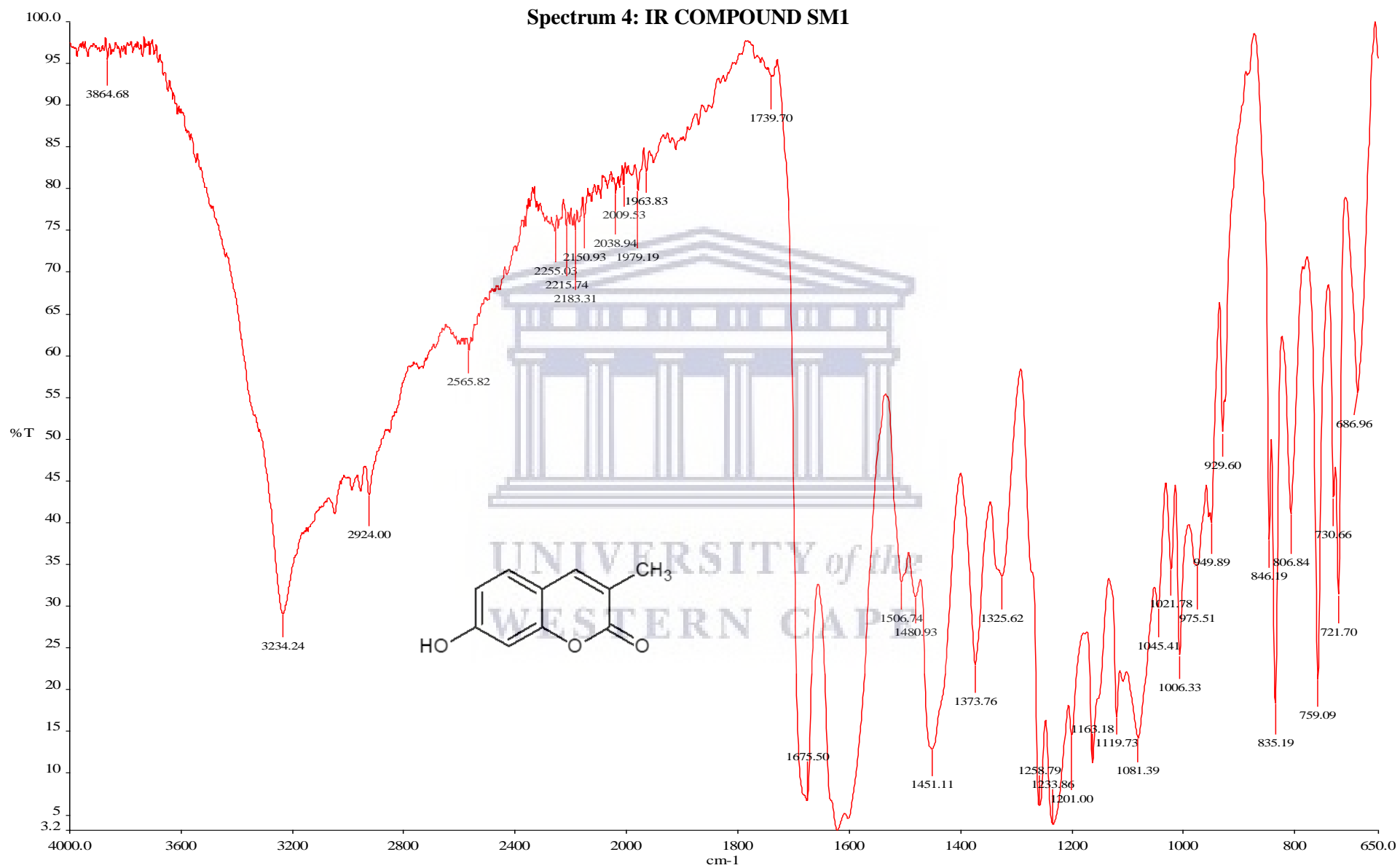
## Spectrum 3: HR-MS COMPOUND SM1

SM 1  
MS\_Direct\_191210\_29n 22 (0.120) Cm (14:29)

1: TOF MS ES-  
6.73e4

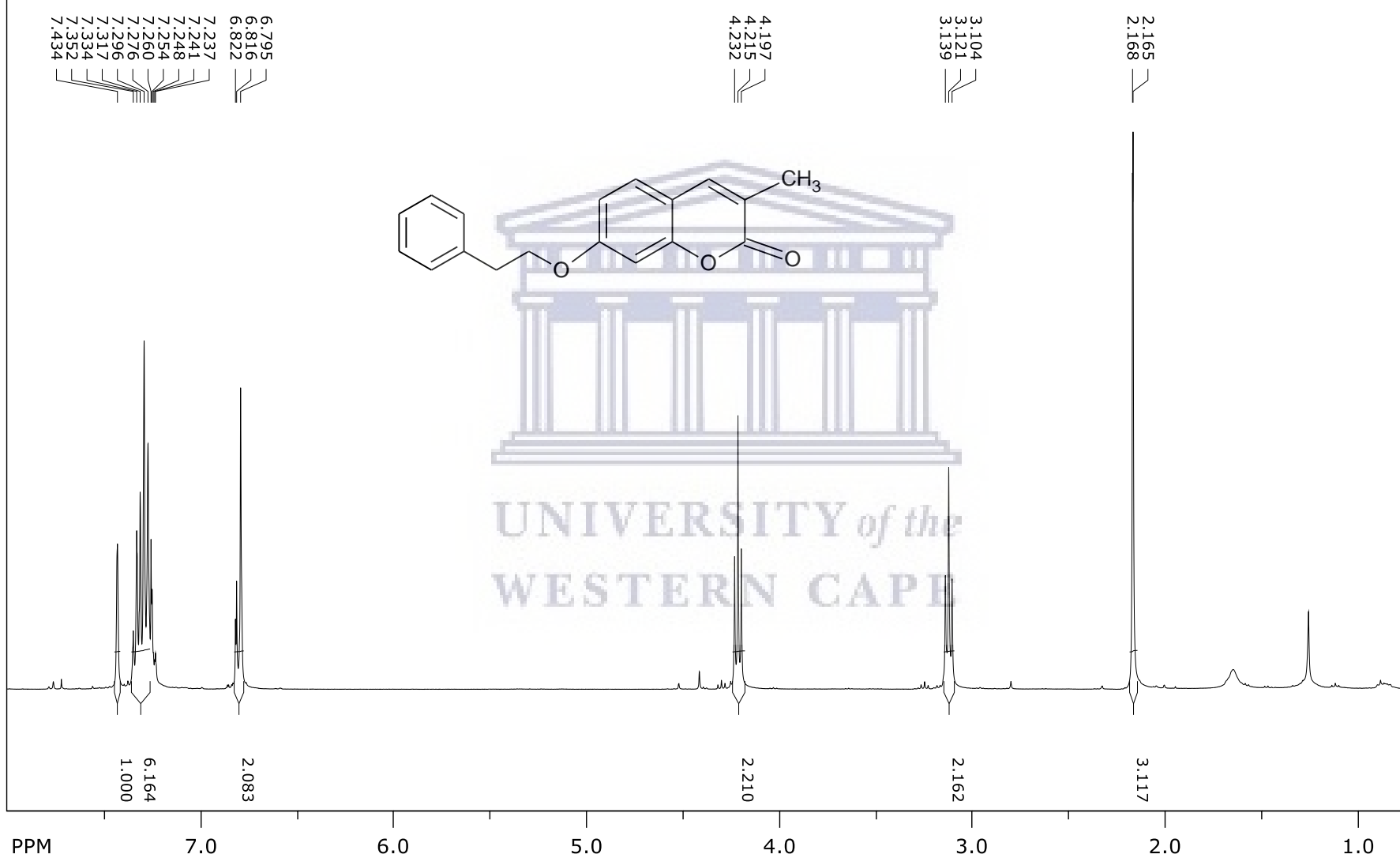


UNIVERSITY of the  
WESTERN CAPE



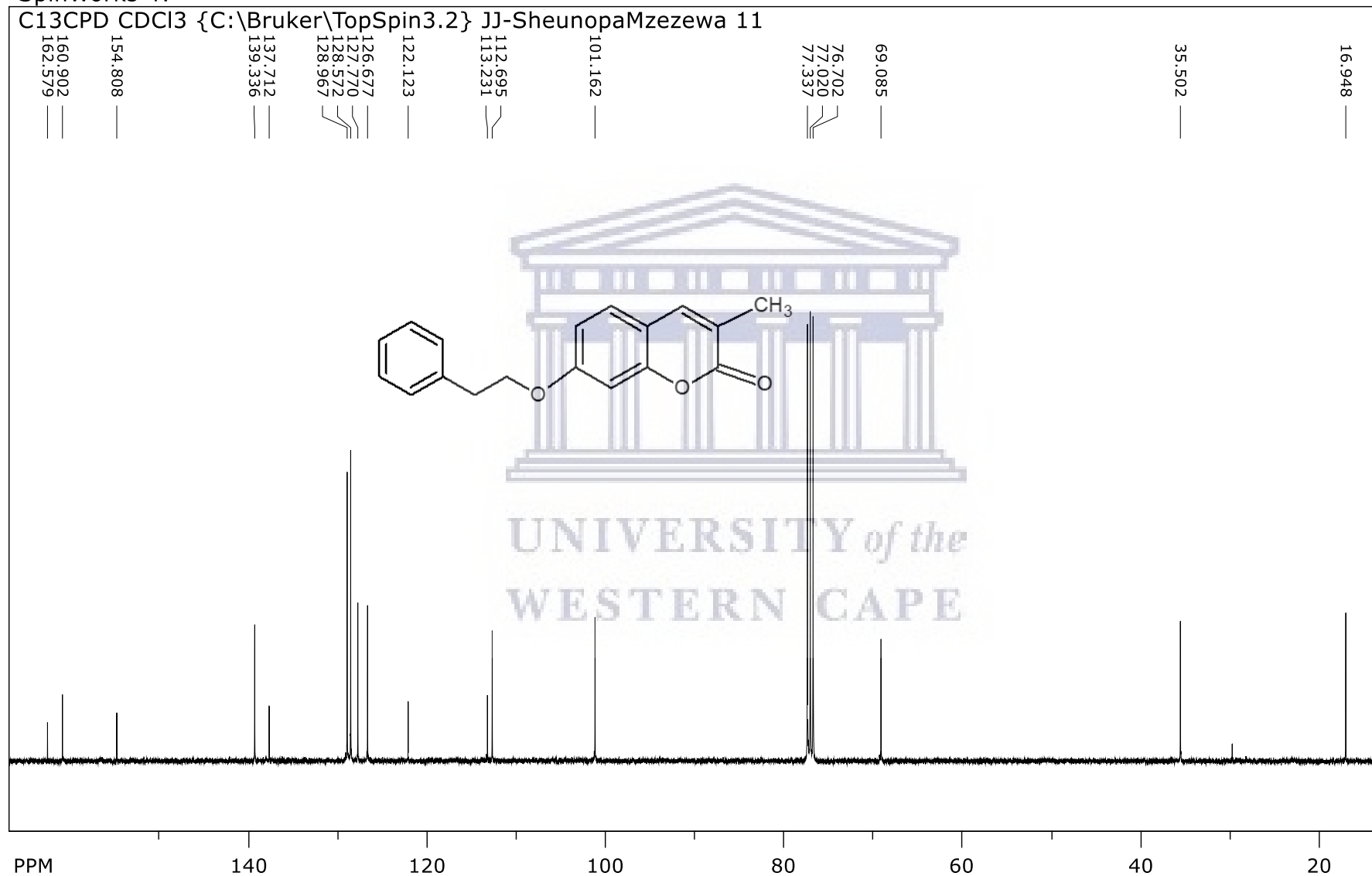
Spectrum 5:  $^1\text{H}$  NMR COMPOUND SM2A

SpinWorks 4:

PROTON CDCl<sub>3</sub> {C:\Bruker\TopSpin3.2} JJ-SheunopaMzezewa 11UNIVERSITY of the  
WESTERN CAPE

Spectrum 6:  $^{13}\text{C}$  NMR COMPOUND SM2A

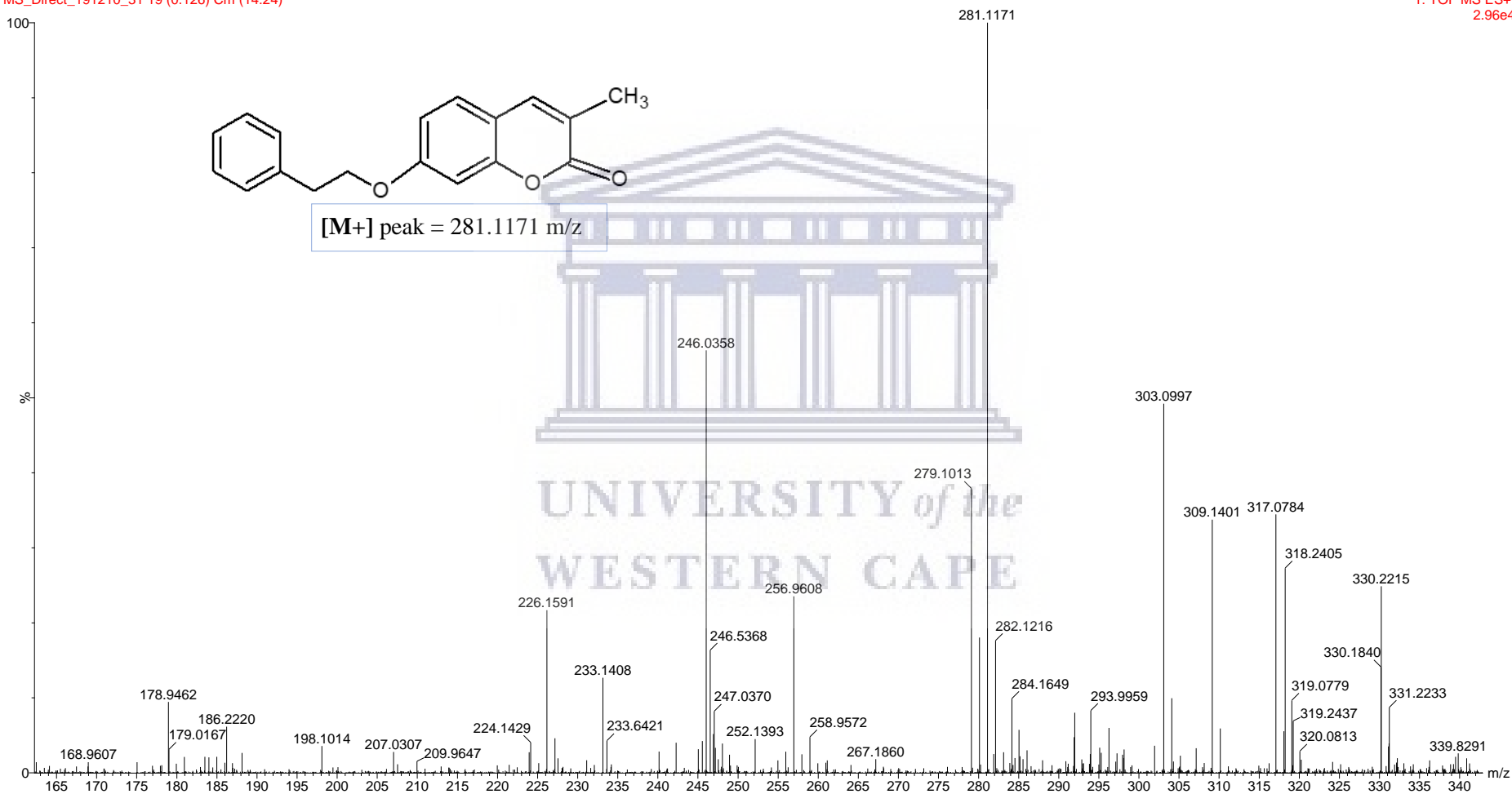
SpinWorks 4:

C13CPD CDCl<sub>3</sub> {C:\Bruker\TopSpin3.2} JJ-SheunopaMzezewa 11UNIVERSITY of the  
WESTERN CAPE

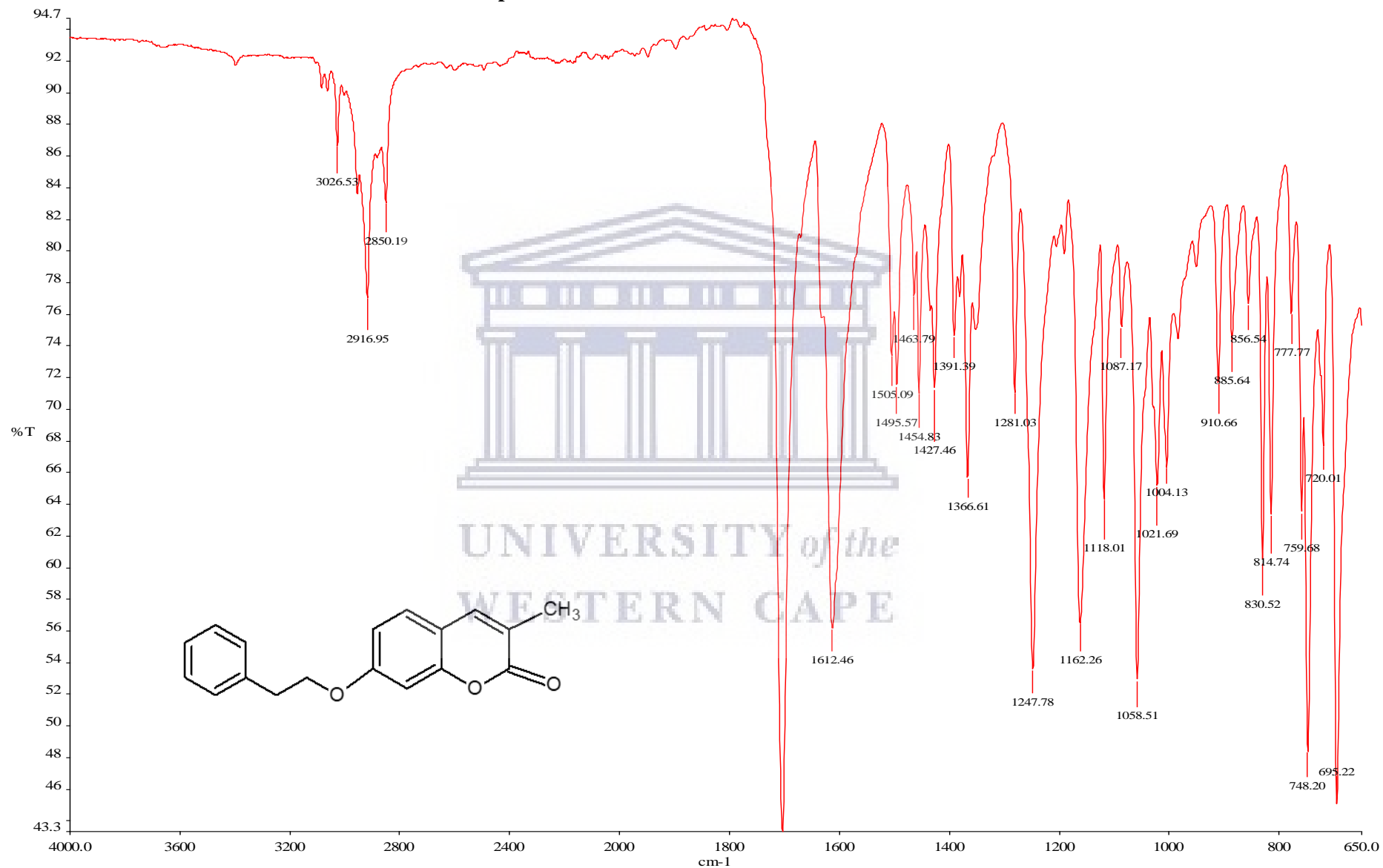
## Spectrum 7: HR-MS COMPOUND SM2A

SM 2A

MS\_Direct\_191210\_31 19 (0.126) Cm (14:24)

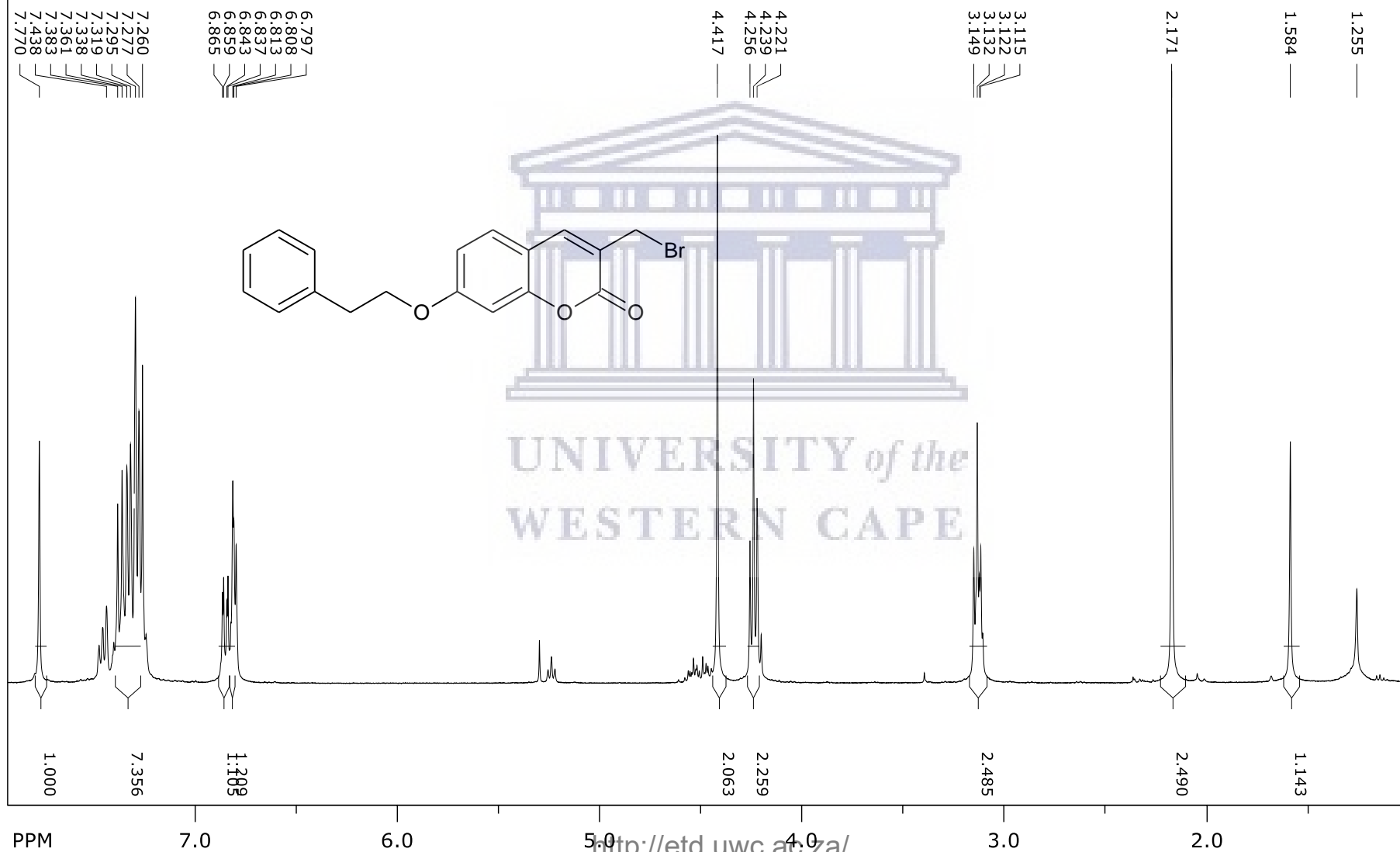
1: TOF MS ES+  
2.96e4

Spectrum 8: IR COMPOUND SM2A



Spectrum 9:  $^1\text{H}$  NMR COMPOUND SM3A

SpinWorks 4:

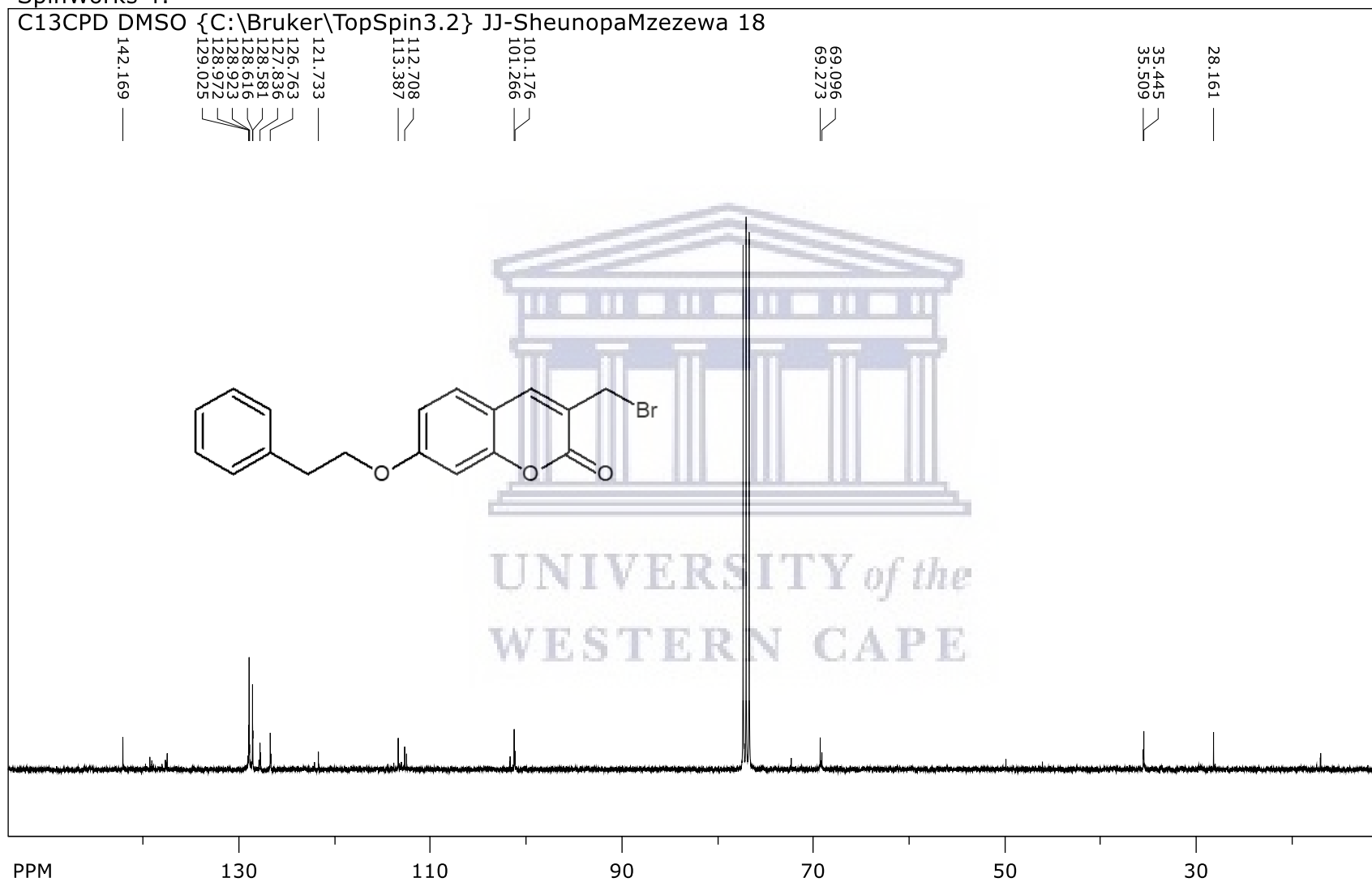
PROTON CDCl<sub>3</sub> {C:\Bruker\TopSpin3.5pl7} JJ-SheunopaMzezewa 19



Spectrum 10:  $^{13}\text{C}$  NMR COMPOUND SM3A

SpinWorks 4:

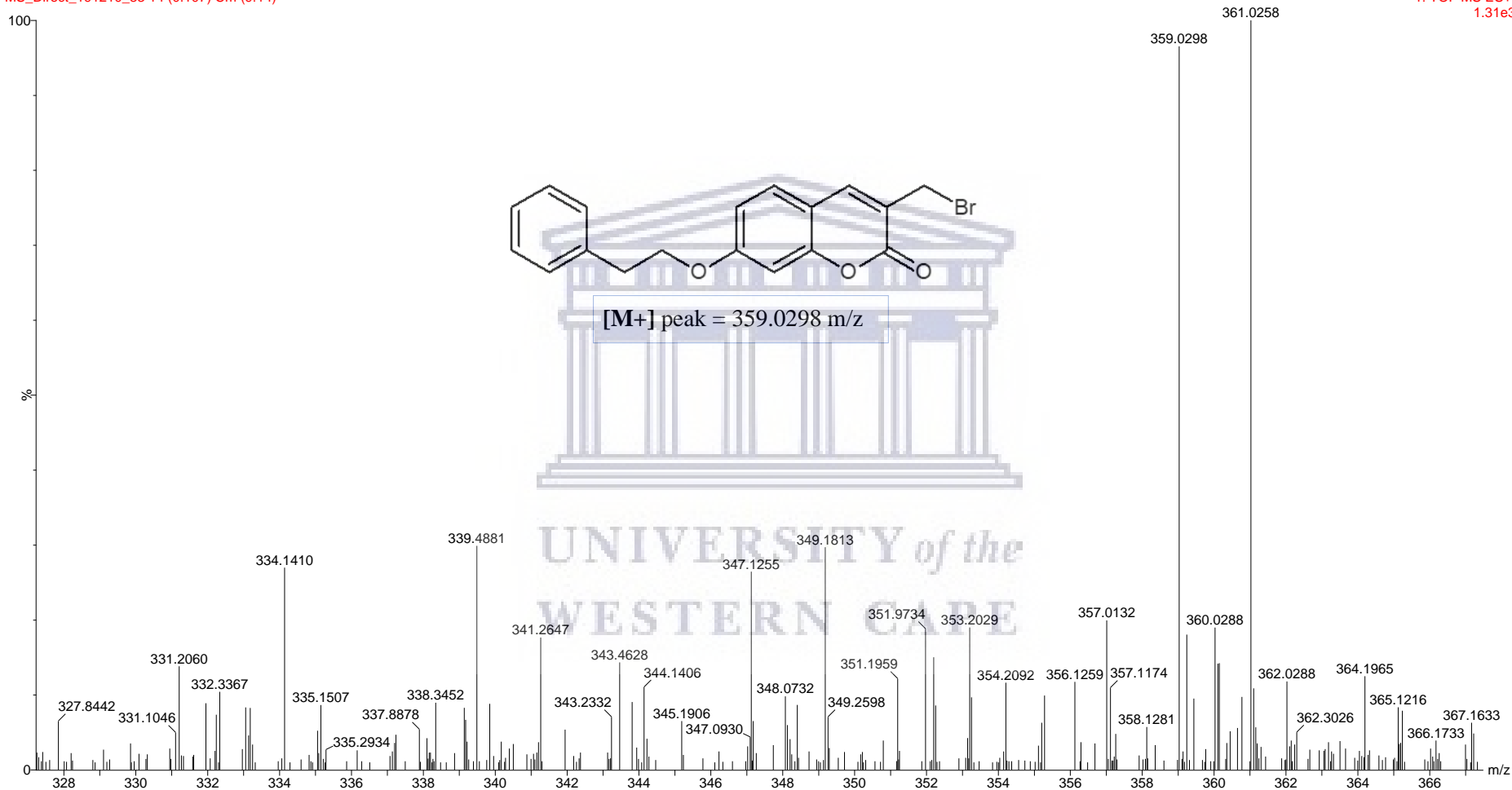
C13CPD DMSO {C:\Bruker\TopSpin3.2} JJ-SheunopaMzezewa 18

UNIVERSITY of the  
WESTERN CAPE

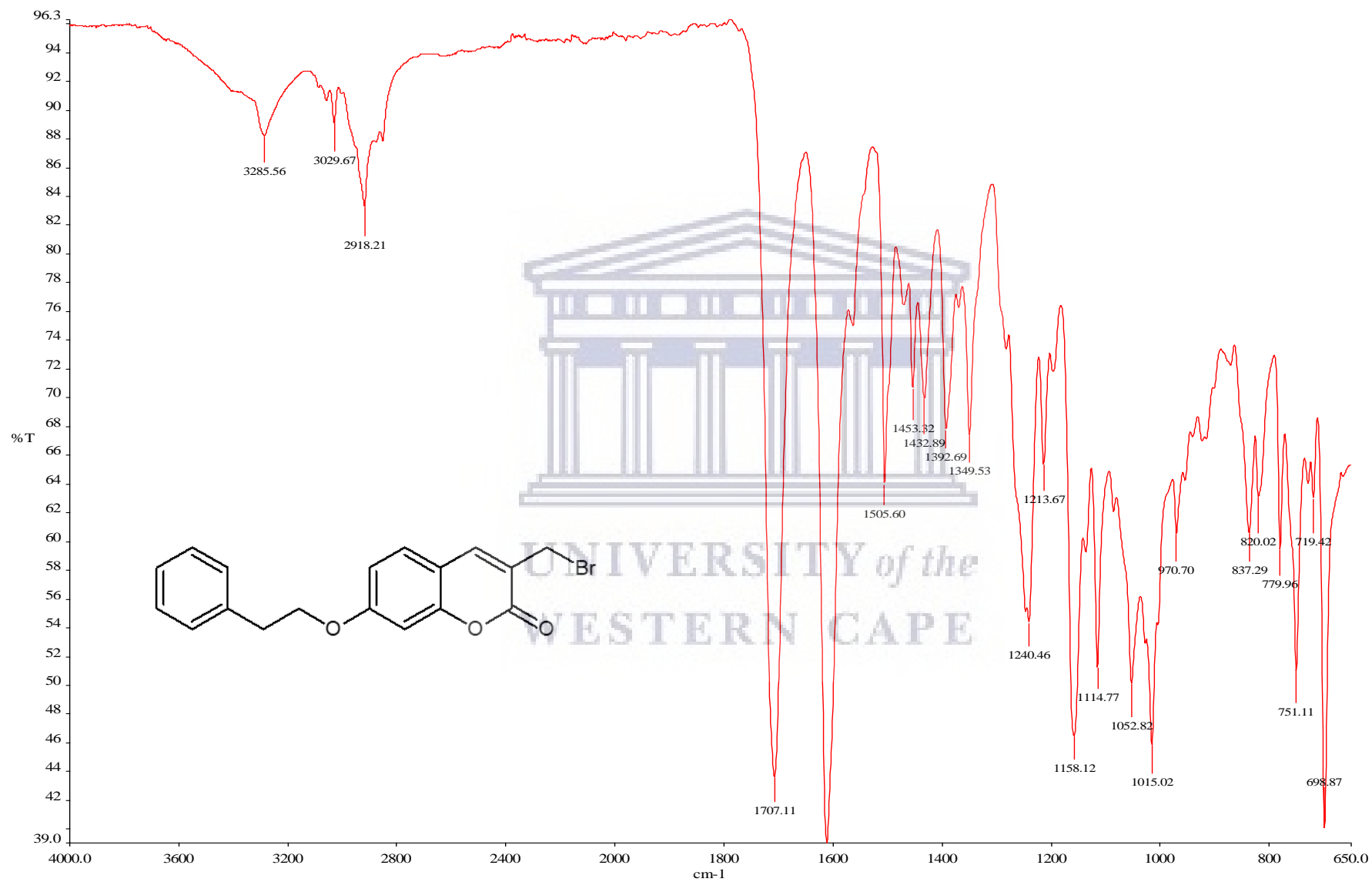
## Spectrum 11: HR-MS COMPOUND SM3A

SM 3A

MS\_Direct\_191210\_33 14 (0.107) Cm (9:14)

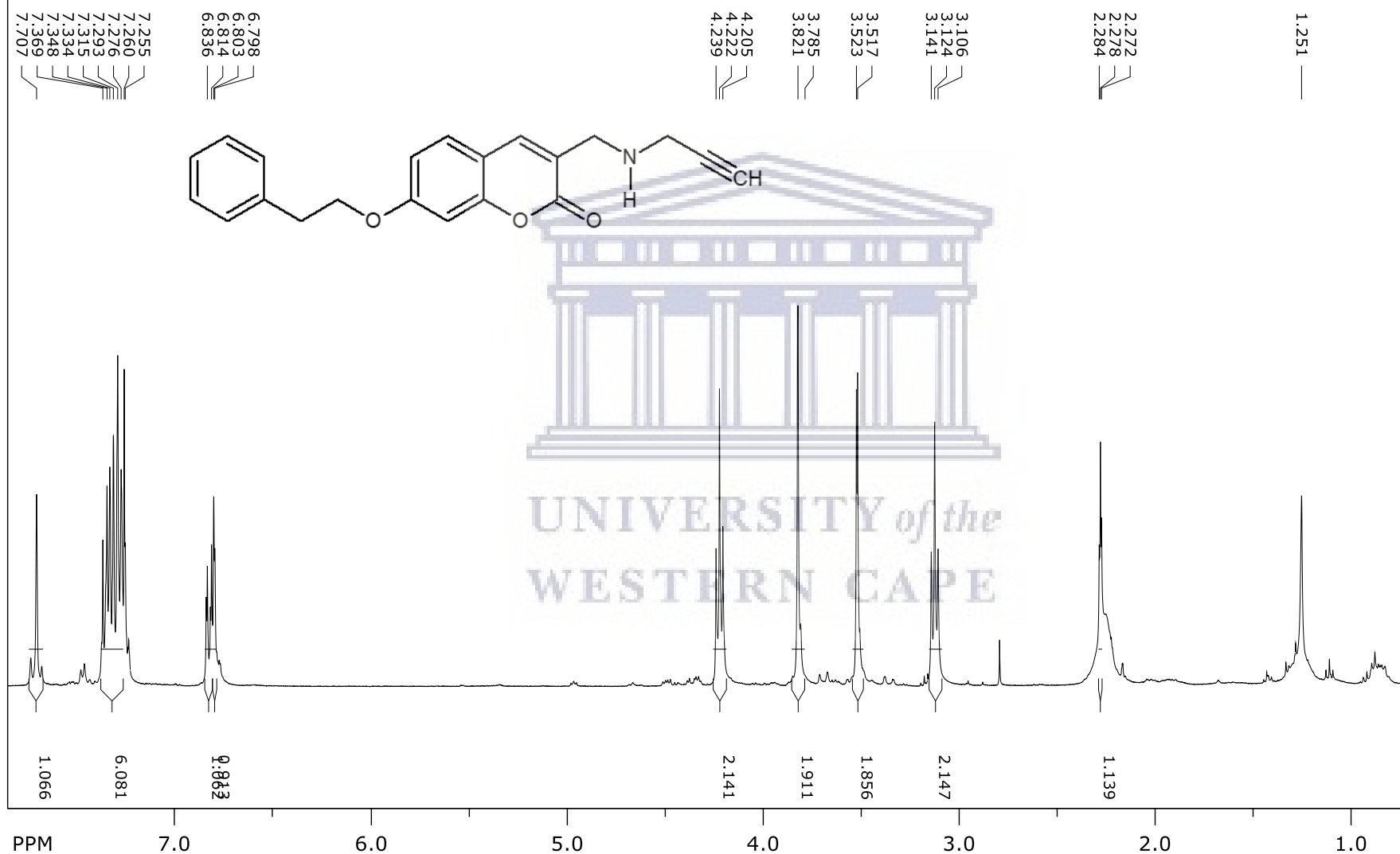
1: TOF MS ES+  
1.31e3

Spectrum 12: IR COMPOUND SM3A



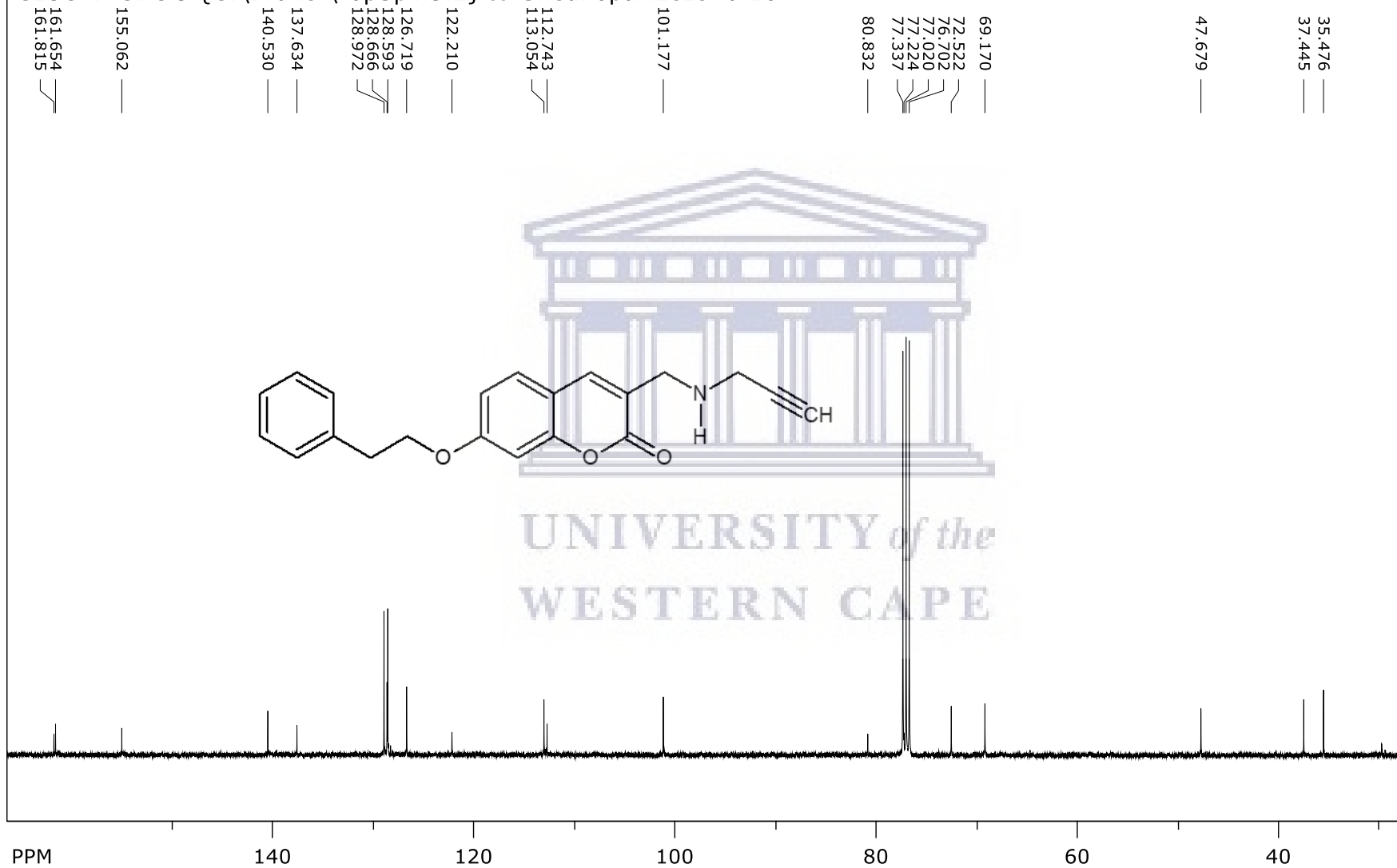
Spectrum 13: <sup>1</sup>H NMR COMPOUND SM4A

SpinWorks 4:

PROTON CDCl<sub>3</sub> {C:\Bruker\TopSpin3.2} JJ-SheunopaMzezewa 10

Spectrum 14:  $^{13}\text{C}$  NMR COMPOUND SM5A

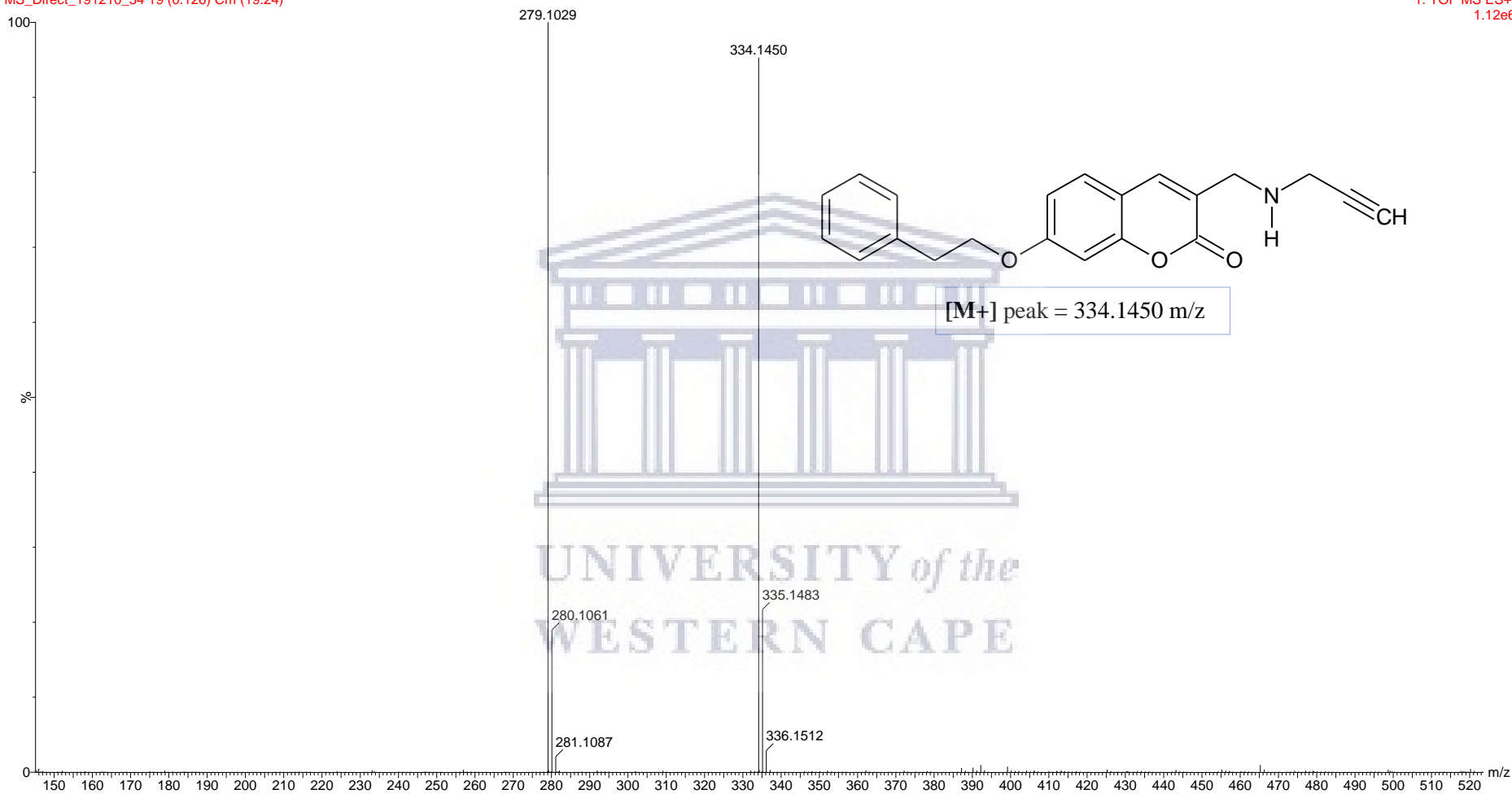
SpinWorks 4:

C13CPD CDCl<sub>3</sub> {C:\Bruker\TopSpin3.2} JJ-SheunopaMzezewa 10

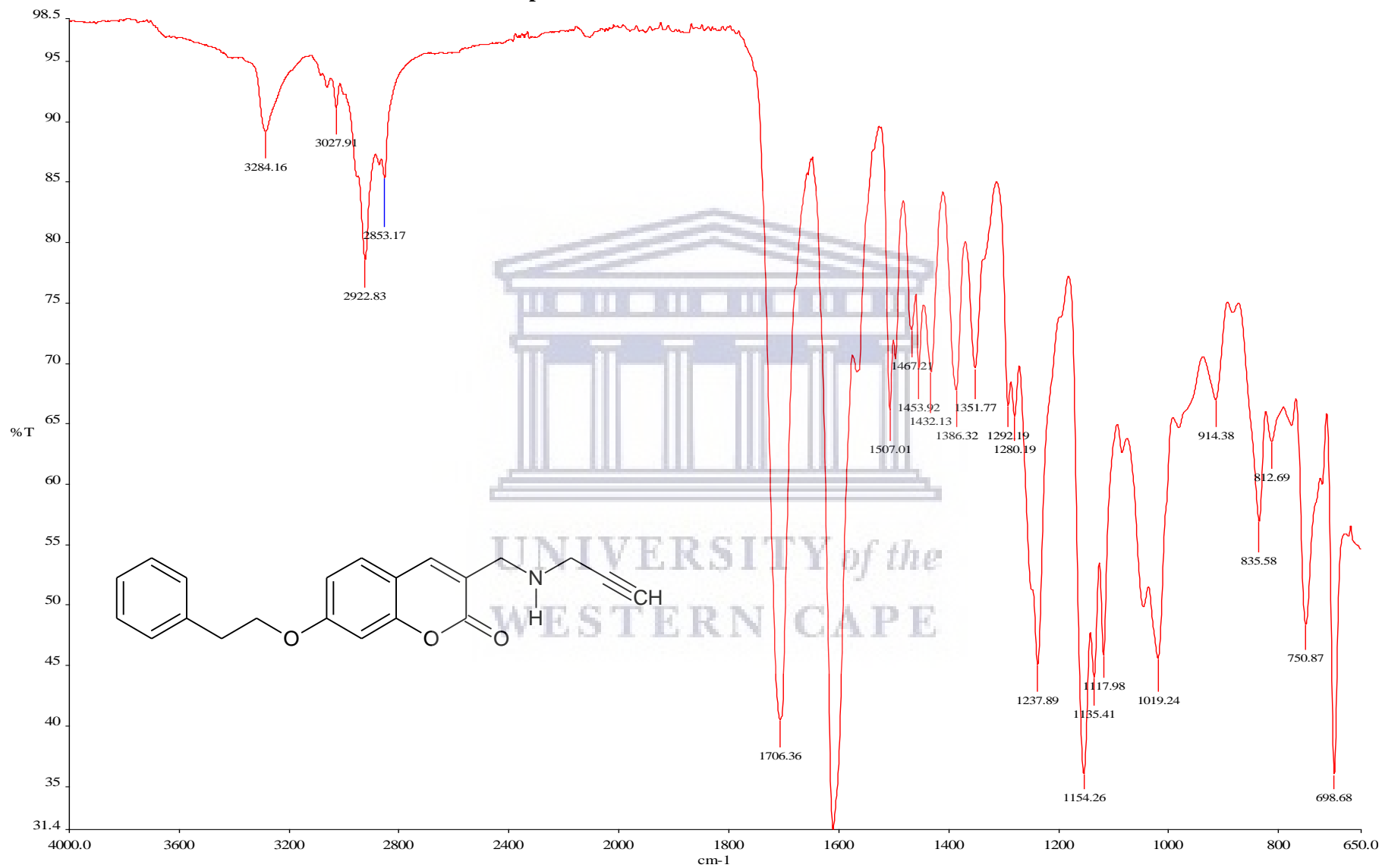
## Spectrum 15: HR-MS COMPOUND SM4A

SM 4A

MS\_Direct\_191210\_34 19 (0.126) Cm (19:24)

1: TOF MS ES+  
1.12e6

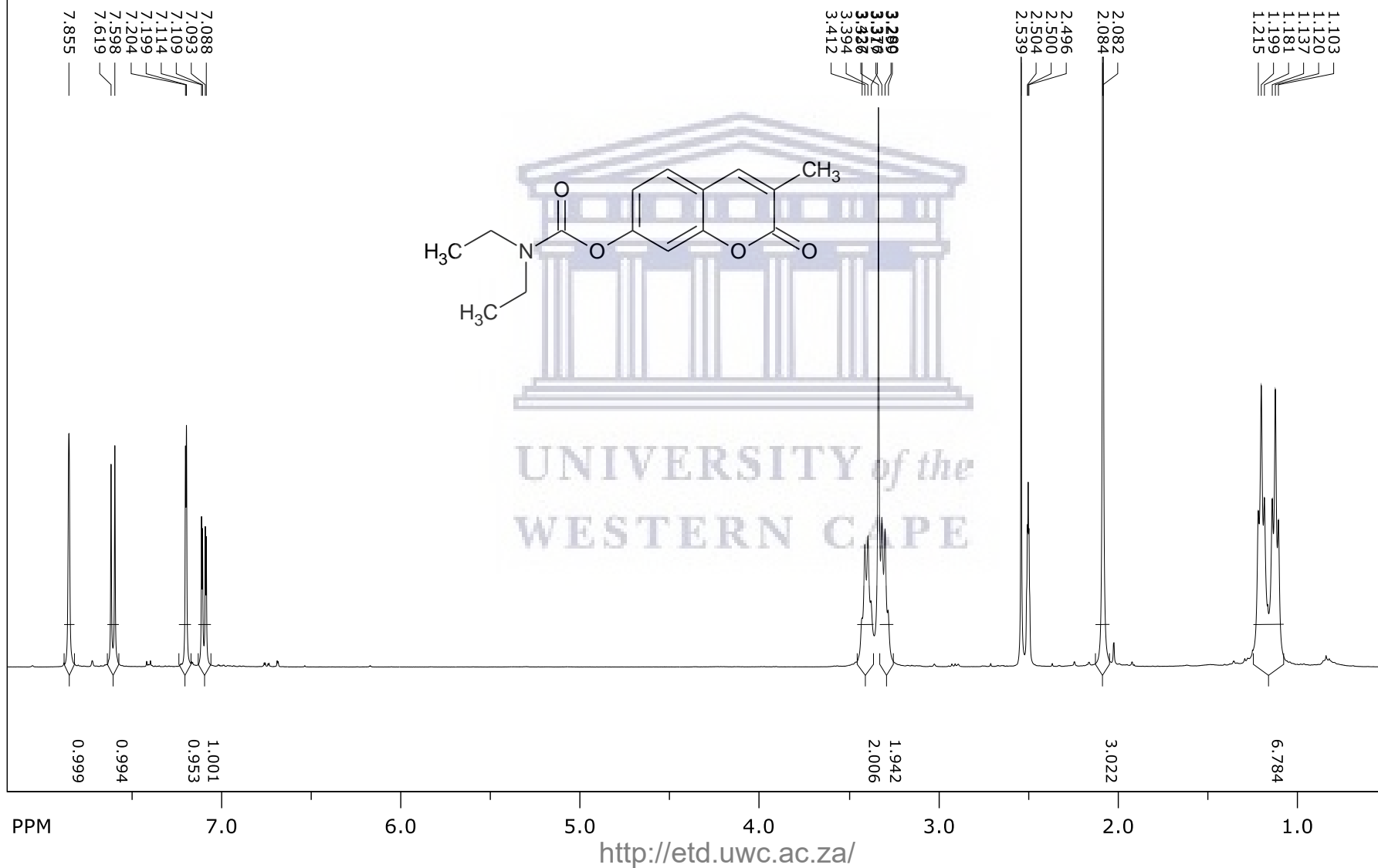
Spectrum 16: IR COMPOUND SM4A



Spectrum 17:  $^1\text{H}$  NMR COMPOUND SM2B

SpinWorks 4:

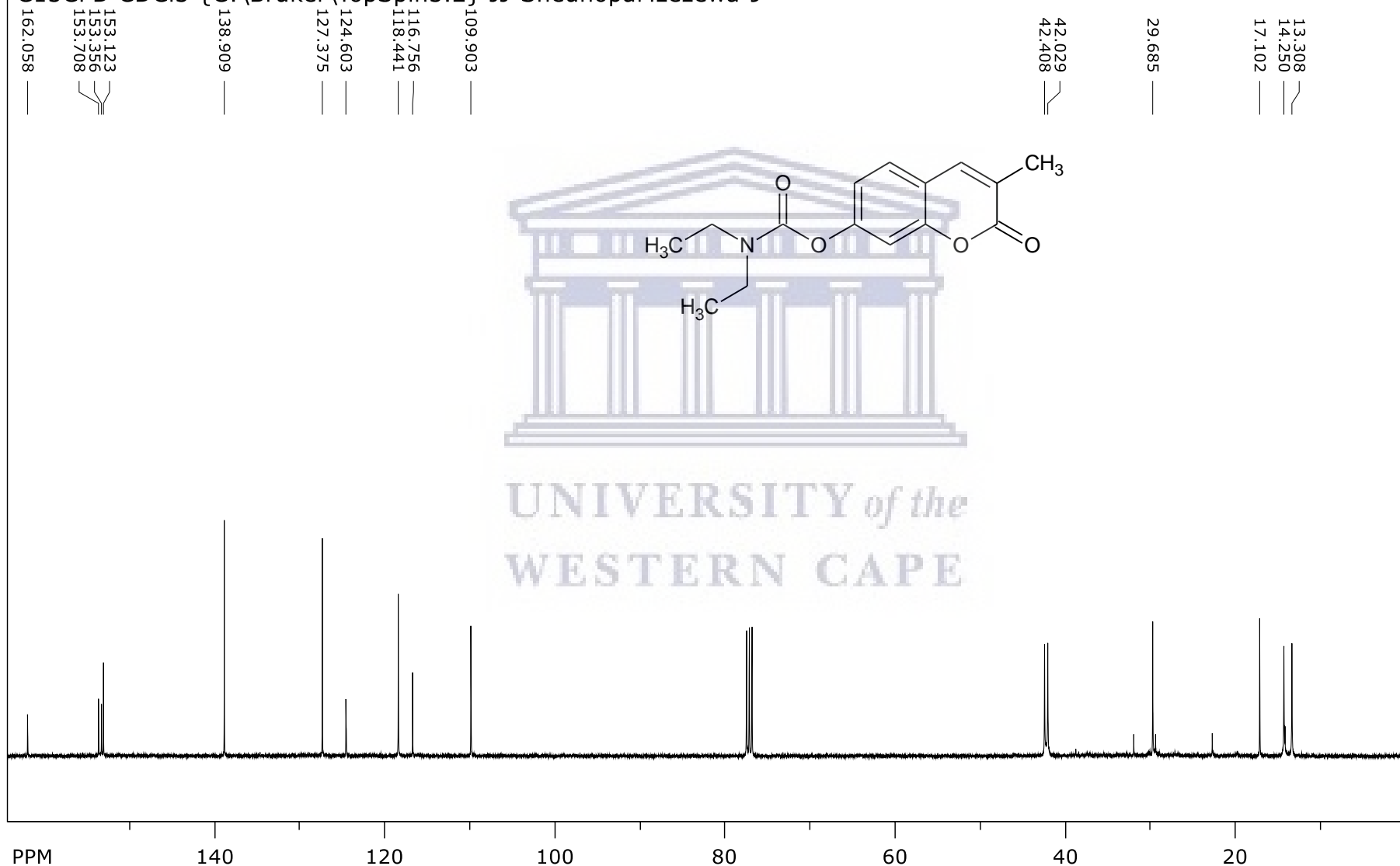
PROTON DMSO {C:\Bruker\TopSpin3.2} JJ-SheunopaMzezewa 19





Spectrum 18:  $^{13}\text{C}$  NMR COMPOUND SM2B

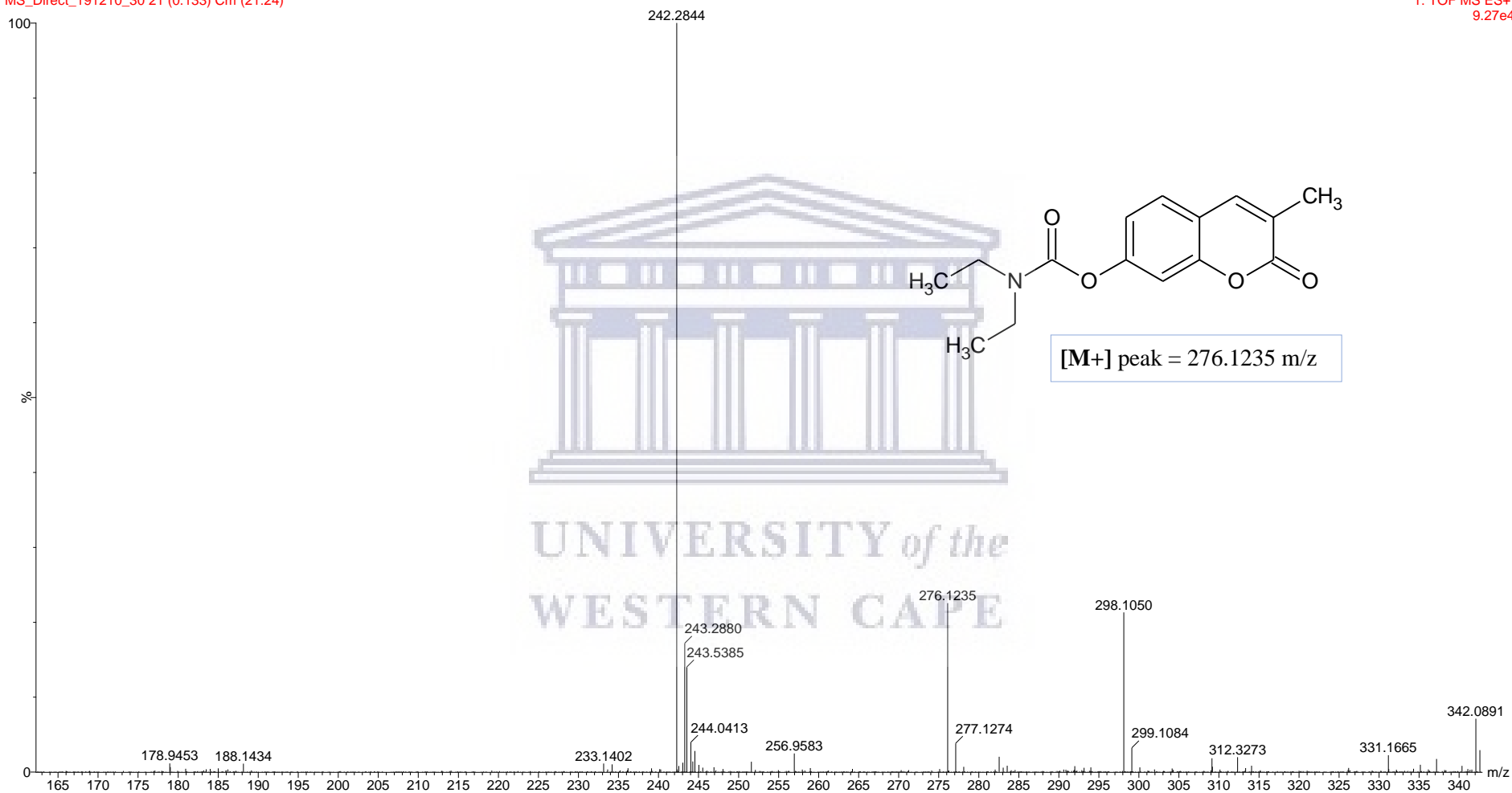
SpinWorks 4:

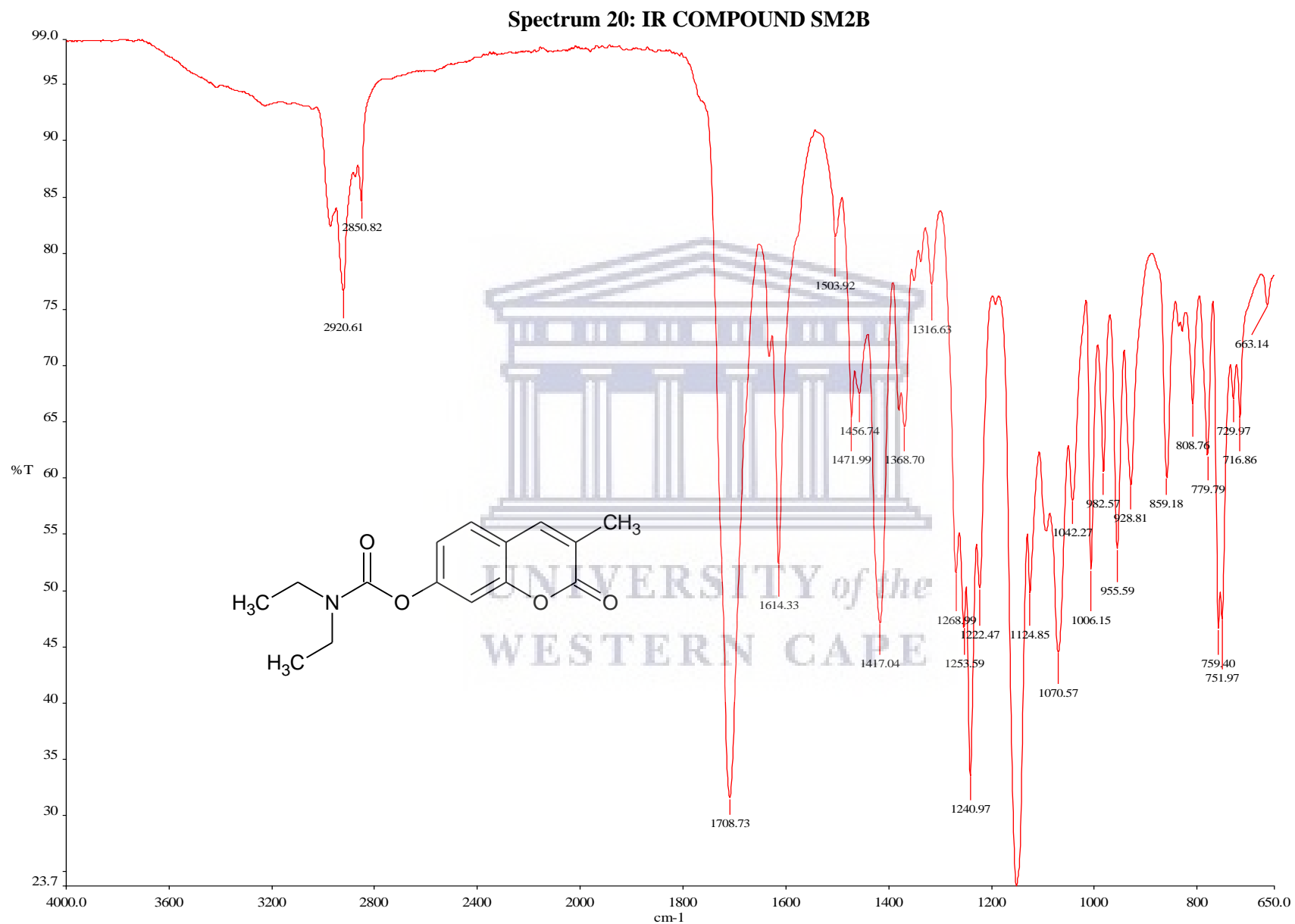
C13CPD CDCl<sub>3</sub> {C:\Bruker\TopSpin3.2} JJ-SheunopaMzezewa 9UNIVERSITY of the  
WESTERN CAPE

## Spectrum 19: HR-MS COMPOUND SM2B

SM 2b

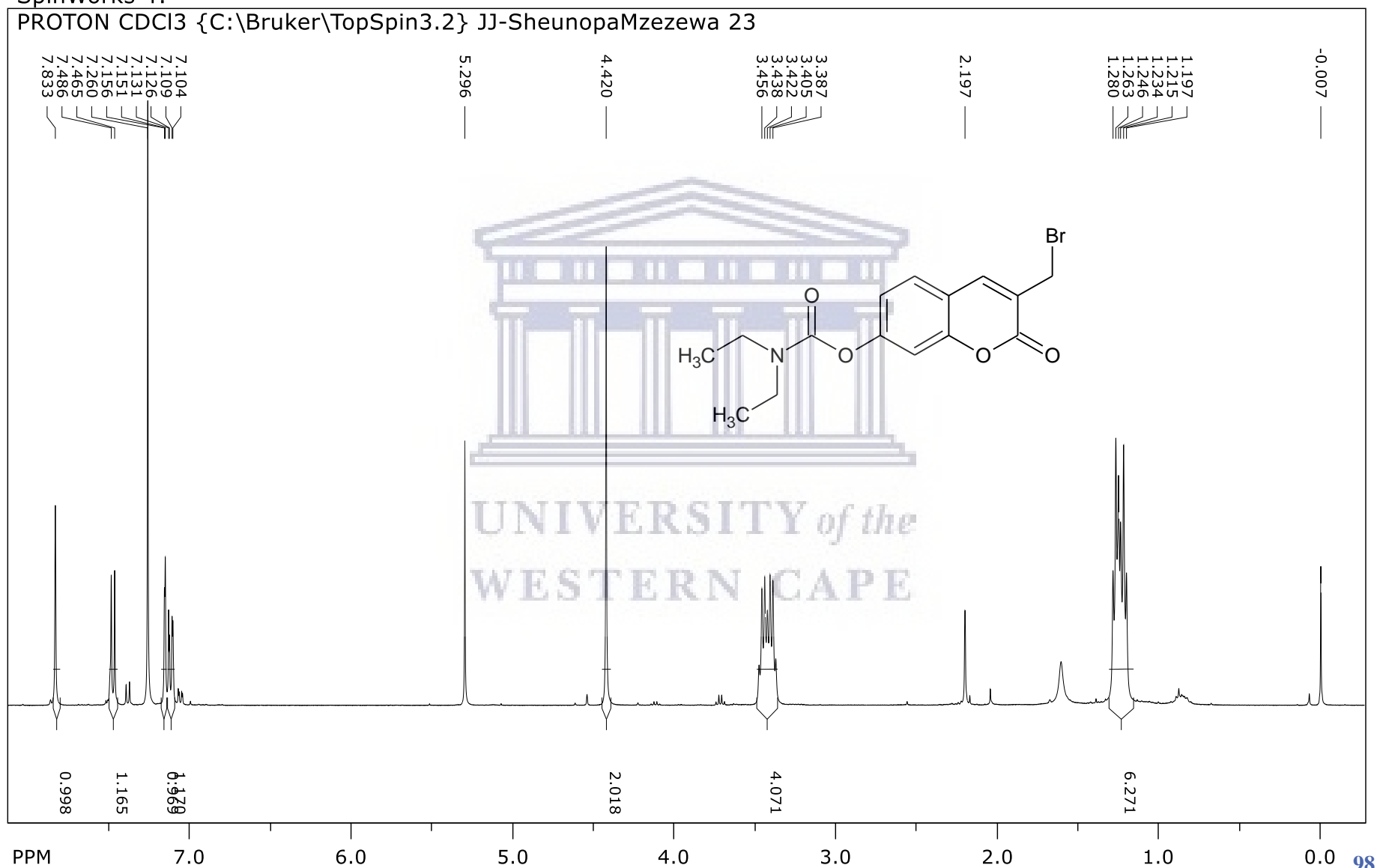
MS\_Direct\_191210\_30 21 (0.133) Cm (21:24)

1: TOF MS ES+  
9.27e4UNIVERSITY of the  
WESTERN CAPE



Spectrum 21: <sup>1</sup>H NMR COMPOUND SM3B

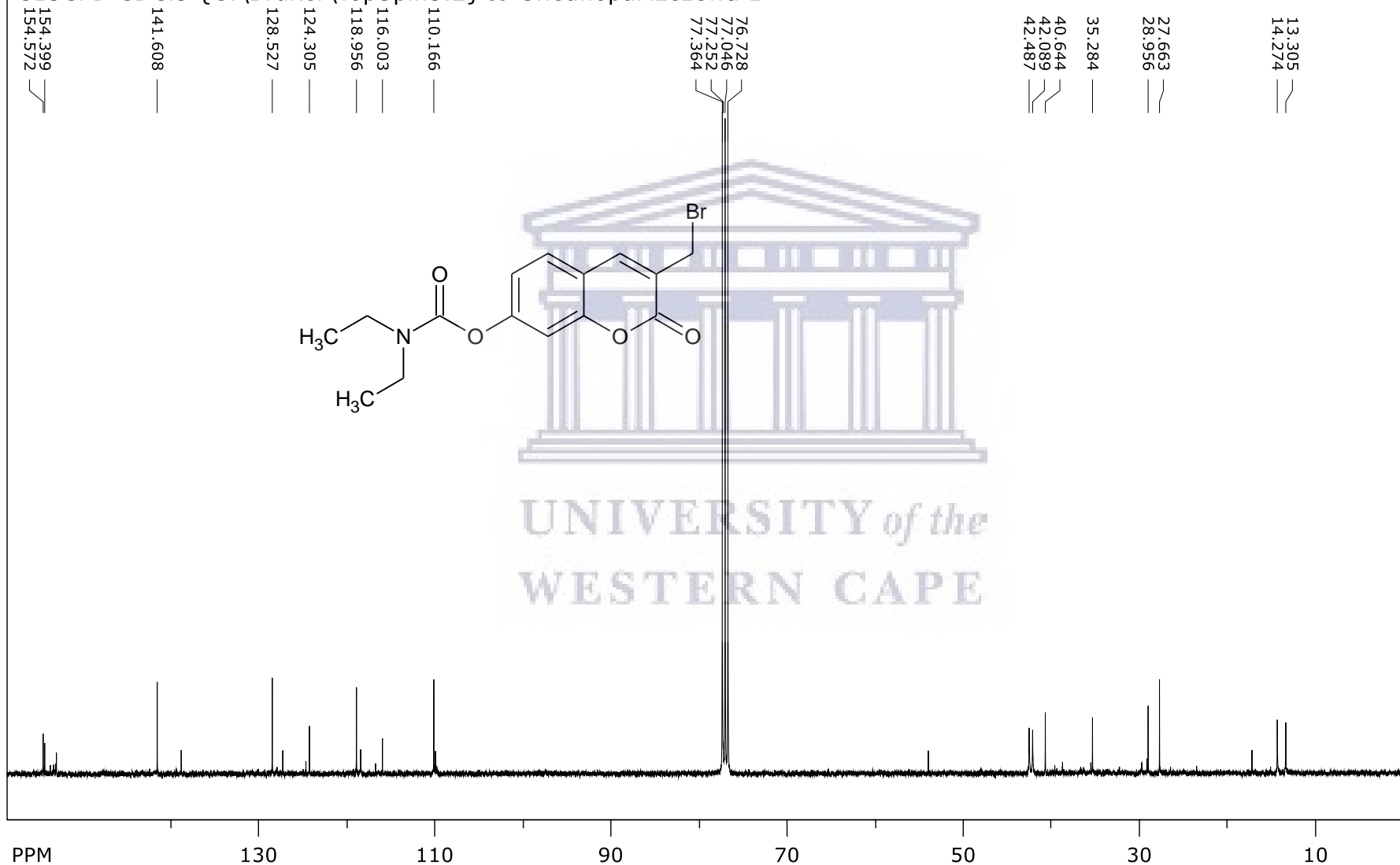
SpinWorks 4:

PROTON CDCl<sub>3</sub> {C:\Bruker\TopSpin3.2} JJ-SheunopaMzezewa 23

Spectrum 22:  $^{13}\text{C}$  NMR COMPOUND SM3B

SpinWorks 4:

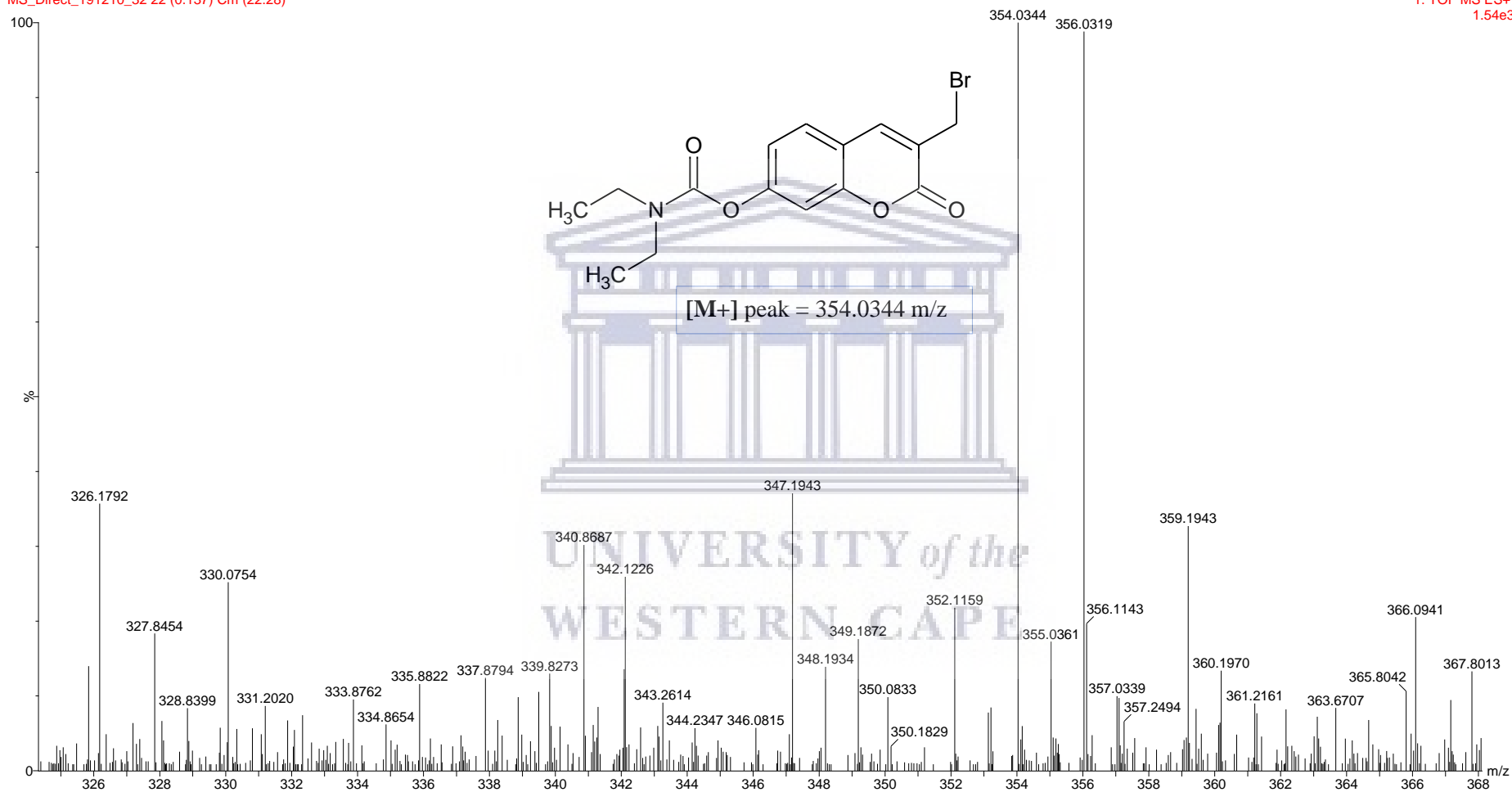
C13CPD CDCl3 {C:\Bruker\TopSpin3.2} JJ-SheunopaMzezewa 1



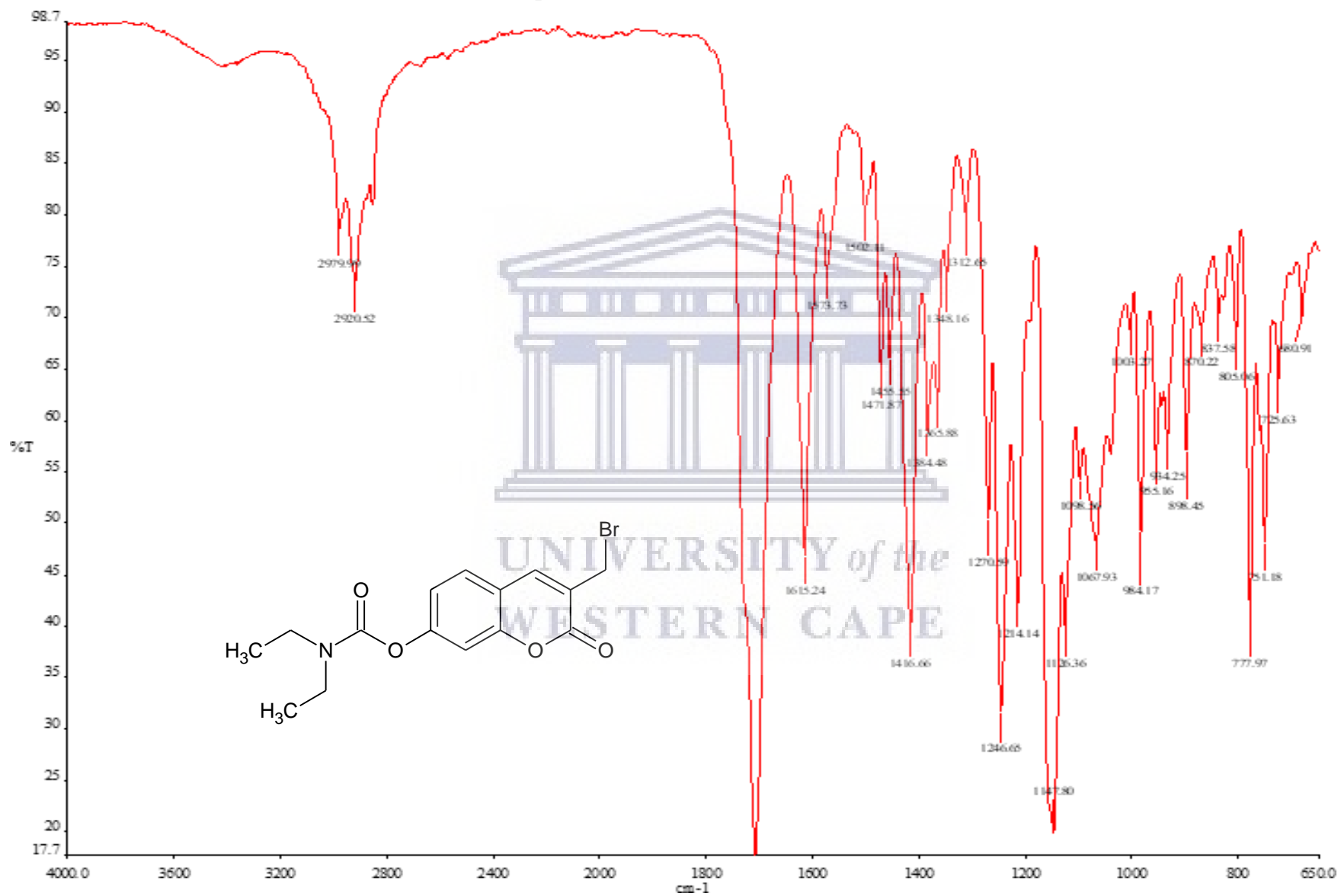
## Spectrum 23: HR-MS COMPOUND SM3B

SM 3B

MS\_Direct\_191210\_32 22 (0.137) Cm (22:28)

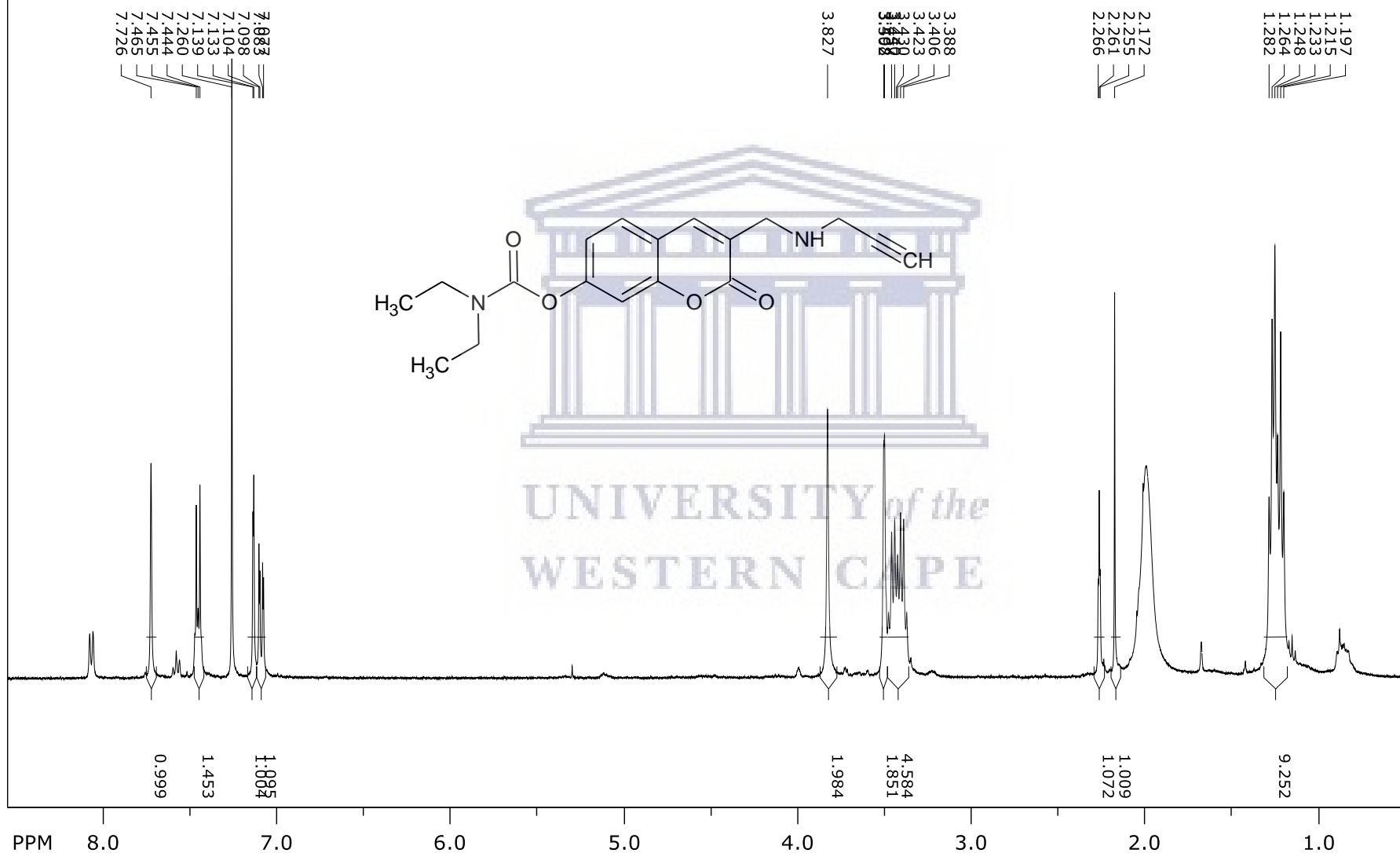
1: TOF MS ES+  
1.54e3

Spectrum 24: IR COMPOUND SM3B



Spectrum 25: <sup>1</sup>H NMR COMPOUND SM5A

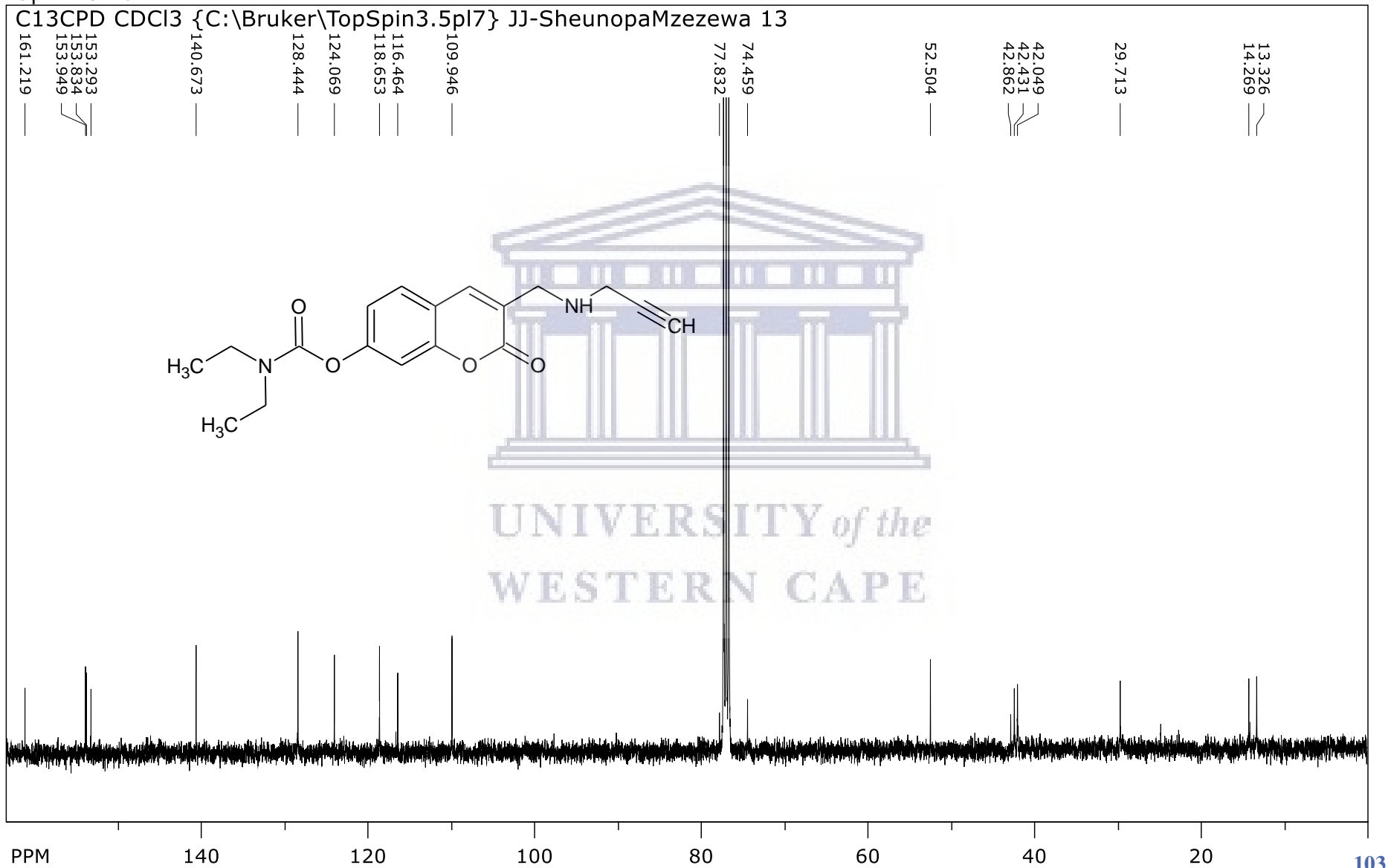
SpinWorks 4:

PROTON CDCl<sub>3</sub> {C:\Bruker\TopSpin3.2} JJ-SheunopaMzezewa 24



Spectrum 26:  $^{13}\text{C}$  NMR COMPOUND SM5A

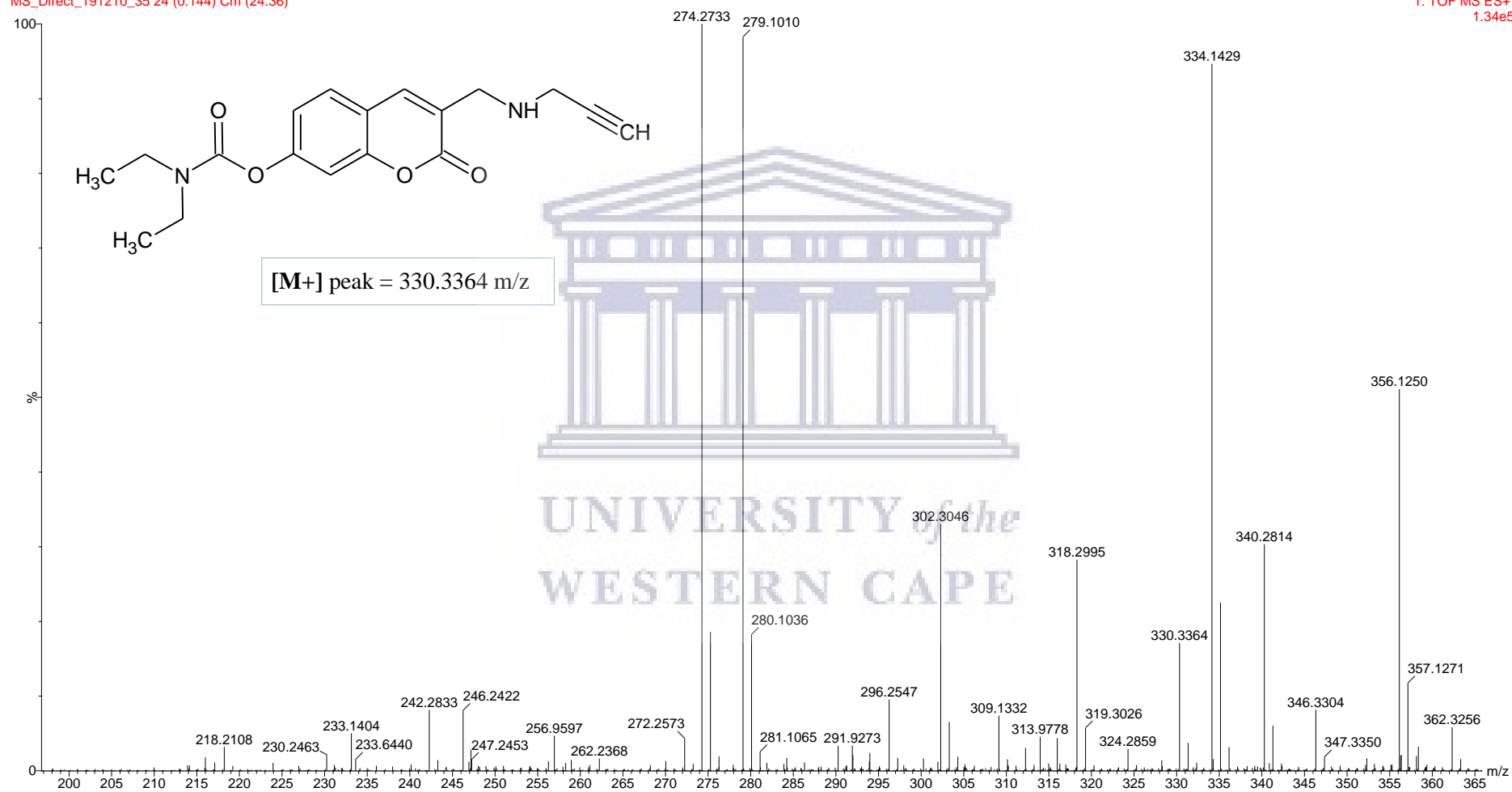
SpinWorks 4:



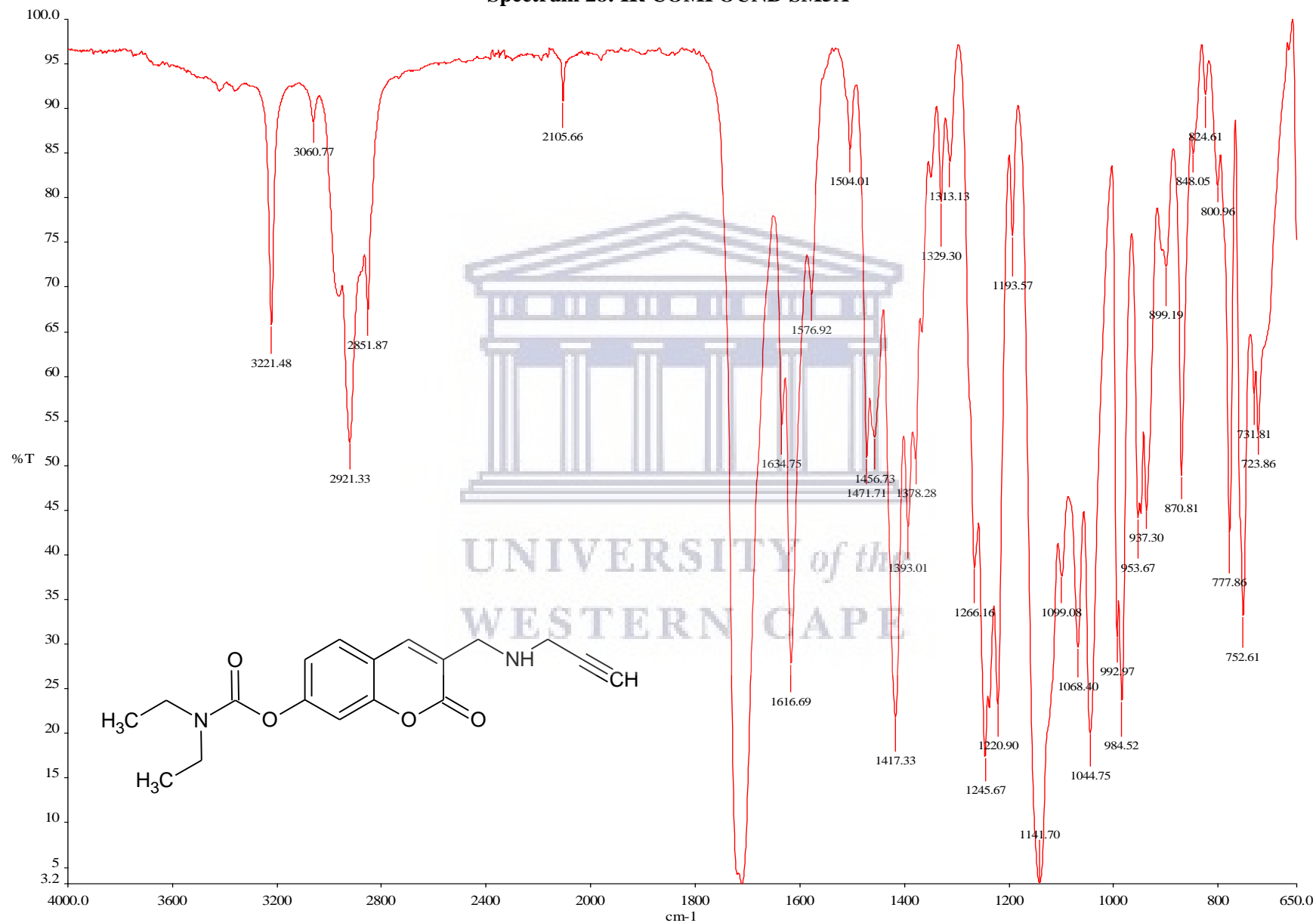
## Spectrum 27: HR-MS COMPOUND SM5A

SM 5A

MS\_Direct\_191210\_35 24 (0.144) Cm (24:36)

1: TOF MS ES+  
1.34e5

Spectrum 28: IR COMPOUND SM5A



<http://etd.uwc.ac.za/>